PRECIPITATION-HARDENING CHARACTERISTICS OF TERNARY COBALT-ALUMINUM-X ALLOYS

by

Charles Samuel Lee

A Dissertation Submitted to the Faculty of the

DEPARTMENT OF METALLURGICAL ENGINEERING

In Partial Fulfillment of the Requirements
For the Degree of

DOCTOR OF PHILOSOPHY
WITH A MAJOR IN METALLURGY

In the Graduate College

THE UNIVERSITY OF ARIZONA

1 9 7 1

THE UNIVERSITY OF ARIZONA

GRADUATE COLLEGE

I hereby recommend that this dissertation prepared under my direction by Charles Samuel Lee

entitled PRECIPITATION-HARDENING CHARACTERISTICS OF TERNARY COBALT-ALUMINUM-X ALLOYS

be accepted as fulfilling the dissertation requirement of the degree of DOCTOR OF PHILOSOPHY

David J. Meyer — Dissertation Director — 3/2/71 — Date

After inspection of the final copy of the dissertation, the following members of the Final Examination Committee concur in its approval and recommend its acceptance:*

Louis J. Demer	3/4/71
K. L. Kratzer	3/5/71
John W. Anthony	3/17/71
H. A. Wriedt	3/19/71

*This approval and acceptance is contingent on the candidate's adequate performance and defense of this dissertation at the final oral examination. The inclusion of this sheet bound into the library copy of the dissertation is evidence of satisfactory performance at the final examination.

STATEMENT BY AUTHOR

This dissertation has been submitted in partial fulfillment of requirements for an advanced degree at The University of Arizona and is deposited in the University Library to be made available to borrowers under rules of the Library.

Brief quotations from this dissertation are allowable without special permission, provided that accurate acknowledgment of source is made. Requests for permission for extended quotation from or reproduction of this manuscript in whole or in part may be granted by the head of the major department or the Dean of the Graduate College when in his judgment the proposed use of the material is in the interests of scholarship. In all other instances, however, permission must be obtained from the author.

SIGNED: 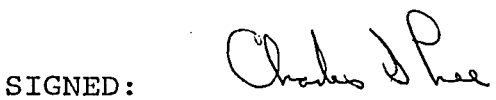

ACKNOWLEDGMENTS

The problems of completing a dissertation in absentia are so many and varied, that it is an almost impossible task to adequately give credit to all those individuals and organizations who deserve it.

Initially let me gratefully acknowledge the help of my advisor, Dr. D. J. Murphy, who encouraged me in my work and who, most importantly, performed the difficult tasks of monitoring my work via reports and arranging all the administrative details associated with a project done in absentia.

To my colleague-in-absentia, Dr. H. H. Keith, special thanks for his numerous helpful suggestions and informative discussions.

Finally, I am indebted to the many branches of the U. S. Navy whose facilities and financial assistance made it possible for me to complete this work. In particular, let me acknowledge the Engineering Department at the U. S. Naval Academy and the Naval Ship Research and Development Center at Annapolis whose personnel were most generous both in terms of time and use of facilities.

TABLE OF CONTENTS

TABLE OF CONTENTS--Continued

LIST OF ILLUSTRATIONS

LIST OF ILLUSTRATIONS--Continued

LIST OF ILLUSTRATIONS--Continued

LIST OF TABLES

LIST OF TABLES--Continued

ABSTRACT

Five precipitation-hardenable ternary cobalt-base alloy systems containing 4.25 weight percent aluminum with titanium, niobium, tantalum, molybdenum, and tungsten as the third element were melted and evaluated as to their precipitation-hardening characteristics. Hardening phases were electrolytically extracted from alloys aged up to 1000 hours in the 600°C to 900°C temperature range.

Based upon the evaluation of these systems, three quartenary alloys with compositions Co-4Al-15Cr-10Ta, Co-4Al-15Cr-20Mo, and Co-4Al-15Cr-25W were melted and similarly evaluated after aging for times from 0.1 to 1000 hours at 800°C.

The results of the investigation of the ternary alloys showed that Ti additions promoted the highest percentage increase in hardness, but that overaging of the $AlCo_2Ti$ hardening phase was very rapid.

The effects of the Nb and Ta additions to the Co-4Al matrix were somewhat similar in that both were considerably more effective as solid solution strengtheners than as precipitation hardening agents. Hardening in the Ta alloys was the result of the presence of primary and precipitated γCo_2Ta ($MgNi_2$ type) which, upon aging, transformed to the cubic

αCo_3Ta. Similarly, in the alloys containing Nb, the Laves phase Co_2Nb ($MgNi_2$ type) was generally present. Two phases previously reported in the literature for the Co-Nb binary system were confirmed. The Co-4Al-5Nb alloy aged for 1000 hours at 700°C contained an ordered fcc phase with a_o = 3.655 Å, while this same alloy aged at 800°C contained a hexagonal phase having the parameters a = 5.94 Å and c = 6.89 Å.

The cellular precipitation of Co_3Mo in the Co-Al-Mo alloys produced very high hardnesses in that alloy system. Temperatures of 900°C were required to overage these structures within the 1000-hour test interval.

In the Co-Al-W systems, an ordered fcc superlattice, or coherent precipitate, having a parameter of a_o = 3.595 Å was found. Precipitation of this phase resulted in continuous increases in hardness for aging times up to 1000 hours at 800°C.

Additions of 15 weight percent Cr to the basic Co-4Al-10Ta, Co-4Al-20Mo, and Co-4Al-25W alloys changed their aging behavior; and in the case of the latter two alloys, the R and Mu phases, respectively, appeared.

Aluminum additions to alloys of Co containing the refractory metals or Ti generally result in a stabilization of the fcc Co matrix and a resulting decrease in the tendency for the formation of non-cubic phases in the matrix. This effect seemed especially strong in the alloys containing

Ta and W where the formation of rhombohedral βCo_3Ta and hexagonal Co_3W were suppressed. Chromium additions to the ternaries containing Al tended to destabilize the fcc matrix and promoted the formation of non-cubic phases.

CHAPTER 1

PHYSICAL METALLURGY OF COBALT AND ITS PRECIPITATION-HARDENABLE ALLOYS

1.1 Cobalt - A General Review

In recent years the demand for high temperature alloys for gas turbines has forced the metallurgist to reconsider the Co-base systems which historically have served a minor role compared to the Ni-base alloys. The predominance of the Ni-base alloys was based upon the lower cost and availability of Ni as well as upon these alloys being somewhat less complicated metallurgically. At the present time, however, it appears that the service temperature capability of these Ni alloys has been nearly maximized so that the 40°C melting point advantage of Co is reason enough to pursue the formulation of new alloys based upon this element for high-temperature applications.

In an excellent state-of-the-art review, Sims (1969) has stated the case for and against the Co-base alloys. In short, while the Co alloys exhibit superior hot-corrosion resistance and display a flatter stress-rupture/time-temperature relationship, they are deficient in low-temperature short-time yield strength, oxidation resistance and structural stability. It is perhaps this last point—

metallurgical stability—which represents the most serious problem in Co alloys since Co, unlike Ni, undergoes an fcc to hcp transformation upon cooling below 417°C. This structural change in the matrix eliminates the possibility of obtaining a coherent hardening precipitate in the matrix since it is extremely unlikely that a precipitate can transform simultaneously with the matrix. For this reason, no Co-base precipitation-hardened alloys are in general use other than those in which the precipitates are carbides. In this respect, they differ from the major Ni-base systems which are hardened by the precipitation of intermetallic compounds as well as various carbides.

It is well known that certain elements, when alloyed with Co, notably C, Ta, Nb, Zr, Ti, V, Fe, Mn, and Ni, tend to stabilize its fcc structure to lower temperatures where the transformation is more sluggish. This stabilization is thought to be due to changes in stacking-fault energy resulting from the alloying. Thus, elemental additions which promote a high stacking-fault energy in the fcc lattice result in alloys which inherently contain less of the hexagonal regions accompanying partial dislocations. Sims considers that these "stacking faults warn of proximity to the hcp structure, and can be regarded as a precursor to more massive hcp formation." Viewed in this light, elemental additions which result in high stacking-fault energies are to be preferred in Co alloys. Other elements such as Si, Cr, Mo, and

W are generally regarded as hcp stabilizers and thus, perhaps, to be avoided.

Because of the importance of this fcc-hcp transformation in Co alloys, a great deal of effort has been expended in its study and in precise lattice parameter determinations for both phases. Vincent and Figlarz (1967) in a very careful study of pure Co have determined the fcc structure to have a_o = 3.5446 Å, while the hcp parameters are a = 2.5071 Å, c = 4.0695 Å with a c/a ratio of 1.6232.

1.2 Selection of Alloying Elements

As an effort toward increasing the understanding of precipitation in potentially useful Co systems, the present study covers precipitation of intermetallic compounds in Co-Al ternary alloys with the objective of determining if longtime stability is possible in these systems.

Many previous studies have looked at the various precipitation-hardenable Co binaries. In all of these studies, the major findings have been that significant hardening is possible but the stability of the precipitates is uniformly poor. A good review of these binary studies is given in a compilation by Fritzlen et al. (1959). More recently, a series of studies of Co-Cr ternaries with the refractory metals has established essentially the same results, namely, that longtime stability at high temperature is not achieved in these systems (Drapier, deBrouwer, and Coutsouradis, 1965).

When considering alloying elements suitable as additions to Co, two considerations are paramount. These are oxidation resistance and metallurgical stability combined with a reasonably strong matrix. Chromium has historically been added to both Ni and Co superalloys for its oxidation resistance. Although not as potent in this respect as is Cr, Al is also regarded as a contributor toward oxidation resistance. Also, being fcc, Al should import stability to the fcc Co matrix in opposition to the Cr which, as stated previously, is an hcp promoter. The selection of 4.25 w/o (weight percent) Al for all alloys in this study was primarily based on the use of this approximate amount in the AiResist series of alloys which exhibit good oxidation resistance and adequate stress rupture properties (AiResearch, 1968). Because of strength considerations, this value represents perhaps the maximum amount which might practically be added. In addition to its value as an aid to oxidation resistance, Al also forms a system with Co suitable for hardening by precipitation of the CoAl intermetallic compound.

The selection of Nb, Ta, Mo, W, and Ti as ternary additions to the basic Co-4Al matrix was based upon two considerations. First, these elements form precipitation-hardenable alloys with Co. The study by Drapier et al. (1965), which evaluated the effects of refractory metal additions (Nb, Ta, Mo, W) in Co-Cr matrices, found substantial hardening in all systems; however, the hardening potential of

these elements with Al in Co has not been studied to date. Secondly, these elements are also solid solution strengtheners. Coutsouradis (1964) has tabulated the effect upon the melting point of the Co solid solution per additions of one w/o of these elements and found that the changes in the melting point were -39°, -18°, -4.5°, +0.55°, and -36°C for Nb, Ta, Mo, W, and Ti, respectively. It is to be noted that W is the only element which increases the melting point. The Ti additions were included to determine whether that element would form a ternary precipitate as it does in the Ni-base alloys where it and Al are the hardening elements.

The weight levels of the ternary additions were chosen to straddle the solvus line and thus determine the effect, if any, of Al upon the solid solubility of the ternary elements. The selection of 15 w/o Cr to the quartenary alloys corresponds approximately to the minimum amount of that element which past experience has proven to be necessary for adequate oxidation resistance.

1.3 Cobalt Alloy Systems

There have been several large-scale programs in recent years oriented towards Co-alloy development. Several of the more extensive of these have been those of Rizzo and Lherbier (1966) and Rausch and Simcoe (1960).

Because of the large number of elements employed in those investigations, the effects of individual elements

were often masked. The following sections will discuss precipitation occurring in binary and ternary Co systems where careful study has documented the effect of the individual elements involved. To be considered are the binaries of Co with Al, Nb, Ta, Ti, Mo, and W. A review of these systems will greatly aid in the understanding of the hardening behavior of the Co-Al-X ternary alloys. Especially noticeable is the large number of different phases reported as existing in the same system by the various investigators. This is an indication of the great difficulty in obtaining equilibrium phases in systems where intermediate precipitates occur and reaction rates are sluggish. This sluggishness is especially apparent in alloys containing the high melting point refractory metals.

1.3.1 Cobalt-Aluminum

The effects of Al additions to Co are not entirely agreed upon. It is generally accepted that large additions have a deleterious effect on creep-rupture strength (Wheaton, 1965). Efforts to obtain a strengthening gamma prime precipitate such as the $Ni_3(Al,Ti)$, which exists in the Ni systems, have not been successful in the Co alloys. As discussed earlier, this problem is related to the loss of coherency and subsequent rapid overaging of the precipitates in a matrix which is always tending toward reversal to the hcp structure. Indeed, even the oxidation retardation

qualities, usually ascribed to Al in Co alloys, have been questioned (Sims, 1969).

A study of the Co-Al phase diagram (Fig. 1) shows one very important feature. In the Co-rich end of the binary system, with alloys up to 34 w/o Al, the intermetallic CoAl (CsCl type) exists as a potential hardening phase. This phase was, in fact, determined by Lee (1967) to contribute to the hardening of AR-213, a castable high Al alloy with excellent oxidation resistance. Bradley and Seager (1939)

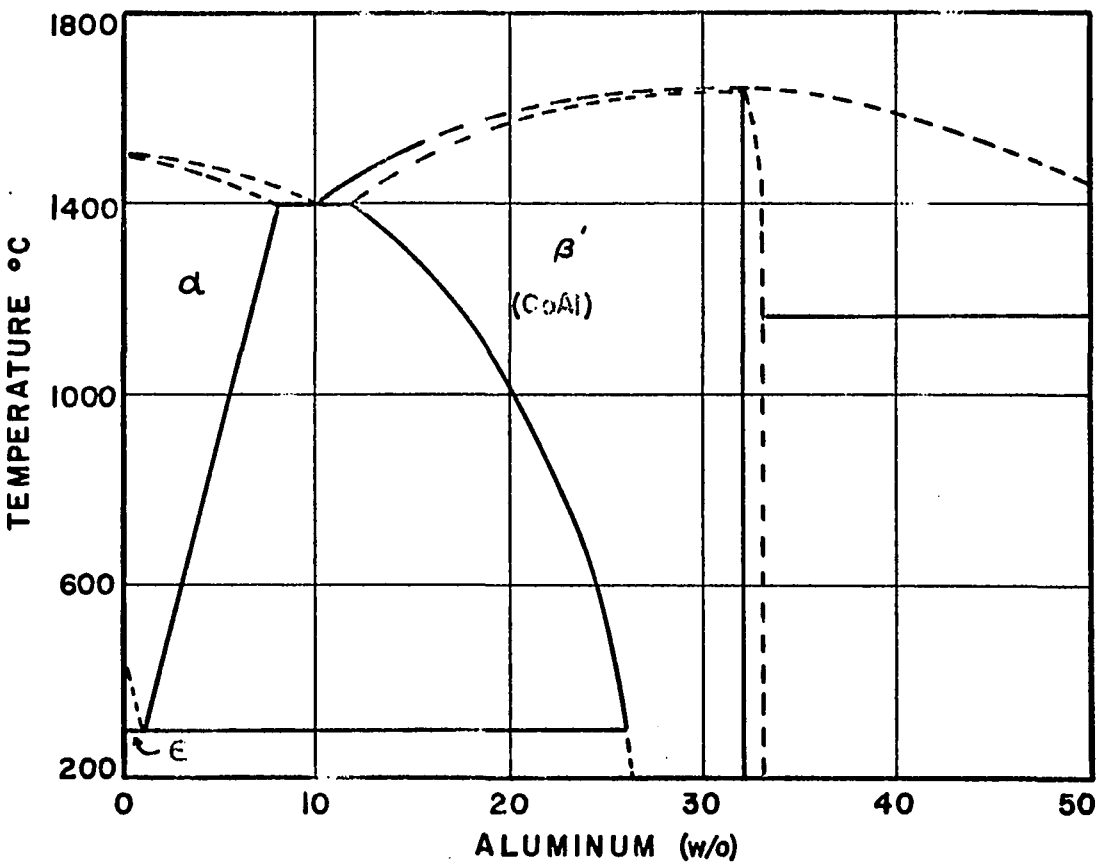

Fig. 1. The Co-Al Phase Diagram

found that the lattice parameter of this phase could range from 2.8506 to 2.8564 Å depending on the relative amounts of Co and Al. Interestingly, this intermetallic at the stoichiometric composition has a congruent melting point of 1620°C. However, because of the large solubility of this compound for Co, its melting point drops to 1400° at 23 a/o (atomic percent) (12 w/o) Al. This effectively reduces the value of CoAl as a high temperature hardening compound. Data presented by Fritzlen et al. (1959) show that in binary Co-Al alloys overaging is relatively rapid at temperatures above 600° to 700°C.

1.3.2 Cobalt-Niobium

In this binary system (Fig. 2) the two most commonly reported phases in Co-rich alloys are the Laves phases Co_2Nb having both the hexagonal $MgNi_2$ and the cubic $MgCu_2$ structures (Fig. 7) (Wallbaum, 1941). These phases form from a eutectic reaction at 1235°C when the Nb content exceeds the maximum solubility of 7.5 w/o (4 a/o). The Nb solubility then falls to a value of approximately 1 a/o at room temperature.

Instead of the stoichiometric Co_2Nb, Wallbaum reported the $MgNi_2$ structure as $Co_{2.19}Nb_{0.81}$. Saito and Beck (1960) determined that the composition for this structure was actually closer to the Co_3Nb. In their study, the cubic

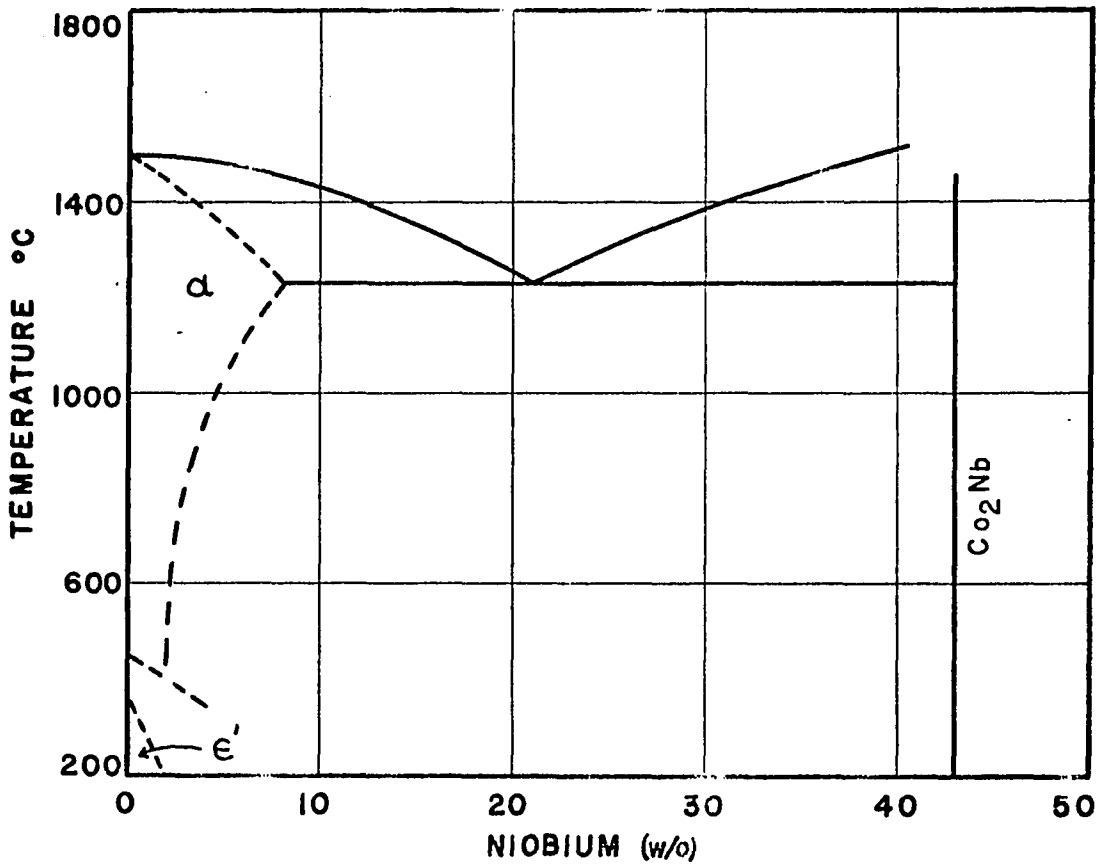

Fig. 2. The Co-Nb Phase Diagram

$MgCu_2$ type occurred only at the higher Nb concentration of 27.3 to 32.6 a/o.

In addition to the Laves phases, Piearcey, Jackson and Argent (1962-63) have reported a hexagonal precipitate in dilute (<6.29 a/o Nb) Co-Nb alloys. Chemical analyses of their extracted residues suggested a composition of Co_5Nb_2 for this phase.

Kokorin and Chuistov (1966) have indicated that an intermediate phase does in fact exist prior to the formation

of the equilibrium Co_2Nb phase. Unfortunately, they do not report any attempt to determine the structure of this phase except to note that it was not the equilibrium phase reported by Piearcey, Jackson and Argent.

Kokorin and Chuistov (1968) have recently found an ordered fcc structure (Cu_3Au type) in a Co-4 a/o Nb alloy which was aged for one hour at 800°C after being quenched from 1200°C. A lattice parameter of $a_o = 3.654$ was reported.

In Co-Nb ternaries with Ni, Piearcey et al. (1962-63) found the third Laves type ($MgZn_2$) to be stabilized by the Ni; while in ternaries with Cr, Drapier et al. (1965) found the $MgNi_2$ form to be present.

Most of the above studies showed similar results in that the increase in hardness was associated with the precipitation of the needle-like Laves phases in the matrix. In general, aging at 600°C produced the maximum hardness in the binary system and aging temperatures greater than 800°C caused overaging in less than one hour. It is quite evident, however, from the many unidentified phases reported and from the discrepancies between investigations that the Co-Nb phase diagram still remains somewhat in doubt especially in the low Nb region.

1.3.3 Cobalt-Tantalum

In the Co-rich end of this system (Fig. 3), Laves phases also form from a eutectic reaction at 1276°C when the Ta content exceeds 13 w/o (4 a/o).

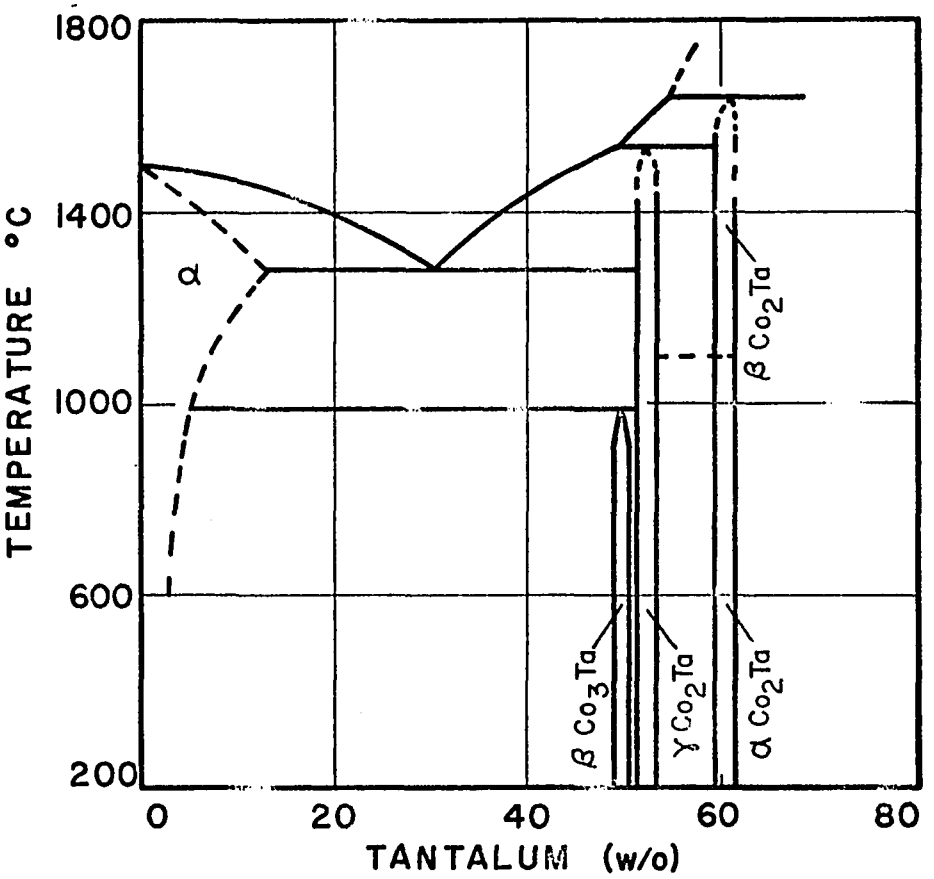

Fig. 3. The Co-Ta Phase Diagram

As with the Nb system, Wallbaum (1941) reported both a cubic ($MgCu_2$) and a hexagonal ($MgNi_2$) form of the Co_2Ta Laves phase. Korchynsky and Fountain (1959) later confirmed the presence of the alternate hexagonal $MgZn_2$ type at the

stoichiometric composition. In addition, they reported a metastable ordered face-centered cubic αCo_3Ta phase (Cu_3Au type). Progressive aging transformed this phase into βCo_3Ta having a hexagonal structure. In their precipitation-hardened alloys containing 5 to 15 w/o Ta, overaging occurred at temperatures above 600°C prior to 1000 hours.

In a later analysis of the intermetallic phases existing in this system, Dragsdorf and Forgeng (1962) confirmed the presence of all three Laves phases plus the α and β forms of the Co_3Ta. As in the previously mentioned study, they also ascribed a hexagonal four-layered structure to the βCo_3Ta.

The βCo_3Ta compound was also reported to be the equilibrium hardening phase for Co-Cr-Ta alloys aged in the 600° - 1000°C temperature range (Drapier and Coutsouradis, 1968). This acicular precipitate was identified as rhombohedral and not hexagonal as proposed earlier. The authors suggested that the initial αCo_3Ta precipitate formed as an ordered coherent phase in the cubic matrix. After prolonged aging during which the βCo_3Ta formed, it was also observed that portions of the matrix had transformed to the hexagonal-close-packed structure. It is now generally accepted that this βCo_3Ta represents the equilibrium precipitate for the alloys containing less than 50 w/o Ta.

1.3.4 Cobalt-Titanium

The Co-rich side of this system (Fig. 4) lends itself well to hardening by precipitation. From a maximum solubility of 10.7 w/o at 1200°C, the solubility of Ti in Co decreases to less than 2 w/o at room temperature. In alloys containing less than 22 w/o Ti, only a Co_3Ti hardening phase has been found. Fountain and Forgeng (1959) established the existence of this Cu_3Au type phase having the ordered fcc structure. Their work helped to clarify much conflicting

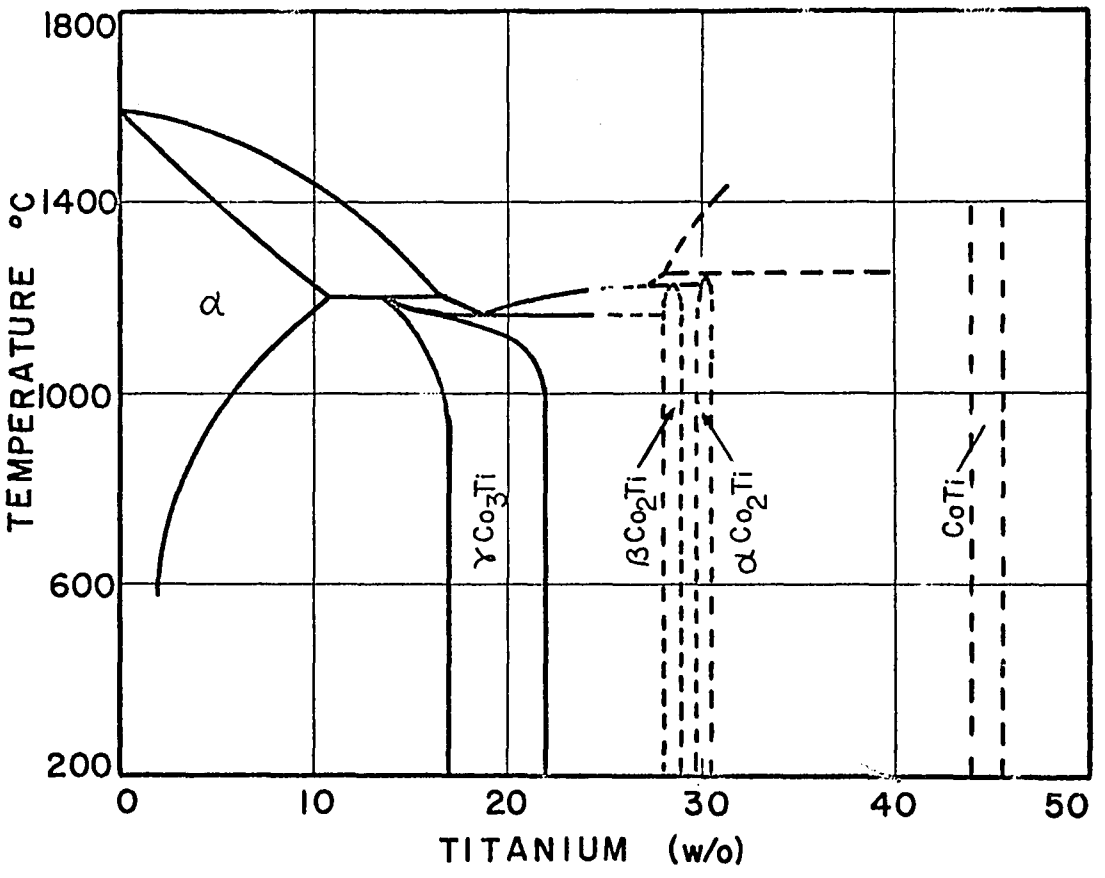

Fig. 4. The Co-Ti Phase Diagram

data concerning that region in the phase diagram between Co solid solution and the previously reported Co_2Ti phase. Interestingly, no superlattice lines were noted in their x-ray analysis of this compound.

Bibring and Manenc (1959) and Fountain, Faulring and Forgeng (1961) later confirmed the ordered nature of this phase in their analyses of its precipitation behavior. The aging response of Co_3Ti in the Fountain and Forgeng study showed that, in general, overaging occurred at temperatures above 700°C in less than 1000 hours.

At compositions greater than 21.7 w/o Ti, the Laves phases Co_2Ti are formed. As in the other systems discussed, both the $MgNi_2$ hexagonal and the $MgCu_2$ cubic forms have been found with the cubic form stable in the range of Ti contents greater than 30 w/o.

In the Co-Ti-Al system, two ternary compounds, $TiCo_2Al$ and Ti_2CoAl_2 have been reported (Markov, 1966). The $TiCo_2Al$ phase has been confirmed as having the Cu_2MnAl Heusler type structure; that is, having an ordering of the body-centered atom positions in the ternary CsCl type structure. (See Fig. 8, page 24.)

1.3.5 Cobalt-Molybdenum

A recent study (Quinn and Hume-Rothery, 1963) has clarified some of the inconsistencies existing in this system. Cobalt can dissolve a maximum of 26 w/o (18 a/o) Mo

at 1335°C (Fig. 5). Alloys containing between 26 and 55 w/o Mo freeze in a eutectic reaction at this temperature. At temperatures below 1025°C, two phases exist as potential hardeners—hexagonal Co_3Mo and rhombohedral-hexagonal Co_7Mo_6. The Co_3Mo compound was apparently responsible for the high hardness (Rockwell C-65) obtained by aging a Co-15 w/o Mo alloy in the study of Sykes and Graff (1935). Bibring and Graf (1961) have shown that this phase precipitates in the hexagonal regions of the matrix. The lattice parameters for

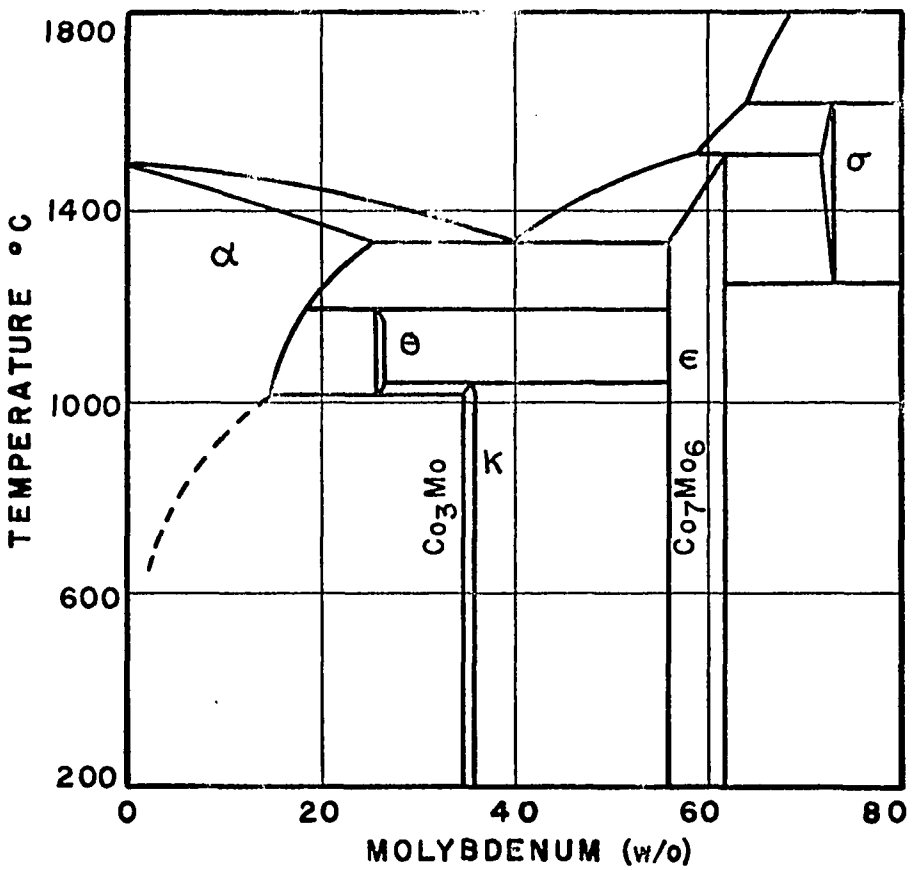

Fig. 5. The Co-Mo Phase Diagram

the hexagonal matrix are a = 2.507 Å, c = 4.070 Å; while those of the Co_3Mo are a = 5.130 Å, c = 4.128 Å. Since the basic parametric difference is a doubling of the "a" parameter, these authors conclude that the formation of the Co_3Mo phase basically involves an ordering on the close-packed basal planes without any change in the axial direction.

Lux and Bollman (1961) studied the hardening characteristics of Co-Cr-Mo ternaries with Cr at the 11-18 w/o level. In their analyses of the residues obtained from aged specimens, no confirmed observation was made of the presence of Co_3Mo, although Co_7Mo_6 was present in all specimens examined.

In studies of this same ternary, Rideout and Beck (1953) discovered an "R" phase (see Section 2.1.2) in alloys quenched from 1200°C. Komura, Sly, and Shoemaker (1960) later identified this Mo-Co-Cr phase as rhombohedral. The presence of the R phase as a precipitate formed by aging a Co-17Cr-13Mo alloy for 20 to 100 hours at 800°C was confirmed by Drapier et al. (1965).

1.3.6 Cobalt-Tungsten

As is the Co-Mo system, the Co-W system (Fig. 6) is amenable to hardening by precipitation. Sykes (1933) obtained a maximum hardness of Rockwell C-65 in an alloy containing 35 w/o W. In fact, most of the Co-W intermetallic compounds are isotypic with those of the Co-Mo system. This

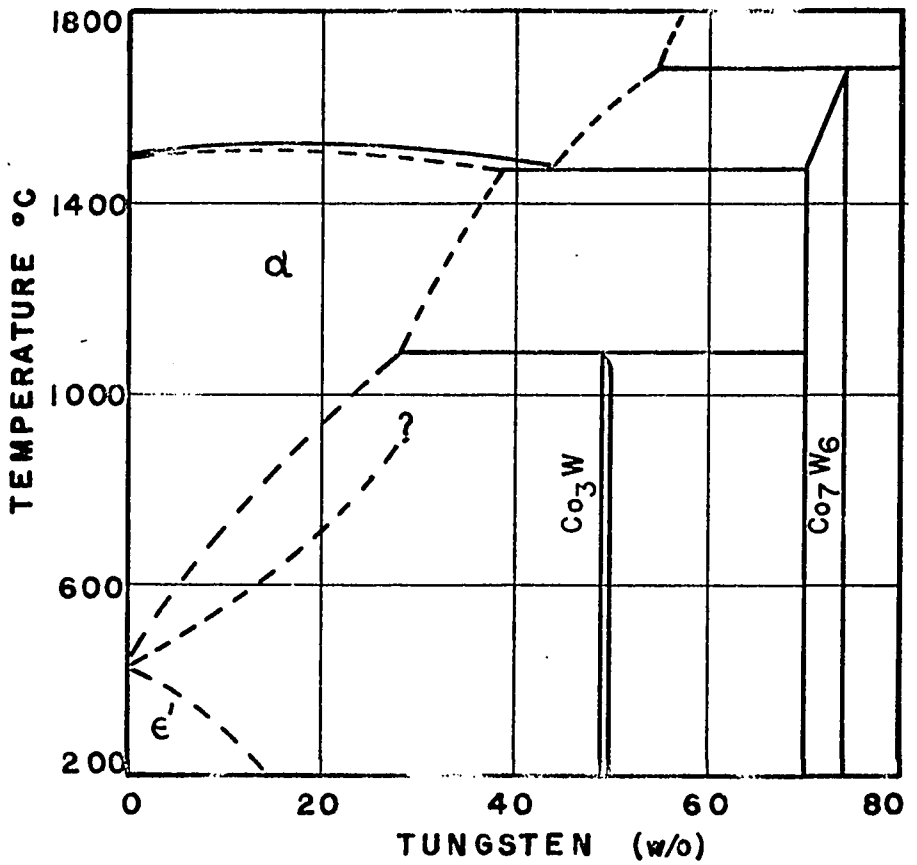

Fig. 6. The Co-W Phase Diagram

similarity extends even to the maximum solubility of W in Co which is 17.5 a/o (38 w/o) at 1471°C. At this temperature, a eutectic reaction results in the formation of Co solid solution plus Co_7W_6. Further cooling to below 1093°C results in the peritectoid reaction of Co solid solution with Co_7W_6 to form Co_3W.

In their study of the Co-W system, Neumeier and Holman (1967) refined the reaction isotherm temperatures to those listed above and in addition determined that a certain solubility for Co exists in both Co_7W_6 and Co_3W.

Adkins, Williams and Jaffee (1960) obtained very high hardnesses in an investigation of Co-W binary and ternary alloys, and attributed this increase primarily to the precipitation of Co_3W. In an alloy of Co-25W-1Al, they found that the Al was an alpha solid solution stabilizer but was not effective in increasing hardness over that of the Co-W binary.

Cobalt-tungsten-chromium ternary alloys were found by Drapier et al. (1965) to be hardened by the hexagonal Co_3W which precipitated preferentially in the hcp regions of the solid solution. This preferential precipitation of the Co_3W in the hcp phase was noted by Bibring and Graf (1961). They also postulated the existence of a hexagonal transition phase accompanying the precipitation of the Co_3W.

CHAPTER 2

INTERMETALLIC COMPOUNDS IN COBALT ALLOYS

The intermediate phases and intermetallic compounds found in Co binary and ternary alloys exist in a wide variety of crystal structures. Since optimum hardening precipitates are generally close-packed coherent structures, the crystalline arrangement of the precipitate is extremely important in determining its potential usefulness. In the following sections, the crystal structures of those phases present in the previously considered Co systems will be discussed.

2.1 Topologically Close-packed Structures

These structures are those whose formation is dependent upon both relative size considerations and electronic configurations. Historically, their presence has been associated with brittleness and a decrease in strength in alloys in which they appear. Among these structures are the Laves phases and the R and Mu phases.

2.1.1 Laves Phases

More Laves phases have been found to exist, 220, than any other type of phase known. These phases have

generally been classed as size-compounds; that is, they form AB_2 compounds whose diametric ratio $d_A:d_B$ is ideally $\sqrt{3/2}:1$ (1.225:1). At this ratio, A atoms touch A atoms and B touch B so that atoms can be packed together to achieve an average coordination number of 13.33 (Elliott, 1956). In practice, these phases have been observed at ratios of from 1.05 to 1.68 (Dwight, 1961). Dwight concluded therefore that it was only necessary that the A atom be larger than the B and that these partner elements have the ability to expand or contract to approach the ideal ratio. Additionally, there are many possible Laves phases, based on favorable ratios, which do not exist. Thus, it is apparent that size consideration, while important, is not the sole criterion in the formation of the Laves phases.

Three types of AB_2 Laves phases exist; the cubic $MgCu_2$ type and the hexagonal $MgZn_2$ and $MgNi_2$ types. In the cubic structure (Fig. 7), the large A atoms exist in a diamond cubic array. Forming the interstices in which these A atoms sit, are tetrahedra of the smaller B atoms. With this arrangement, the stacking in the <111> directions is the familiar ab, a.... The a and b "layers," however, are actually double layers of the A atoms in which these atoms are vertically aligned over each other (Hume-Rothery and Raynor, 1962).

The hexagonal types are also formed by the stacking of these double layers, the $MgZn_2$ structure being ab, a...

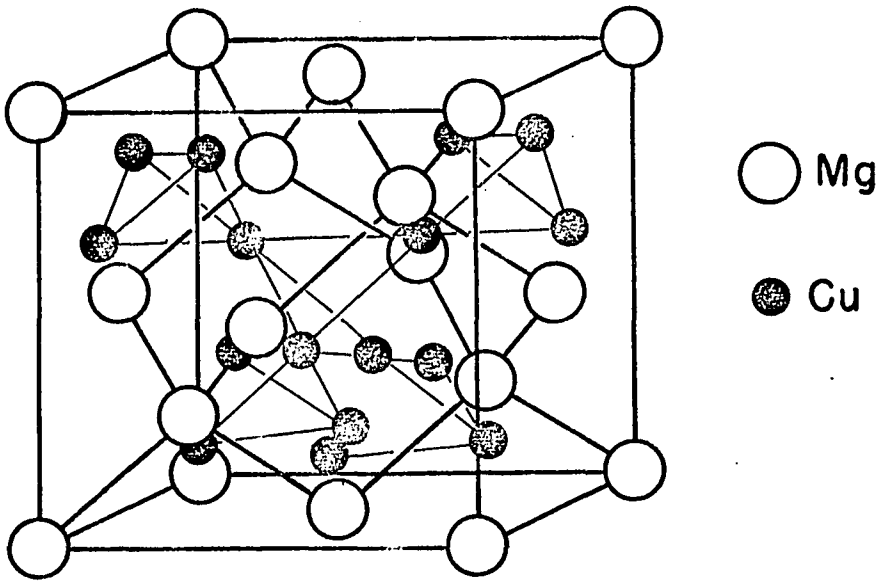

Fig. 7. The $MgCu_2$ Structure

and the $MgNi_2$ form being abac, a.... A great deal of effort has been concentrated by many investigators in attempting to predict which of the possible Laves structures will form based upon a prediction of the electron to atom (e/a) ratio. In his study, Elliott (1956) concluded, "allotropy is the exception rather than the rule and occurs only for those binary phases that have electron:atom ratios near a critical value." Unfortunately, this prediction process involves various assumptions as to the proper value of valence for the transition elements such as Co. In these elements, "effective valences" can vary depending on the nature of neighboring atoms. Nevertheless, great success has been made in the correct prediction of Laves forms by this approach.

2.1.2 R and Mu Phases

The R and Mu phases, along with the better known sigma and others, belong to a class of phases known as "electron compounds." Their occurrence in structural alloys has been studiously avoided because of their brittleness and the loss of toughness they impart to alloys. In addition, the precipitation of these phases reduces matrix strength by lowering the concentration of solid solution strengtheners and oxidation retarders. Their crystal structure is rather complex and they generally are found in alloys of the transition elements Co, Ni, and Fe.

The R phase was discovered by Rideout and Beck (1953) in their studies of the Co-Cr-Mo system. It has not been found in binary alloys and its composition range is considered to be fairly small. The crystal structure of this phase was found by Komura, Sly, and Shoemaker (1960) to be rhombohedral with 53 atoms per unit cell. The nominal ratio of the elements in this Co-Cr-Mo compound is approximately 49:21:30. The lattice constants determined were:

Rhombohedral	Hexagonal
a = 9.011 Å	a = 10.903 Å
α = 74°27.5'	c = 19.342 Å
	c/a = 1.774

Alloys containing the R phase were not as brittle as those containing sigma, nor is the phase itself as brittle as sigma.

The Mu phase, also rhombohedral, is structurally related to R but has only 13 atoms per cell. Co_7Mo_6, Co_7W_6 and their Fe isomorphs have the Mu-phase structure. At the ideal stoichiometric ratio, the parameters for Co_7W_6 are:

Rhombohedral	Hexagonal
$a = 8.990$ Å	$a = 4.752$ Å
$\alpha = 30°39'$	$c = 25.68$ Å
	$c/a = 5.404$

A ternary Mu phase exists in the aforementioned Co-Cr-Mo system. In this system, the R and Mu phases both had approximately the same hardness.

2.2 Body-centered Cubic Structures

Although many variations of the bcc structures exist, only those pertinent to this investigation will be discussed here.

The familiar ordered CsCl structure is the second most common intermetallic structure following the Laves phases.

In this binary structure, the A sites (Fig. 8) are occupied by one atomic species and the B and C sites by the

other. Compounds exhibiting this structure are CoAl and CoTi among others.

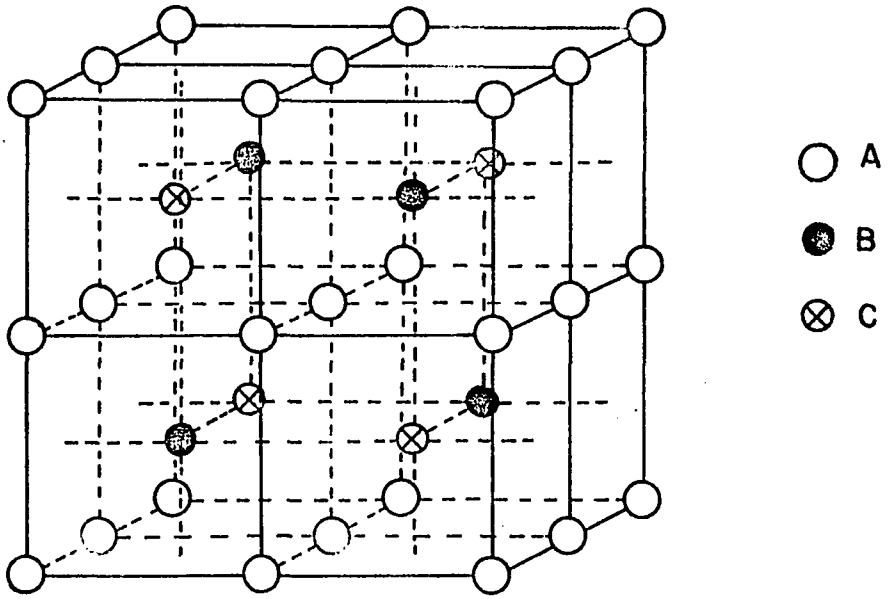

Fig. 8. Body-centered Cubic Model

Two variations of this structure can occur in ternary systems. If the B and C sites are occupied randomly by two atomic species, a "ternary CsCl-type" compound results; however, if these two species order by selective occupation of B and C sites, the Cu_2MnAl-type compound is formed. In this case, the lattice parameter is necessarily twice that for the disordered case. The ordered Cu_2MnAl compounds occur only in the correct stoichiometric ratio. Differentiation between the ternary CsCl type and the Cu_2MnAl structures can be made by observing the additional superlattice lines

in an x-ray pattern. The compound $AlCo_2Ti$ is an example of this ordered structure.

2.3 Close-packed Structures

In its elemental form, Co exists in two close-packed configurations, fcc and hcp. The difference between these two forms can be considered in terms of the stacking of close-packed planes. Thus, in the fcc structure, the packing sequence of those planes is abc, a...; whereas in the hcp structure, it is ab, a....

Close-packed structures also occur in great abundance in many Co systems. Beattie (1967) has an excellent tabulation of these structures, which exist in many forms. Those which are pertinent to this investigation are the Cu_3Au cubic type and the Ni_3Sn hexagonal form. As with pure Co, the stacking sequences are abc, a..., and ab, a..., respectively. However, in these structures, the close-packed planes which are arranged in these sequences are Co_3X planes in which each X atom is completely surrounded in its plane by Co atoms (triangular ordering). Each X atom in both of these structures is coordinated entirely by twelve Co atoms (Fig. 9). Examples of these compounds are the cubic Co_3Ta and the hexagonal Co_3Mo phases.

As Sims (1969) notes, it is precisely the formation of these close-packed phases which gives strength to the nickel-base superalloys. Unfortunately, in the Co systems,

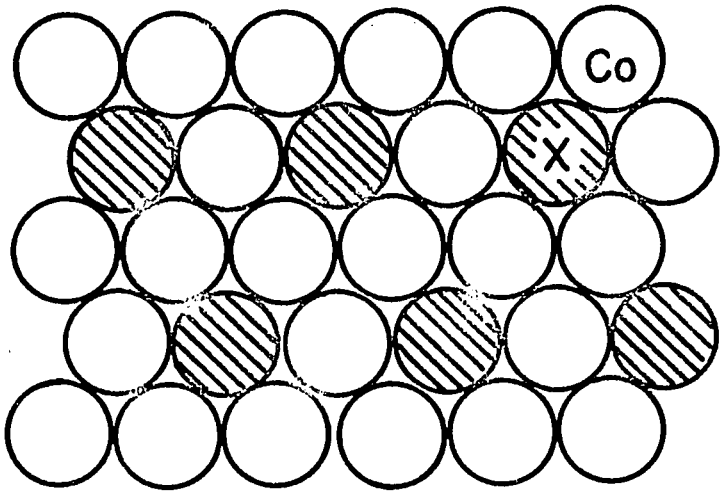

Fig. 9. Close-packed Triangular Ordering

these phases tend to dissolve and/or overage at temperatures below 800°C.

CHAPTER 3

OBJECTIVES

The objective of this investigation of precipitation-hardenable cobalt-aluminum alloys was essentially threefold and consisted of:

a. The preparation of Co-4Al alloys containing ternary additions of Nb, Ta, Mo, W, and Ti, and the evaluation of their responses to heat treatments.

b. The determination of the actual hardening mechanisms in the alloys by microscopy and x-ray techniques.

c. The determination of the effects of Cr additions upon the hardening behavior of several of the more promising ternary systems.

CHAPTER 4

EXPERIMENTAL PROCEDURE

4.1 Procedural Summary

The experimental work consisted of two separate but related sections. In Section I, 17 cobalt-aluminum-X ternary alloys (Table I) were melted, solution treated, and aged for a series of times up to 1000 hours in the 600°C to 900°C temperature range. Hardness measurements and

Table I - Selected Alloys

Section I	Section II
Co+4Al + 5 Nb	
Co+4Al + 10 Nb	Co+4Al+15Cr+10Ta
Co+4Al + 15 Nb	
Co+4Al + 20 Nb	Co+4Al+15Cr+20Mo
Co+4Al + 5 Ta	
Co+4Al + 10 Ta	Co+4Al+15Cr+25W
Co+4Al + 15 Ta	
Co+4Al + 20 Ta	
Co+4Al + 3 Ti	
Co+4Al + 6 Ti	
Co+4Al + 9 Ti	
Co+4Al + 12 Ti	
Co+4Al + 5 Mo	
Co+4Al + 12.5 Mo	
Co+4Al + 20 Mo	
Co+4Al + 10 W	
Co+4Al + 25 W	

photomicrographs were taken at suitable aging times. Following the 1000-hour agings, the hardening precipitates were electrolytically extracted and identified by x-ray diffraction.

In Section II, 15 w/o Cr was added to three of the more promising ternaries examined in Section I, and the procedures outlined above were essentially repeated at the 800° aging temperature. In addition, scanning electron microscopy was employed for a more complete analysis.

A pictorial summary of the experimental procedure is shown in Fig. 10.

4.2 Preparation and Heat Treatment of Specimens

The alloy nomenclature used in the investigation of the Co-4.25 Al-X ternaries was to designate the alloy by the X element and the w/o of that element—thus, the Co-4.25Al-10Ta alloy is listed as 10Ta. Since all quarternary alloys contained 15 w/o Cr, the nomenclature used in those cases was Cr-10Ta.

All alloys of selected composition (Table V, Appendix B) were melted as 15 gm. buttons in an arc-melting furnace utilizing a tungsten electrode over a water-cooled copper hearth. The raw materials were procured in the form shown in Table II. Their complete chemical analyses are listed in Table VI (Appendix B).

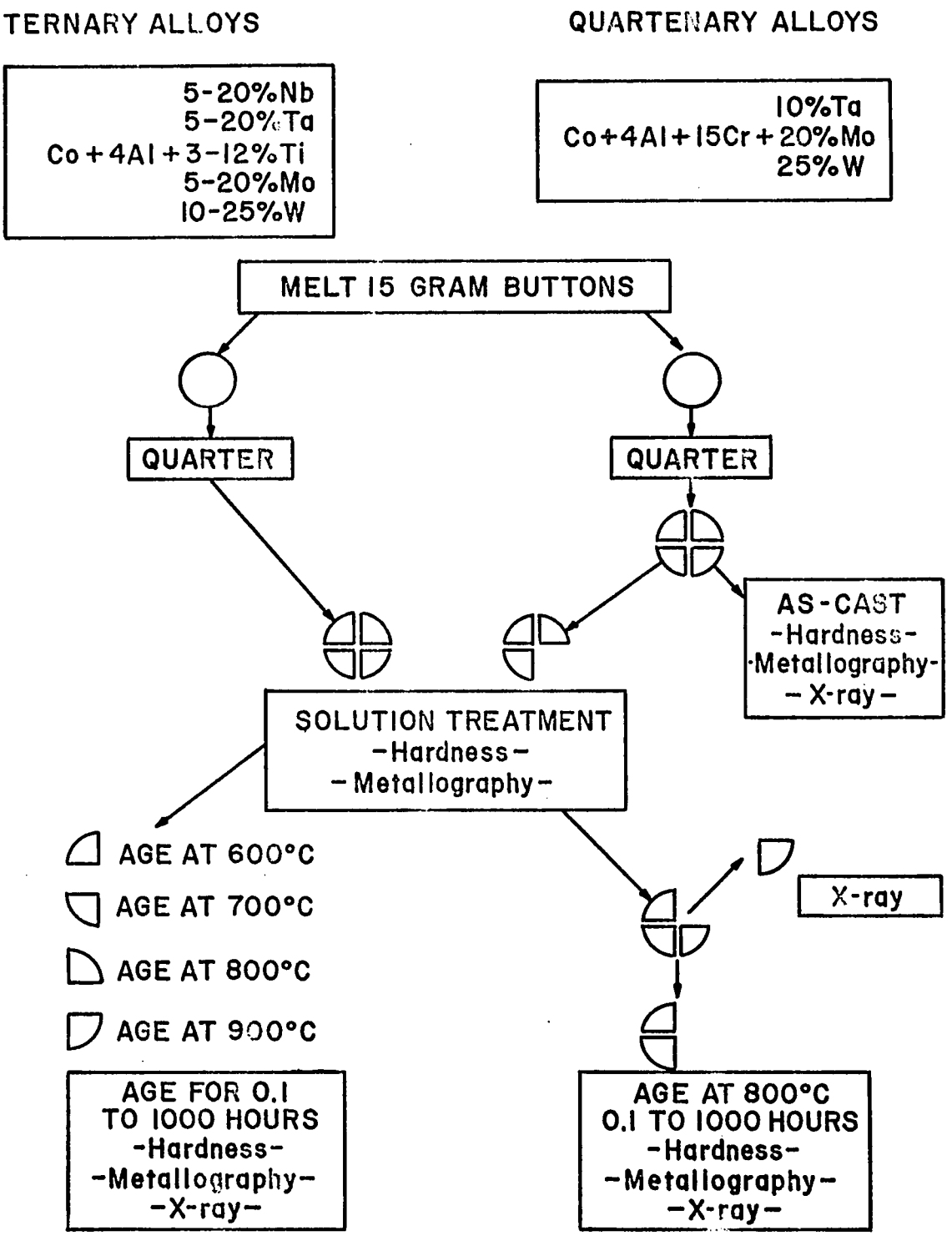

Fig. 10. Procedural Flow-chart

Table II - Raw Materials

Metal	Purity	Form	Metal	Purity	Form
Co	99.94	electrolytic	Mo	99.9	powder
Al	99.9	chunk	W	99.79	powder
Nb	99.7	wire	Cr	99.999	shot
Ta	99.9	wire	Ti	99.73	sponge

The Mo and W powders were compacted and vacuum outgassed at 650°C prior to melting in the arc-furnace in order to prevent loss of material.

The melting procedure was to:

a. weigh the charges
b. evacuate, backfill, and re-evacuate the chamber three times, alternately backfilling with He-Ar-He
c. evacuate to 70 microns
d. backfill to 16" Hg vacuum with helium
e. backfill to 10" Hg vacuum with argon
f. melt

Each button was melted and inverted four times to insure homogeneity except that the buttons containing Mo were melted five times and the buttons containing W, six times. A Ti or Zr "getter" button was always melted prior to the desired buttons in order to eliminate any residual oxygen or nitrogen. Initially, the buttons were weighed after each melting but, since total loss after four meltings was

consistently under 0.2%, this procedure was discontinued. A wet chemical analysis of a Co-5Al-5Ta button showed the following comparison.

Composition as weighed: 90.03%Co-4.92%Al-5.06%Ta

Composition as analyzed: 89.96%Co-4.92%Al-5.09%Ta

Following melting, the buttons were quartered and subsequently encapsulated in fused quartz tubes under a partial pressure of argon. The encapsulated specimens were solution treated for two hours at the selected temperature, then water quenched (Table III).

Table III - Solution Heat Treatments

Alloy Containing	Solution Treatment °C
Nb	1180° - 2h/W.Q.
Ta	1200° - 2h/W.Q.
Ti	1095° - 2h/W.Q.
Mo	1305° - 2h/W.Q.
W	1300° - 2h/W.Q.
Mo+Cr	1285° - 8h/W.Q.
Ta+Cr	1200° - 8h/W.Q.
W+Cr	1350° - 7h/W.Q.

These temperatures were set as high as practicable but not so high as to possibly allow incipient melting to occur because of nonequilibrium freezing following arc-melting.

After the solution treatment, the specimens were evaluated for hardness and microstructure and were then re-encapsulated. Each quarter was subsequently aged at 600°, 700°, 800°, or 900°C for times from 0.1 to 1000 hours. Thus, the same specimen was used to generate all points on each aging curve.

The quartenary alloy systems were similarly treated but were aged only at 800°C.

4.3 Microhardness and Microscopy

The Vickers hardness data were taken using a Leitz microhardness tester with a 200-gm. load. Each datum point plotted represents the average of at least three indentations. Hardness readings were confined to the matrix, where possible, and away from grain boundaries or large agglomerates of primary intermetallic compounds.

Photomicrographs were taken on specimens which were either mechanically or electro-polished as described in Appendix A. Original magnifications were at 500 and 1000 X using a Leitz metallograph. The scanning electron microscopy was performed on a Cambridge Mark II A Stereoscan with the photographs shown in Figs. 49 through 54 being taken at magnifications of 1400 X to 13,000 X. The interpretation of these photographs is discussed in Section V.

4.4 X-ray Diffraction

This work consisted of electrolytically extracting the precipitated intermetallic phases and analyzing these particles using a General Electric XRD-6 diffractometer.

The electrolytic extractions were accomplished by making the specimen the anode while using a pure tantalum cathode. The electrolyte used was that suggested by Brown, Clark and Parker (1957) and was simply a 10% solution of HCl in methanol except for those alloys containing tungsten. For these, a salt solution consisting of 7.5% sodium citrate, 5.0% potassium thiocyanate 1.2% potassium bromide, 0.8% ammonium chloride and 85.5% H_2O was used (Drapier et al., 1965). This was necessary to avoid the large amounts of tungstic acid which formed in the acidic HCl solution. A four-hour extraction using a current density of 0.1 amps/cm^2 gave sufficient residue for identification. A magnetic stirrer in the cell helped accelerate the dissolution of the specimen.

The residue was allowed to settle overnight and then was separated from the solution, washed several times in ethanol and evaporated onto a glass slide.

Cobalt Kα radiation, filtered by iron oxide, was the radiation employed for the diffraction analysis. The specimen was scanned at a speed of 0.4°/minute using a scintillation tube for counting. The x-ray data were read to an

accuracy of 0.05° and non-cubic patterns were then indexed using either a Bunn chart or references in the literature relating to that particular compound. Cubic patterns were indexed simply by inspection of the $\sin^2\theta$ values. Following indexing, the lattice parameters were determined with the aid of a computer program kindly furnished by the General Electric Company. Using an input of 2θ, λ, (h, k, l) and a weighting factor, this program performed a least squares extrapolation of the data to give the lattice parameters. The weighting method employed for this investigation was to assign a weight of unity to all lines with values of 2θ below 90° and a weight of $1/\sin^2 2\theta$ for all values above 90°.

CHAPTER 5

RESULTS AND DISCUSSION

Because of the large number of systems studied and the amount of data generated, the results will be discussed in two parts—a heat treatment and microscopy section followed by an analysis of the x-ray results. In each case, the alloys will be discussed in the order Nb, Ta, Ti, Mo, and W. The quartenary alloys will be covered along with their corresponding ternary.

5.1 Heat Treatment and Microscopy

The aging response curves for all alloys are shown in Appendix C (Figs. 11-28). The associated microstructures are found in Appendix D (Figs. 29-54). For convenience, most of the discussion of the microstructures has been placed on their facing pages.

The Co-Al-Nb alloys (Figs. 11-14) were all nominally hardened by the precipitation of the Co_2Nb Laves phase ($MgNi_2$-type) and its associated transition phase(s). Alloys with more than 5 w/o Nb all contained some primary Co_2Nb as well as precipitated Co_2Nb. It is evident from the large quantities of this phase in the microstructure of the 5Nb alloy (Fig. 29) that the solubility of Nb in Co is decreased

somewhat by the presence of Al in the matrix. The ability of Co_2Nb to effectively harden the Co-Al matrix is not too great as evidenced by the aging curves. The Co_2Nb needles agglomerated rapidly and overaging occurred for all compositions prior to 1000 hours even at 600°C. Two notable exceptions to this are seen in Figs. 11 and 12 where the 5Nb and 10Nb alloys had not overaged at 700°C even after 1000 hours. The x-ray data, to be discussed later, confirmed the presence of a probable transition phase in these specimens. It should also be noted that the large amounts of Co_2Nb in the 15Nb and 20Nb alloys caused these specimens to crack during quenching, confirming the extremely brittle nature of the Laves phases.

When compared with the data obtained by Piearcey et al. (1962-63) on binary Co-Nb alloys, it is evident from this study that the effects of Al additions upon the aging characteristics of Co-Nb alloys are such as to reduce the degree of hardening which can occur and also to reduce the rate of precipitation. The sluggishness of the reaction indicates that the presence of Al tends to decrease the rate of diffusion of Nb in Co. Piearcey et al. (1962-63) observed substantially this same effect in their study of Ni additions to Co-Nb alloys. Aluminum additions appear, however, to reduce hardening by precipitation to a much greater degree than do Ni additions. Because appreciable hardening did not

appear possible with the Co-Al-Nb systems, no quartenary alloys based upon this system were melted.

The Co-Al-Ta systems (Figs. 15-18) were, in general, similar to the Co-Al-Nb alloys in their aging behavior; however, on an atomic percent basis, hardening by Ta additions appeared to be slightly more effective. As with the alloys containing Nb, significant overaging occurred prior to 1000 hours at both 800° and 900°C. At 600° and 700°C, however, these Co-Al-Ta alloys showed level or rising tendencies in their aging curves even after 1000 hours. Since the earlier data of Korchynsky and Fountain (1959) showed overaging prior to 1000 hours at 700° for binary Co alloys with up to 15 w/o Ta, this indicates that Al additions prolong hardening in the Co-Ta system. The reason for this is probably related to the fact that Al, in stabilizing the fcc matrix, hinders the transformation of metastable cubic αCo_3Ta to rhombohedral βCo_3Ta. The higher hardnesses obtained in the Co-Al-Ta alloys over the Co-Al-Nb alloys are a result of the formation of this ordered αCo_3Ta phase which Dragsdorf and Forgeng (1962) have shown to be coherent with the fcc Co matrix.

Although both the 15Ta and 20Ta alloys contained primary Co_2Ta ($MgNi_2$-type Laves phase), this phase was also observed after aging the 5Ta and 10Ta alloys, indicating that its precipitation preceded the formation of the αCo_3Ta.

Subsequent aging of all Ta alloys resulted in the gradual disappearance of the Co_2Ta and its replacement by the αCo_3Ta.

Since the largest percent increase in hardness occurred with the 10Ta alloy, this composition was selected for study in a quartenary system containing 15 w/o Cr. The Cr addition to the basic 10Ta alloy altered substantially the aging behavior of this alloy (Fig. 28). The solution treated hardness alone was raised from a Vickers hardness of 254 to 335 due to the solid-solution strengthening. The percentage increase in hardness after aging was actually slightly less in the Cr-10Ta alloy than in the ternary 10Ta alloy aged at 800°C. Overaging was observed at 1000 hours in both alloys although the process was predictably more sluggish in the quartenary system. The addition of Cr to the Co-Al-10Ta matrix lowered the solubility of the matrix for Ta; and it can be seen in Fig. 46 that, unlike the ternary 10Ta alloy, the Cr-10Ta system contained primary Co_2Ta. Subsequent aging transformed this phase into the αCo_3Ta. Comparison of the aging results for the Co-4Al-15Cr-10Ta quartenary with the work of Drapier et al. (1965), who studied a Co-15Cr-8Ta alloy, showed the following. Aluminum additions, as with the Nb alloys discussed previously, tend to reduce the amount of hardening which can occur in Co-Ta alloys. In the alloy containing Al, the precipitate even after 1000 hours at 800°C was the metastable cubic αCo_3Ta; whereas,

in the Co-Cr-Ta ternary, the rhombohedral βCo_3Ta was found after only 16 hours at 800°C. Thus, the stabilizing effect of Al on the ordered fcc precipitate is quite apparent.

The Co-Al-Ti alloys were quite hardenable (Figs. 19-22) although with 9 and 12 w/o Ti, the large amounts of primary hard phase, Co(Al,Ti), tended to obscure the precipitation effects. A study of this ternary is actually better based upon the Co-Al system than upon the Co-Ti system, since the ternary precipitate was crystallographically related to the bcc CoAl compound and not the fcc γCo_3Ti.

After solution treating, even the 3Ti alloy contained some second phase (Fig. 37-A). Subsequent aging brought out appreciable precipitate at all temperatures. This precipitation was both of the cellular type at grain boundaries and of a general nature in the matrix. Although high hardnesses were measured in these cellular areas, the general precipitate in the matrix did not produce much of a hardness increase. For example, a 3Ti specimen aged for 10 hours at 700°C had a matrix hardness of 227 while the hardness of the adjacent cellular regions measured 435. These cellular regions (Fig. 38-E) caused the high hardnesses evident in the aging curves for the 6Ti series of alloys. The hardnesses were not persistent, however, and overaging of the Co(Al,Ti) compounds (Fig. 38-F) occurred very rapidly even at temperatures as low as 600°C. Data by Boesch, presented in the

reference by Fritzlen et al. (1959), indicated that Co-Ti binary alloys containing 3, 6, and 9 w/o Ti were all significantly hardened by the precipitation of cubic Co_3Ti. It is evident from the present study that the addition of the 4 w/o Al completely changes the hardening mechanism from one based on Ti to one based on Al and Ti in concert. Because of the rapid overaging of the precipitate even at 600°C for the lower Ti compositions, no quartenary alloys, containing Ti, were melted.

The aging curves for the Co-Al-Mo alloys are shown in Figs. 23-25 and the associated microstructures in Figs. 41-43. All the alloys in this system were hardened by precipitation of the Co_3Mo phase either in a cellular manner originating at the grain boundaries or as a general precipitate in the matrix. The 5Mo alloy did not harden to any great extent because of the small volume of precipitate available. At temperatures of 600° and 700°C, where the solubility of Mo is smaller, some Co_3Mo precipitated along grain boundaries. With 12.5 and 20 w/o Mo present (Figs. 24 and 25), the hardening became quite pronounced and persistent. This was especially evident for the 700°C aging temperature where the hardnesses were still rising after 1000 hours. The structures responsible for this hardness (Figs. 42-D and 51) were of a cellular nature with alternating layers of Co solid solution and Co_3Mo. This cellular precipitate

in the 20Mo alloy coalesced at the higher aging temperatures with a resultant drop in hardness after 100 hours at the 800° and 900°C aging temperatures.

In the study by Sykes and Graff (1935) of a Co-15 w/o Mo alloy, appreciable hardness increases were noted after aging at 600°C for only five hours. In this study, by contrast, the precipitation process was much retarded. This can be explained by the fcc stabilizing effect of Al in the matrix. As mentioned in section 1.3.5, the precipitation of Co_3Mo occurs preferentially in the hcp portion of the matrix; hence, if the fcc lattice is stabilized by Al, the entire precipitation process is retarded.

Because of the high persistent hardnesses found in these alloys, a Co-4Al-15Cr-20Mo quartenary alloy was melted and aged at 800°C. The as-cast structure (Fig. 47-A) consisted of stringer-like arrays of R phase in the Co solid solution. This phase then agglomerated during solution treatment. Additional R phase precipitated during aging to give a large increase in hardness in the alloy (Fig. 28). The peak hardness for this alloy occurred at approximately 50 hours, after which it fell fairly rapidly.

Lux and Bollman (1961) determined the aging characteristics for a Co-15Cr-20Mo alloy in which they found the hardening precipitate to be Co_7Mo_6. In this study, the presence of 4 w/o Al in the quartenary alloy resulted in the formation, not of Co_7W_6, but of the R phase alone. Neither

of these rhombohedral phases is really desirable because of their brittleness. This quartenary is therefore not considered very useful at the levels of Al and Cr which were evaluated.

The Co-Al-W ternaries with 10 and 25 w/o W displayed especially interesting aging curves (Figs. 26 and 27) and microstructures (Figs. 44, 45, and 53). It is obvious (Fig. 26) that there was not enough precipitate in the 10W alloy at 800° and 900°C to promote much of a hardness increase. On the other hand, at 600° and 700°C, the kinetics of the precipitation were so slow that peak hardnesses were not reached even after 1000 hours. With 25 w/o W, however, hardening was appreciable at 600°, 700°, and 800°C after 1000 hours. In comparison with this behavior, an aging study of a Co-25W alloy by Adkins et al. (1960) showed overaging at 700° after only 64 hours and at 800° after only 16 hours. In their study, a maximum Vickers hardness of 710 was obtained by aging this alloy at 700°C - a much higher hardness than that obtainable with Al present. The authors attributed the hardness increases in the Co-25W alloy primarily to the decomposition of the supersaturated fcc solid solution into hcp solid solution plus hexagonal Co_3W. In the present study, however, no Co_3W was detected in any of the Co-Al-W alloys analyzed. Instead, a fine ordered fcc

phase (Fig. 53) was found in all aged specimens. This phase will be discussed in more detail in the next section.

Because of the very promising hardening behavior of the Co-4Al-25W alloy, a quartenary with 15 w/o Cr was melted and aged at 800°C (Fig. 28). Although appreciable hardening occurred, overaging was very rapid and took place in less than 500 hours. The precipitate in this alloy was found to be rhombohedral Co_7W_6, which existed as both a primary phase formed during casting, and as a precipitated phase (Figs. 48 and 54). Thus, the fcc stabilizing effect of the Al is destroyed by the presence of a significant amount of Cr, and the stability of the ternary alloy does not hold with Cr additions.

5.2 Crystallographic Phase Identification

All identification of the phases discussed in the preceding section was accomplished by powder x-ray diffraction techniques using the precipitated phases collected by electrolytic dissolution of the various specimens. These patterns were then matched against references in the literature or tabulated data in the Fink Index (1966) for identification.

5.2.1 The Co-Al-Nb System

The Co-Al-Nb alloys were difficult to analyze in terms of trying to put together a complete picture of

precipitation corresponding to the various compositions and aging temperatures. The 15Nb and 20Nb alloys were, however, very simple in that they contained only Co_2Nb ($MgNi_2$ type) either in the as-cast structure or in the aged condition. The residues collected from the 20Nb alloy aged for 1000 hours at 600° and at 900°C both contained only this phase (Table VII). (Note: Table VII and all subsequent tables are located in Appendix B.) The lattice constants determined were a = 4.747 Å, c = 15.494 Å, and c/a = 3.271. This compares with the values a = 4.729 Å, c = 15.43 Å, and c/a = 3.262 which Wallbaum (1941) found for the Laves phase of composition $Co_{2.19}Nb_{0.81}$ and with those of Saito and Beck (1960), who reported a = 4.740 Å, c = 15.45 Å, and c/a = 3.259. The slightly larger size of the unit cell probably corresponds to the presence of some of the larger Al atoms.

With the 5Nb and 10Nb alloys, the precipitation behavior was more complex. The x-ray pattern for residues extracted from the 5Nb alloy aged for 1000 hours at 900°C contained only lines corresponding to precipitated Co_2Nb (Table VIII) while the pattern for the specimen aged at 600°C contained lines of Co_2Nb plus two unidentified peaks corresponding to d-spacings of 2.236 and 2.137 Å. No d-spacings for either fcc or hcp Co have these values.

Residues for this same alloy aged for 1000 hours at 700°C showed the strong presence of an ordered fcc phase

(Table IX) with a lattice parameter of 3.655 Å plus the weaker presence of a second unidentified phase. This parameter for the cubic phase corresponds extremely well with the value of 3.654 Å reported by Kokorin and Chuistov (1968), who were the first to record the presence of a Cu_3Au type phase in the Co-Nb system corresponding to the cubic αCo_3Ta whose existence had previously been well established in the Co-Ta system. It is worthwhile to note that for the aged 5Nb alloy, its highest hardness (Fig. 11) occurred at 700°C where this cubic Co-Nb compound was detected. This suggests that some coherency effect is involved since the microstructure did not show any appreciable differences in volume percent of precipitate for the 600° and 800°C aged specimens. As mentioned above, there was a second unidentified phase observed after the 700°C aging. Although this phase was not the prominent one, its presence was marked and, based upon its three strongest peaks, it was thought to be Co_2Nb. Examination of the residue from the specimen aged at 800°C showed otherwise. All of the major lines of this pattern corresponded to those found by Piearcey et al. (1962-63) (ASTM card No. 15-465) and which were identified in that study as belonging to an hexagonal structure whose parameters were given as a = 5.89 Å, c = 6.83 Å, with c/a = 1.16. Chemical analysis of the residues in the Piearcey study suggested a composition near to Co_5Nb_2. To check this result,

an alloy of composition Co_5Nb_2 was melted in this study and aged at 800°C for 280 hours. The only phase present was found to be the Laves phase Co_2Nb. The lines for this unidentified phase (Table X) were then indexed on the basis of the hexagonal cell used by Piearcey and the parameters were found to be a = 5.94 Å, c = 6.89 Å, c/a = 1.16. Thus, good agreement is found with the aforementioned work. It seems probable that this hexagonal phase is a transition phase found only in dilute Co-Nb alloys where the amount of Nb is less than 6 a/o and perhaps considerably lower. Those lines which could not be indexed on the basis of an hexagonal pattern corresponded to the stronger lines of the Co_2Nb pattern.

The x-ray patterns for the residues from 10Nb alloys differed somewhat from those of the 5Nb specimens. A cubic Cu_3Au type (possibly Co_3Nb) with a_o = 3.655 Å (Table XI) and the hexagonal Co_2Nb with a = 4.728 Å, c = 15.426 Å, c/a = 3.263 were both found in the specimen aged at 700°C, while the 900°C aging produced only the Co_2Nb Laves phase with a = 4.756 Å, c = 15.477 Å, and c/a = 3.254.

From the above, it is evident that an aging temperature of 900°C results solely in the precipitation of the Co_2Nb Laves phase; while at lower temperatures, the Co_2Nb appears along with both a cubic and an hexagonal phase. These latter two phases may represent transition phases or may be stable since they did exist after 1000 hours at

temperature. Since both of these phases had been previously reported in the binary Co-Nb system, the effect of Al may be one of merely altering their relative stability with time.

5.2.2 The Co-Al-Ta System

The precipitation pattern for the alloys containing Ta was perhaps even more complex than for those containing Nb. As noted from the photomicrographs (Figs. 35 and 36), some primary γCo_2Ta ($MgNi_2$ type Laves phase) was present following solution treating. In addition, this phase was also observed to precipitate in aged specimens. The parameters (Table XII) determined from the residue of the 10Ta alloy aged at 600°C for 1000 hours were a = 4.754 Å, c = 15.503 Å, c/a = 3.26. These values compare with Wallbaum's a = 4.722 Å, c = 15.39 Å, c/a = 3.26 for the composition $Co_{2.19}Ta_{0.81}$ and the values of a = 4.70 Å, c = 15.42 Å, c/a = 3.28 obtained by Dragsdorf and Forgeng (1962). Although the Co_2Ta phase was perhaps not the equilibrium one, it was the only phase found in the Co-Al-Ta alloys aged at 600°C. In alloys aged at 700°, 800°, and 900°C, this phase transformed to the ordered fcc αCo_3Ta. This Cu_3Au type structure (Table XIII) had a lattice parameter a_o = 3.646 Å which compares with the 3.647 Å value determined by Dragsdorf and Forgeng. It was this phase which was responsible for the hardening in the Co-Al-Ta alloys. In the Co-Ta binary systems, the equilibrium phase at 600° to 900°C should be the rhombohedral

βCo_3Ta for alloys containing between 7 and 49 w/o Ta. The fact that both the 10Ta and 20Ta alloys contain αCo_3Ta even at 900°C indicates that Al is a potent stabilizer for this fcc matrix and its cubic precipitate.

Considering the aging of the 10Ta alloy at successively higher temperatures from 600° to 900°C, an interesting pattern was apparent. The solution treated structure contained no second phase; however, aging at 600°C resulted in the precipitation of γCo_2Ta. At 800°C, the residue after 1000 hours was primarily the cubic αCo_3Ta. Several extraneous lines also appeared in the pattern for this phase. At 900°C, the pattern was quite complex. The predominant phase was still αCo_3Ta; however, the strongest lines of Co_2Ta were present along with several peaks of medium intensity whose presence may be ascribed to the rhombohedral βCo_3Ta. Unfortunately, the strongest peaks for βCo_3Ta are coincident with those of αCo_3Ta so identification is not precise. It does appear, however, that the αCo_3Ta is not an equilibrium phase in this Co-Al-Ta system, but rather a very stable transition phase which approaches equilibrium very slowly, even at 900°C.

Because the Co-Al-Ta system exhibited a reasonable hardening capability, a quartenary Co-4Al-15Cr-10Ta alloy was melted and aged at 800°C. This alloy (Figs. 46, 49, and 50) contained primary γCo_2Ta as cast. The parameters (Table XIV) were a = 4.764 Å, c = 15.503 Å, c/a = 3.25. Aging this

alloy resulted, as with the ternary system, in the primary γCo_2Ta reverting to a mixture of cubic αCo_3Ta needles with a lattice parameter a_o = 3.659 Å (Table XV) plus the still predominant hexagonal Co_2Ta Laves phase. The parameters of the Laves phase after aging were a = 4.766 Å, c = 15.536 Å, c/a = 3.26. No βCo_3Ta lines appeared in the residue patterns for this alloy.

5.2.3 The Co-Al-Ti System

The Co-Al-Ti alloys, with from 3 to 12 w/o Ti, all contained the same phases after both the solution and aging heat treatments. Instead of the expected Co_3Ti, the compound $AlCo_2Ti$ was identified. This Cu_2MnAl type compound (Fig. 8) is simply an ordered ternary CsCl-type compound. The lattice parameter determined from the extracted residue of the 12Ti alloy aged at 900°C for 1000 hours was a_o = 5.845 Å (Table XVI). This compares well with the value of 5.847 Å reported by Markov (1966). A similar pattern for the 3Ti alloy gave a_o = 5.818 Å. The $AlCo_2Ti$ phase is really a hybrid of CoTi (a_o = 2.991 Å) and CoAl (a_o = 2.862 Å), both of which have the CsCl structure. An average lattice parameter for these two structures would be a_o = 2.927 Å. The determination of whether or not the phase in the current study was simply the ternary CsCl structure with a_o = 2.923 Å or the ordered version with a doubled parameter was based upon the presence of the weak superlattice lines. If the

crystallographic planes with all odd integers such as the (111), (311), (331), (115), and (135) are deleted from the pattern in Table XVI, and the remaining indices are then halved, the parameter would then be that of the ternary CsCl compound. The presence of these planes, however, shows the preferential ordering of the Al and Ti atoms and gives rise to a unit cell of twice the size, namely 5.845 Å. It is perhaps quite probable that the alloys contained both ordered and unordered amounts of this component since the Al and Ti were not present in the stoichiometrically correct amounts for 100% $AlCo_2Ti$.

A second phase, considered to be an impurity phase, was also identified in the residues for all alloys containing Ti. This CsCl type compound with a_o = 3.226 Å (Table XVII) could not be isolated metallographically, nor could it be identified by its parameter.

5.2.4 The Co-Al-Mo System

In the Co-Al-Mo system, all alloys were hardened by the precipitation of hexagonal Co_3Mo. This phase was present in specimens containing from 5 to 20 w/o Mo and was found at all aging temperatures between 600° and 900°C. For the various compositions and aging treatments. the parameters ranged for a values between 5.113 Å to 5.146 Å, and for c values between 4.107 Å to 4.130 Å. The average values obtained from six different extractions were a = 5.128 Å,

c = 4.120 Å, c/a = 0.803. These values compare with the a = 5.11 Å, c = 4.12 Å, c/a = 0.803 values obtained by Quinn and Hume-Rothery (1963). A typical pattern for this phase is given in Table XVIII. Various unidentified peaks were present in the residue patterns for all of the alloys containing Mo. No consistent occurrence was noted in these peaks except for one medium intensity peak having a range of d-spacings from 2.257 Å to 2.282 Å. The constant appearance and disappearance of lines in this alloy system suggests that the Al in the alloy is affecting the attainment of equilibrium by stabilizing the fcc matrix. Evidence for this is seen by noting the extremely strong (002) reflection for Co_3Mo (Table XVIII) as compared to the weaker (201) reflection which should be the stronger of the two. Part of the reason for the apparent strength of the (002) reflection must be that it diffracts at the same Bragg angle as does the close-packed (111) plane from the fcc matrix. Many of the extra lines in these patterns could be matched with those of the hcp or fcc Co matrix; however, it is also possible that they are the result of the presence of a transition phase in the lattice. Such a transition phase, accompanying the precipitation of Co_3Mo, has been suggested for the Co-Mo binary system by Bibring and Graf (1961).

The addition of 15 w/o Cr to the Co-4Al-20Mo alloy resulted in the formation of a completely different hardening

phase. In the as-cast condition, the alloy contained a mixture of fcc cobalt solid solution having a parameter a_o = 3.620 Å plus the rhombohedral phase designated by Beck (Rideout and Beck, 1953) as the R phase and having the parameters a = 9.027 Å, α = 74.42° (Table XIX). These values compare with a = 9.011 Å, α = 74.46° found by Komura et al. (1960). Extractions analyzed after solution treatment and aging both contained only the R phase although the lattice parameters after aging at 800°C for 1000 hours had changed slightly to a = 9.092 Å, α = 74.54° (Table XX). No other phases were detected in this quartenary alloy.

5.2.5 The Co-Al-W System

Of all the systems investigated, the Co-Al-W alloys were the most interesting in terms of their precipitation behavior. The expectations were for the formation of an hexagonal Co_3W type compound isotypic with Co_3Mo. In actuality, neither Co_3W nor Co_7W_6 was detected in the residue of the aged 10W and 25W alloys. Instead, the hardening in both alloys resulted from the formation of a cubic Co-W superlattice or precipitate with the Cu_3Au structure. Examination of the aging curves (Figs. 26 and 27) shows that the hardening process is still going on after 1000 hours at temperatures of 800°C and below. This, of course, indicates a very sluggish precipitation reaction. The photomicrographs in Figs. 44 and 45 show the matrix precipitation as a general

darkening only. The scanning electron microscope (Fig. 53) revealed no distinct precipitate even at 10,500 X, but instead showed a uniformly textured matrix. The volume of extracted material for both alloys was very great initially, indicating a large amount of hardening phase. X-ray analyses of these extractions all gave the same major pattern, namely an ordered fcc lattice with a_o varying only between the values of 3.593 to 3.599 Å. A typical pattern is presented in Table XXI. All possible reflection lines were present in this ordered structure. A similar pattern taken from 200 mesh filings of the bulk alloy gave a lattice parameter of 3.597 Å (Table XXII) and was devoid of superlattice lines. Thus, there was no appreciable difference in size between the matrix and the ordered phase. Spectroscopic analyses of the Co-4Al-25W alloy and its extracted residue revealed that the residue contained approximately two-thirds the amount of Al and approximately the same amount of W as did the parent matrix.

If one presumes the possibility of a cubic $Co_3(W,Al)$ type phase similar to those found in the Co-Ta and Co-Nb systems, a reasonable assumption for the length of the Co-(W,Al) bond could be derived from the Co-W bond in the close-packed hexagonal Co_3W where this length in the basal plane is the a parameter divided by 2 or 5.128 ÷ 2 = 2.564 Å. Assuming this distance to be valid for the fcc system gives

$a_o = 2.564\ \sqrt{2} = 3.627$ Å. Considering that the c/a ratio for the hexagonal Co_3W is less than that required for a hard-sphere model and that the diameter of the Al atom is greater than the W atom, the predicted value of 3.627 Å is not too different from the average value of $a_o = 3.595$ Å actually found. To see if the actual compound Co_6WAl existed, a button of this composition was melted. The resulting pattern revealed the presence of Co_7W_6 only.

It is probable, therefore, that the ordered cubic pattern found for the Co-Al-W alloys represents a pre-precipitate or superlattice which is present in the Al stabilized fcc matrix. This stabilization is not difficult to understand if it is noted that on an atomic percent basis, the 25W alloy actually contains more Al than W (10.55 to 9.41 a/o). Since, unlike the other systems investigated, no extraneous lines appeared in any of the x-ray patterns, it is possible that this Cu_3Au type phase is in fact an equilibrium one. Although the Al obviously tended to stabilize the fcc structure in Co, the residue from the 10W alloy aged at 700°C contained an appreciable amount of hexagonal Co along with the cubic phase.

In addition to the hardening phase, each residue sample from the aged 25W alloy contained a small amount of a second Cu_3Au type phase with an average $a_o = 3.971$ Å (Table XXIII). Although its pattern was weak, it was readily

detectable and is probably an impurity of some kind since the lattice parameter could not be matched with any known compound. Although its significance is not apparent, the parameter of this phase decreased from a value of 3.975 Å for the 600°C aging to 3.970 Å at 800°C and 3.968 at 900°C.

As it did in the Co-Mo alloys, the addition of 15 w/o Cr to the Co-4Al-25W alloy completely changed the nature of the precipitate. The as-cast microstructure contained the rhombohedral Co_7W_6 phase (Table XXIV) with the parameters a = 8.984 Å, α = 30.64°. This compares well with Neumeier and Holman's (1967) values of 8.957 Å and 30.67° for Co saturated Co_7W_6. This same Mu phase was also the only one present following aging, although the parameters had changed to a = 8.960 Å, α = 30.68°.

5.3 Summary of Results

The following table (Table IV) lists the various phases found in the different alloy systems under the conditions stated.

In general, all the ternary systems investigated were precipitation hardenable to some extent, although Al additions to the Co-X binaries generally resulted in a decrease in the maximum obtainable hardnesses. The effects of Al were least in the alloys containing Nb and Mo where the phases present were those which could be predicted from the binary diagrams alone. This study did confirm the presence

Table IV - Summary of X-ray Data

Alloy	Conditions	Phases Present
5Nb	600°C/1000 hours	Co_2Nb
	700°C/1000 hours	Cu_3Au phase + Co_2Nb
	800°C/1000 hours	Hexagonal phase + Co_2Nb
	900°C/1000 hours	Co_2Nb
10Nb	700°C/1000 hours	Co_2Nb + Cu_3Au phase
	900°C/1000 hours	Co_2Nb
20Nb	600°C/1000 hours	Co_2Nb
	900°C/1000 hours	Co_2Nb
5Ta	700°C/1000 hours	αCo_3Ta
10Ta	600°C/1000 hours	γCo_2Ta
	800°C/1000 hours	αCo_3Ta
	900°C/1000 hours	αCo_3Ta + γCo_2Ta + βCo_3Ta?
20Ta	600°C/1000 hours	γCo_2Ta
	800°C/1000 hours	αCo_3Ta + γCo_2Ta + βCo_3Ta?
	900°C/1000 hours	αCo_3Ta + γCo_2Ta + βCo_3Ta?
Cr-10Ta	As cast	γCo_2Ta
	Solution treated	γCo_2Ta
	800°C/1000 hours	αCo_3Ta + γCo_2Ta
3Ti	600°C/1000 hours	$AlCo_2Ti$ + unk. cubic
	900°C/1000 hours	$AlCo_2Ti$ + unk. cubic
12Ti	900°C/1000 hours	$AlCo_2Ti$ + unk. cubic

Table IV, Continued

Alloy	Conditions	Phases Present
5Mo	700°C/1000 hours	Co_3Mo
12.5Mo	700°C/1000 hours	Co_3Mo
	800°C/1000 hours	Co_3Mo
20Mo	600°C/1000 hours	Co_3Mo + hcp Co
	800°C/1000 hours	Co_3Mo
	900°C/1000 hours	Co_3Mo
Cr-20Mo	As cast	R phase + fcc Co
	Solution treated	R phase
	800°C/1000 hours	R phase
10W	700°C/1000 hours	Cu_3Au phase + hex Co
25W	600°C/1000 hours	Two Cu_3Au phases
	800°C/1000 hours	Two Cu_3Au phases
	900°C/1000 hours	Two Cu_3Au phases + fcc Co
Cr-25W	As cast	Co_7W_6 + fcc Co
	Solution treated	Co_7W_6
	800°C/1000 hours	Co_7W_6
Co_6WAl	Solution treated	Co_7W_6

of both a hexagonal and a cubic phase, previously reported by other investigators, but not shown on the existing Co-Nb phase diagram. Aluminum additions to the Co-Ti system resulted in the precipitation of ordered bcc $AlCo_2Ti$ instead of the ordered fcc Co_3Ti. This $AlCo_2Ti$ phase was not a stable hardening precipitate. In the Co-Ta system, the presence of Al stabilized the fcc matrix to such an extent that the equilibrium rhombohedral βCo_3Ta only appeared, if at all, after 1000 hours, at which time the major second phase was still fcc αCo_3Ta. Perhaps the greatest deviation from expected behavior occurred in the Co-Al-W alloys where the hardening was very sluggish and where the hardening phase was not Co_3W but instead a superlattice or precipitate which was probably coherent with the matrix. Chromium additions to the ternaries containing Ta, Mo, and W did not improve the hardening behavior of any of these systems, but resulted instead in the formation of brittle R and Mu phases in the Mo and W alloys, respectively.

On an atomic percent basis, Ti additions to the Co-4Al matrix promoted the greatest hardening increase but this increase was also sustained for the shortest time interval due to rapid overaging of the precipitate. Nb and Ta additions were about equally effective in hardening ability; however, these elements were considerably better as solid solution strengtheners than as contributors to precipitation

hardening. The Group VI B elements Mo and W were similar in their hardening effects in that overaging had not yet occurred even after 1000 hours at 800°C for alloys containing 7.7 a/o Mo and 9/4 a/o W. Although, as previously discovered, the mode of hardening was different for the two systems, these elements appeared to be the most useful for strengthening the Co-Al matrix.

5.4 Suggestions for Further Work

Several areas of study appear promising enough to warrant further work. First, it is obvious that Al additions to Co stabilize the fcc structure. Quantitative stacking-fault energy determinations should be made to see how effective Al is compared with other known fcc stabilizers.

This study has confirmed that there are phases existing in the Co-Al-Nb system which are exactly those reported in the Co-Nb system, but not included in published diagrams. Further work should be undertaken to complete the Co rich end of this diagram to determine the equilibrium phases.

It is recognized that equilibrium is very difficult to reach in Co binaries and alloys with the refractory elements. With this in mind, long-time studies of Co-Al-Mo and Co-Al-W alloys should be undertaken to see just how stable these systems are for times over 1000 hours. Perhaps by

optimizing the Al and refractory metal content, a coherent cubic precipitate, such as was found in the Co-Al-W system, might be preserved and optimized, thus forming the basis for a useful alloy.

CHAPTER 6

CONCLUSIONS

Additions of each of the five elements Nb, Ta, Ti, Mo, and W to a Co-4Al matrix resulted in the formation of a precipitation hardenable alloy system. Comparison of the relative hardening effects of each element was difficult because of the wide range of elemental solubilities in the Co-Al matrix and the major differences in their precipitation behavior. Nevertheless, certain conclusions became apparent:

a. On an atomic percent basis, Ta additions resulted in a higher degree of hardening than did additions of the chemically similar Nb. In neither alloy system could overaging be suppressed above 700°C for times up to 1000 hours. The hardening phase in the Co-Al-Nb systems was primarily Co_2Nb whereas in the alloys containing Ta both Co_2Ta and αCo_3Ta were present.

b. The Co-Al-Ti system was very amenable to precipitation hardening especially for alloys with approximately 6 w/o Ti. However, the rapid overaging (prior to 1000 hours even at 600°C) of the $AlCo_2Ti$ precipitate greatly exceeded that of other precipitates studied.

c. Molybdenum, in the form of the precipitate Co_3Mo, proved to be the most potent hardener of the elemental additions studied. High hardnesses were retained even after 1000 hours at 800°C indicating potential usefulness for alloys based upon this system.

d. The least tendency to overage was exhibited by the Co-Al-W system wherein the hardening was attributed to the formation of a cubic Cu_3Au type superlattice. Although the hardnesses were not as high as those attained with the Mo alloys, the apparent stability of the Co-Al-W alloy hardening phenomenon warrants further study of this system.

In the alloys studied, the effects of Al additions depend upon the tendency of this element to stabilize fcc cobalt and therefore to hinder formation of non-cubic precipitates. In this respect, the presence of Al affects the Co-W system to the greatest extent and Co-Mo the least. For example, in the systems containing Ta, the cubic αCo_3Ta is retained in preference to the rhombohedral βCo_3Ta which is the equilibrium phase in the Co-Ta binary system. In alloys with Ti, $AlCo_2Ti$ precipitates rapidly and agglomerates very quickly also. No appreciable changes occur in the Co-Nb system due to the presence of 4 w/o Al.

In contrast to the effect of the Al addition, Cr additions tend to destabilize the fcc Co and thus promote the formation of non-cubic phases in this matrix. Thus, in the

Co-Al-Cr-Mo system, the non-cubic R phase occurs; while in the Co-Al-Cr-W system, the non-cubic Mu phase is the hardening precipitate.

APPENDIX A

OPTICAL AND ELECTRON MICROSCOPY PROCEDURES

1. Optical Metallography

   a. Mechanical Polishing

      (1) The specimens were mounted in bakelite and ground on papers through 600 grit.

      (2) Initial polishing was accomplished on an AB-Microcloth wheel using a 0.3 micron alumina abrasive. This was followed by a final polishing using a similar wheel with 0.05 micron alumina.

      (3) Specimens were then etched with a solution of 60% glycerine, 20% HNO_3 (70%), and 20% HF (48%).

   b. Electropolishing and Etching

      (1) Specimens were ground on papers through 600 grit.

      (2) Polishing was accomplished using a stainless steel cathode in a solution of 60% methanol, 35% ethylene glycol monobutyl ether (butyl cellosolve) and 5% H_2SO_4 (97%).

      (3) Varying polishing parameters were tried for the different alloys but in general a polishing time of 15-30 seconds using approximately 20 volts with a current density of 3 amperes/cm^2 was used.

      (4) Etching reagents varied with the alloys. For many, the solution listed in b.(3) above was

used at 2 volts for 5-10 seconds. In cases where this technique was not successful, etching was often accomplished by electropolishing in an H_2O-5% HCl solution. Where neither of these two was successful, etching was accomplished by immersing the specimen in concentrated HCl, then adding H_2O_2 (30%) dropwise on the specimen until decomposition occurred.

2. Electron Microscopy

   a. Electropolishing was employed in all instances using the technique described above except that the amount of etching was reduced.

APPENDIX B

TABLES OF CHEMICAL ANALYSES AND X-RAY DATA

Table V

Complete Analyses of Alloys

	Co		Al		X		Cr	
Alloy	Wt.%	At.%	Wt.%	At.%	Wt.%	At.%	Wt.%	At.%
5Ta	91.3	89.9	4.0	8.6	4.7	1.5	-	-
10Ta	85.8	87.3	4.2	9.4	10.0	3.3	-	-
15Ta	80.8	85.1	4.2	9.7	15.0	5.1	-	-
20Ta	75.6	82.6	4.3	10.2	20.1	7.2	-	-
5Nb	90.8	88.0	4.2	9.0	5.0	3.1	-	-
10Nb	85.8	84.6	4.3	9.2	10.0	6.3	-	-
15Nb	81.[illegible]	81.3	4.2	9.2	14.8	9.5	-	-
20Nb	75.[illegible]	77.5	4.3	9.5	20.1	13.0	-	-
3Ti	92.5	87.5	4.2	8.7	3.3	3.[illegible]	-	-
6Ti	89.8	84.4	4.2	8.7	5.9	6.9	-	-
9Ti	86.8	81.0	4.3	8.7	9.0	10.3	-	-
12Ti	82.7	77.8	4.2	8.6	11.[illegible]	13.7	-	-
5Mo	90.7	88.1	4.2	8.9	5.1	3.0	-	-
12.5Mo	83.2	83.1	4.2	9.2	12.5	7.7	-	-
20Mo	75.9	78.0	4.2	9.5	19.8	12.5	-	-
10W	85.6	87.2	4.3	9.5	10.1	3.3	-	-
25W	70.8	80.0	4.3	10.6	26.0	9.4	-	-
Cr-10Ta	70.7	70.6	4.2	9.1	10.2	3.3	15.0	17.0
Cr-20Mo	60.8	61.3	4.2	9.3	20.0	12.4	15.0	17.1
Cr-25W	55.5	61.6	4.2	10.2	24.9	8.9	15.4	19.4

Table VI

Analyses of Raw Materials

	Co	Al	Nb	Ta	Mo	W	Cr	Ti
Co	99.94							
Al		99.9						
Nb			99.7					
Ta				99.9				
Mo					99.9	0.01		
W						99.79		
Cr							99.999	0.085
Ti								99.73
Ni	0.036							
Cu	0.002					0.01		
C	0.004							0.011
Fe	0.003					0.01		0.045
S	0.0009					0.005		
Si	0.001							0.014
O						0.04		0.065
Mn	0.0003							0.008
P	0.0003							
Pb	0.0001							
Zn	0.002							
Mg								0.038

Table VII

Co_2Nb Phase, Co-4Al-20Nb (900°C/1000 Hours)

h k l	d (Å)	Intensity
006	2.612	w+
105	2.465	w
110	2.367	m
106	2.178	s-
200	2.048	vw
114	2.019	vs
202	1.982	m
008	1.931	w
203	1.905	w
204	1.811	vw
108	1.746	vw
109	1.573	w
10.10	1.446	vw
215	1.387	vw
300	1.369	vw
10.11	1.343	vw
216	1.330	w+
304	1.289	w+
217	1.269	vw
20.10	1.236	w+
220	1.186	w+
20.11	1.160	vw
21.11	1.042	w
228	1.011	w

Hexagonal

$a = 4.737 \pm .017$ Å

$c = 15.494 \pm .056$ Å

$c/a = 3.271$

w - weak
m - medium
s - strong
v - very

Table VIII

Co_2Nb Phase, Co-4Al-5Nb (900°C/1000 Hours)

h k l	d (Å)	Intensity
006	2.572	w
105	2.462	vw
110	2.372	s-
106	2.182	m
114	2.021	vs
202	1.984	m
008	1.932	m-
203	1.910	w
300	1.369	w
216	1.330	w+
304	1.291	m
20.10	1.235	w
220	1.187	m
21.11	1.042	w
228	1.012	w+

Hexagonal

a = 4.751±.003 Å

c = 15.471±.010 Å

c/a = 3.257

Table IX

Cubic Phase, Co-4Al-5Nb (700°C/1000 Hours)

h k l	d (Å)	Intensity	
110	2.590	vw	
111	2.097	vs	
200	1.825	vw	
210	1.631	vw	
220	1.298	w+	Cubic
221	1.219	vw	$a_o = 3.655 \pm .020$ Å
310	1.158	vw	
311	1.104	m-	
222	1.049	w	

Table X

Hexagonal Phase, Co-4Al-5Nb (800°C/1000 Hours)

h k l	d (Å)	Intensity
110	2.970	w
200	2.572	w
201	2.403	s
003	2.292	s
112	2.230	vw
103	2.089	w
202	2.042	vs
210	1.931	m
220	1.485	w
311	1.396	w
222	1.360	w
400	1.288	vw
115	1.237	w
402	1.201	m
321	1.169	w+
006	1.140	vw

Hexagonal

$a = 6.038 \pm .060$ Å

$c = 6.923 \pm .069$ Å

$c/a = 1.147$

Table XI

Cubic Phase, Co-4Al-10Nb (700°C/1000 Hours)

h k l	d (Å)	Intensity	
110	2.590	w	
111	2.093	vs	
210	1.629	vw	
220	1.298	m+	Cubic
221	1.219	w	$a_o = 3.655 \pm .023$ Å
310	1.158	vw	
311	1.104	s	
222	1.049	vw	

Table XII

γCo_2Ta Phase, Co-4Al-10Ta (600°C/1000 Hours)

h k l	d (Å)	Intensity
006	2.615	vw
105	2.468	w
110	2.370	m+
106	2.184	m+
114	2.021	vs
202	1.986	m
107	1.949	w
008	1.933	w+
203	1.908	w
204	1.814	vw
10.10	1.445	vw
215	1.387	w
300	1.369	w+
216	1.330	m-
304	1.290	m-
217	1.271	vw
20.10	1.235	w+
220	1.186	w+
20.11	1.160	w
21.11	1.042	w
228	1.012	w

Hexagonal

$a = 4.754 \pm .007$ Å

$c = 15.503 \pm .024$ Å

$c/a = 3.261$

Table XIII

αCo_3Ta Phase, Co-4Al-10Ta (800°C/1000 Hours)

h k l	d (Å)	Intensity
100	3.653	m
110	2.581	m
111	2.109	vs
200	1.826	s
210	1.631	w
211	1.489	vw
220	1.289	w+
221	1.215	vw
310	1.152	vw
311	1.099	m-
222	1.052	w
320	1.011	vw
321	0.974	vw

Cubic

$a_o = 3.644 \pm .001$ Å

Table XIV

γCo_2Ta Phase, Co-4Al-15Cr-10Ta (As Cast)

h k l	d (Å)	Intensity
101	4.084	w
004	3.818	vw
102	3.609	w
104	2.804	w
110	2.367	vs
106	2.174	s
200	2.053	w+
114	2.017	vs
202	1.982	s
008	1.918	w
204	1.811	vw
108	1.742	vw
10.10	1.442	w
300	1.370	w+
216	1.329	m
304	1.291	w+
20.10	1.233	w+
220	1.188	m
20.12	1.095	w
21.11	1.044	w+
228	1.012	w

Hexagonal

$a = 4.764 \pm .011$ Å

$c = 15.503 \pm .034$ Å

$c/a = 3.254$

Table XV

αCo_3Ta Phase, Co-4Al-15Cr-10Ta (800°C/1000 Hours)

h k l	d (Å)	Intensity	
100	3.621	w	
110	2.560	w	
111	2.089	vs	Cubic
200	1.816	w	$a_o = 3.659 \pm .004$ Å
210	1.624	w	
311	1.099	w	

Table XVI

$AlCo_2Ti$ Phase, Co-4Al-12Ti (900°C/1000 Hours)

h k l	d (Å)	Intensity	
111	3.368	vw	
200	2.918	w	
220	2.063	vs	
311	1.760	vw	
222	1.683	vw	
400	1.458	m-	Cubic
331	1.337	vw	$a_o = 5.845 \pm .004$ Å
420	1.304	vw	
422	1.191	s	
115	1.123	vw	
440	1.032	m	
135	0.987	vw	

Table XVII

Cubic Phase, Co-4Al-12Ti (900°C/1000 Hours)

h k l	d (Å)	Intensity	
110	2.278	w	
200	1.610	vw	Cubic
211	1.315	vw	$a_o = 3.226$ Å
220	1.139	vw	
310	1.019	vw	

Table XVIII

Co_3Mo Phase, Co-4Al-20Mo (900°C/1000 Hours)

h k l	d (Å)	Intensity
101	3.004	w
110	2.533	w+
200	2.210	w
002	2.053	vvs
201	1.950	s
102	1.845	w
210	1.667	vw
112	1.604	vw
211	1.550	w
202	1.507	w+
301	1.384	vw
103	1.306	m
220	1.280	w+
310	1.229	vw
113	1.209	vw
302	1.200	vw
311	1.183	vw
203	1.167	m
400	1.115	w
222	1.088	w+
401	1.072	w
004	1.031	m-
104	1.001	vw
402	0.977	vw
410	0.970	vw
114	0.952	w
411	0.942	vw

Hexagonal

a = 5.124±.006 Å

c = 4.107±.005 Å

c/a = .802

Table XIX

R Phase, Co-4Al-15Cr-20Mo (As Cast)

h k l*	d (Å)	Intensity
131	2.590	w
401	2.332	m
134	2.299	w+
042	2.285	w
306	2.239	w
217	2.169	m
315	2.157	m
232	2.105	m
410	2.065	s
045	2.030	m
128	2.005	s
324	1.984	vs
413	1.957	w
10.10	1.884	w+
502	1.863	w
309	1.770	w
526	1.363	vw
704	1.297	w
00.15	1.291	vw
12.14	1.284	vw
710	1.249	w
618	1.234	w+
31.14	1.223	w

*hexagonal indices

Hexagonal

$a = 10.918 \pm .158$ Å

$c = 19.386 \pm .280$ Å

$c/a = 1.776$

Rhombohedral

$a_R = 9.027$ Å

$\alpha = 74.42°$

Table XX

R Phase, Co-4Al-15Cr-20Mo (800°C/1000 Hours)

h k l*	d (Å)	Intensity
131	2.603	vw
312	2.525	vw
027	2.393	vw
401	2.335	w
134	2.289	vw
306	2.250	w
217	2.169	vs
315	2.161	vs
404	2.124	m
232	2.109	s
410	2.059	s
045	2.006	m+
128	1.989	m+
324	1.969	m
413	1.954	m
10.10	1.884	w+
502	1.848	w
309	1.772	w
416	1.732	vw
526	1.367	w+
20.14	1.322	w
12.14	1.284	w
609	1.271	w
41.12	1.266	w
710	1.249	w
618	1.234	w+
541	1.208	w
627	1.184	w

*hexagonal indices

Hexagonal

$a = 11.011 \pm .090$ Å

$c = 19.500 \pm .160$ Å

$c/a = 1.770$

Rhombohedral

$a_R = 9.092$ Å

$\alpha = 74.54°$

Table XXI

Cubic Phase, Co-4Al-25W (800°C/1000 Hours)

h k l	d (Å)	Intensity
100	3.555	vw
110	2.522	w
111	2.063	vs
200	1.789	m+
210	1.601	vw
211	1.462	vw
220	1.267	m
310	1.135	vw
311	1.082	s
222	1.037	w+
320	0.996	w
321	0.960	w

Cubic

$a_o = 3.593 \pm .001$ Å

Table XXII

FCC Co Matrix, Co-4Al-25W (800°C/1000 Hours)

h k l	d (Å)	Intensity
111	2.066	vs
200	1.805	w+
220	1.269	w
311	1.085	w+
222	1.038	vw

Cubic

$a_o = 3.597$ Å

Table XXIII

Cubic Phase, Co-4Al-25W (900°C/1000 Hours)

h k l	d (Å)	Intensity	
100	3.954	vw	
110	2.797	vw	
111	2.285	m	Cubic
200	1.979	m	$a_o = 3.968 \pm .0003$ Å
220	1.400	vw	
311	1.195	w	

Table XXIV

Co_7W_6 Phase, Co-4Al-15Cr-25W (As Cast)

h k l*	d (Å)	Intensity
222	4.241	vw
100	4.037	vw
211	3.450	vw
$10\bar{1}$	2.370	vs
210	2.289	w+
433	2.169	m+
444	2.128	vw
321	2.074	vs
$\bar{1}11$	2.044	m-
344	2.021	m-
022	1.954	w
311	1.905	w
432	1.816	vw
244	1.598	vw
310	1.506	vw
$\bar{2}11$	1.368	m-
532	1.326	w+
411	1.302	w+
245	1.290	w
466	1.260	vw
765	1.218	w
$20\bar{2}$	1.185	m-
876	1.087	m-
145	1.040	w+
$\bar{2}22$	1.023	w
256	0.987	vw

*rhombohedral indices

Rhombohedral

$a_R = 8.984 \pm .037$ Å

$\alpha = 30.64 \pm .01°$

Hexagonal

$a = 4.748 \pm .005$ Å

$c = 25.667 \pm .025$ Å

$c/a = 5.406$

APPENDIX C

HEAT TREATMENT CURVES

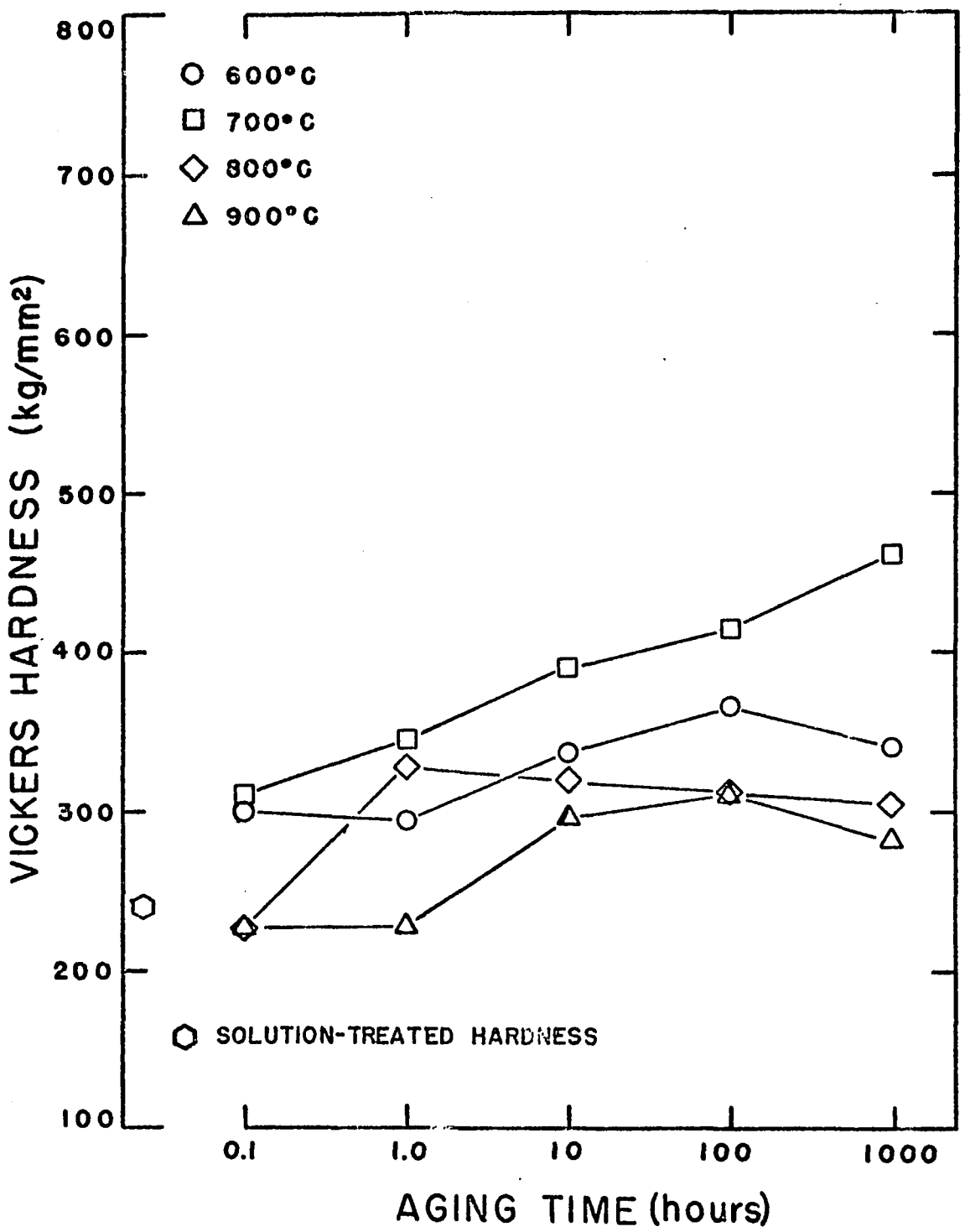

Fig. 11. Aging Curves for Co-4Al-5Nb

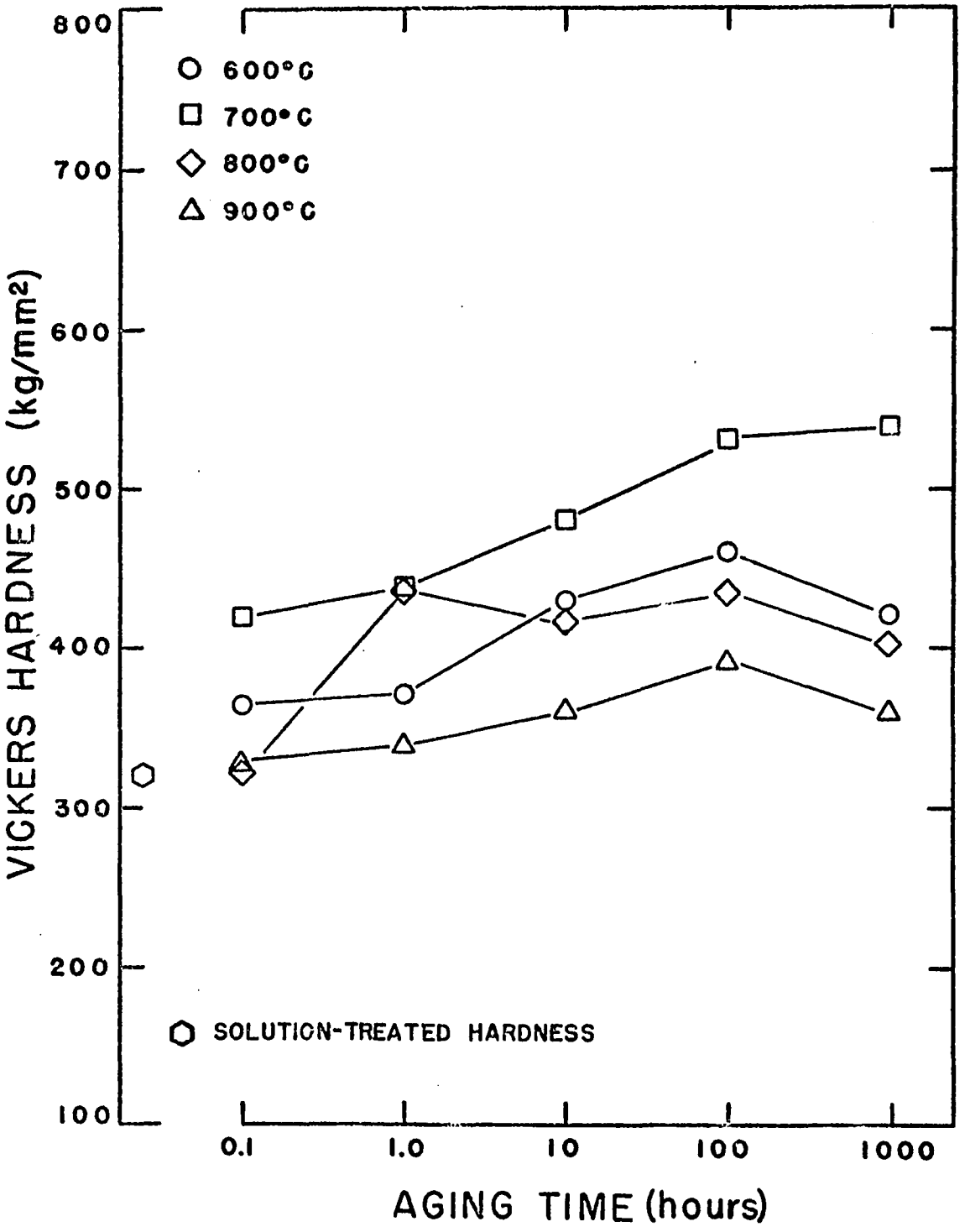

Fig. 12. Aging Curves for Co-4Al-10Nb

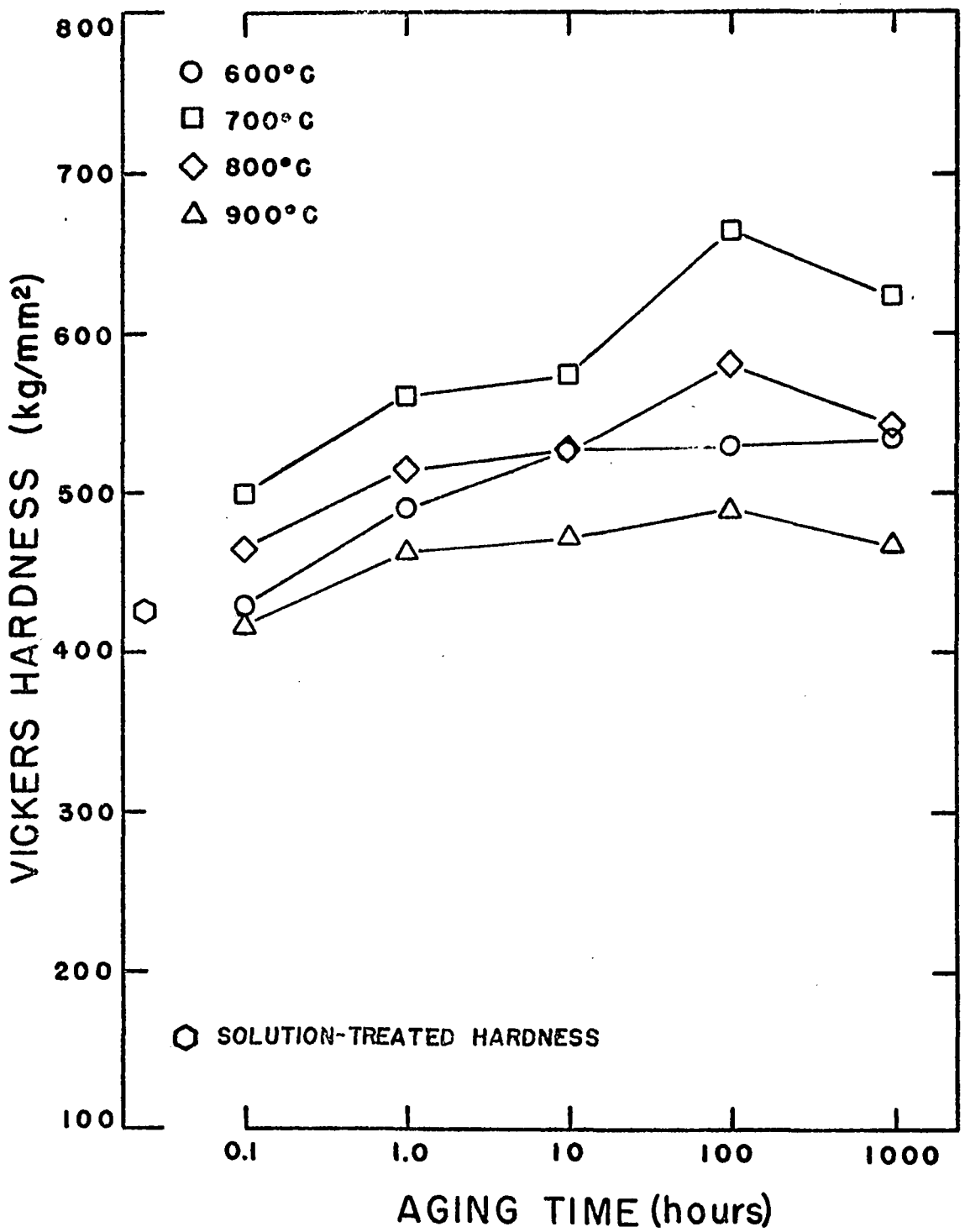

Fig. 13. Aging Curves for Co-4Al-15Nb

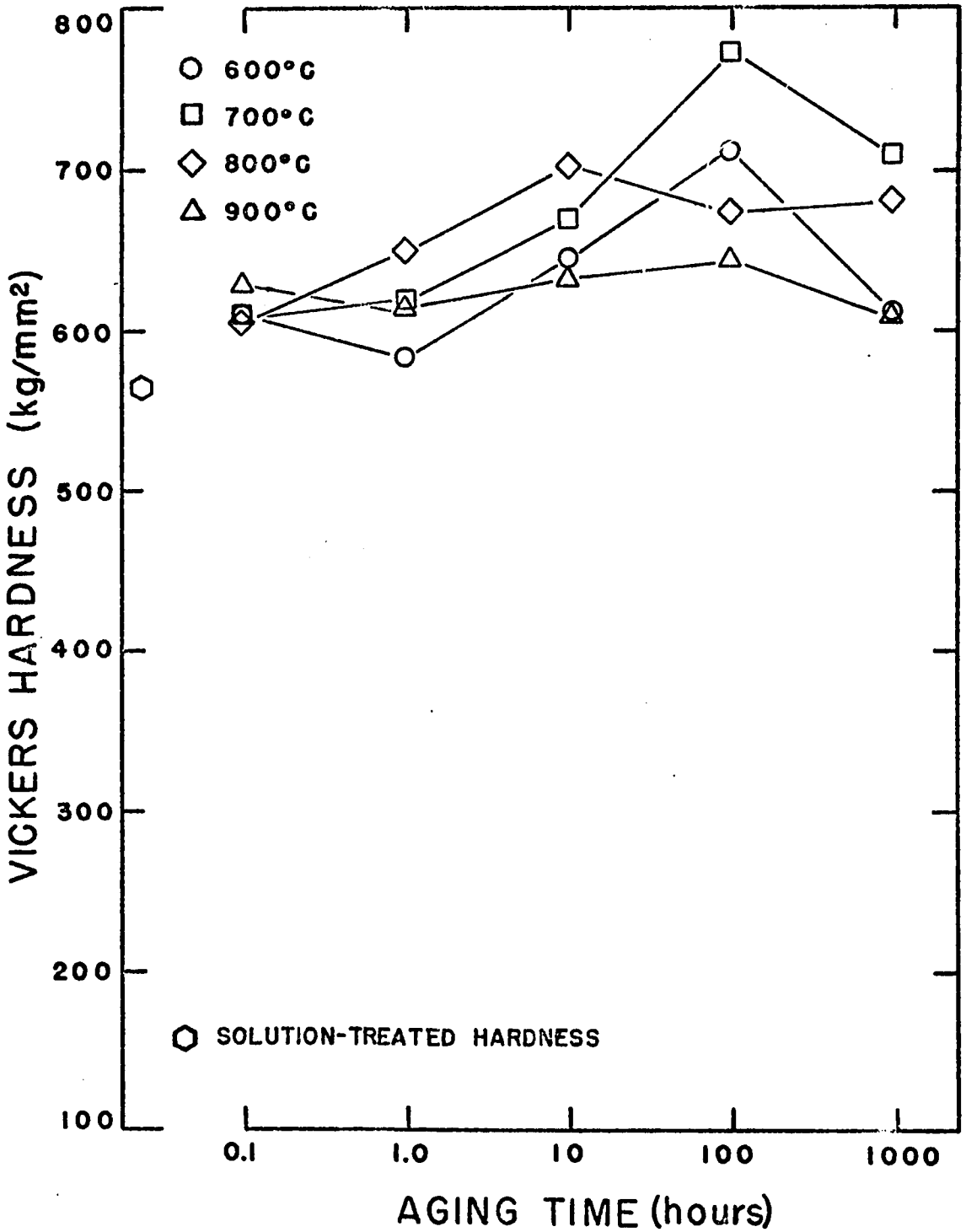

Fig. 14. Aging Curves for Co-4Al-20Nb

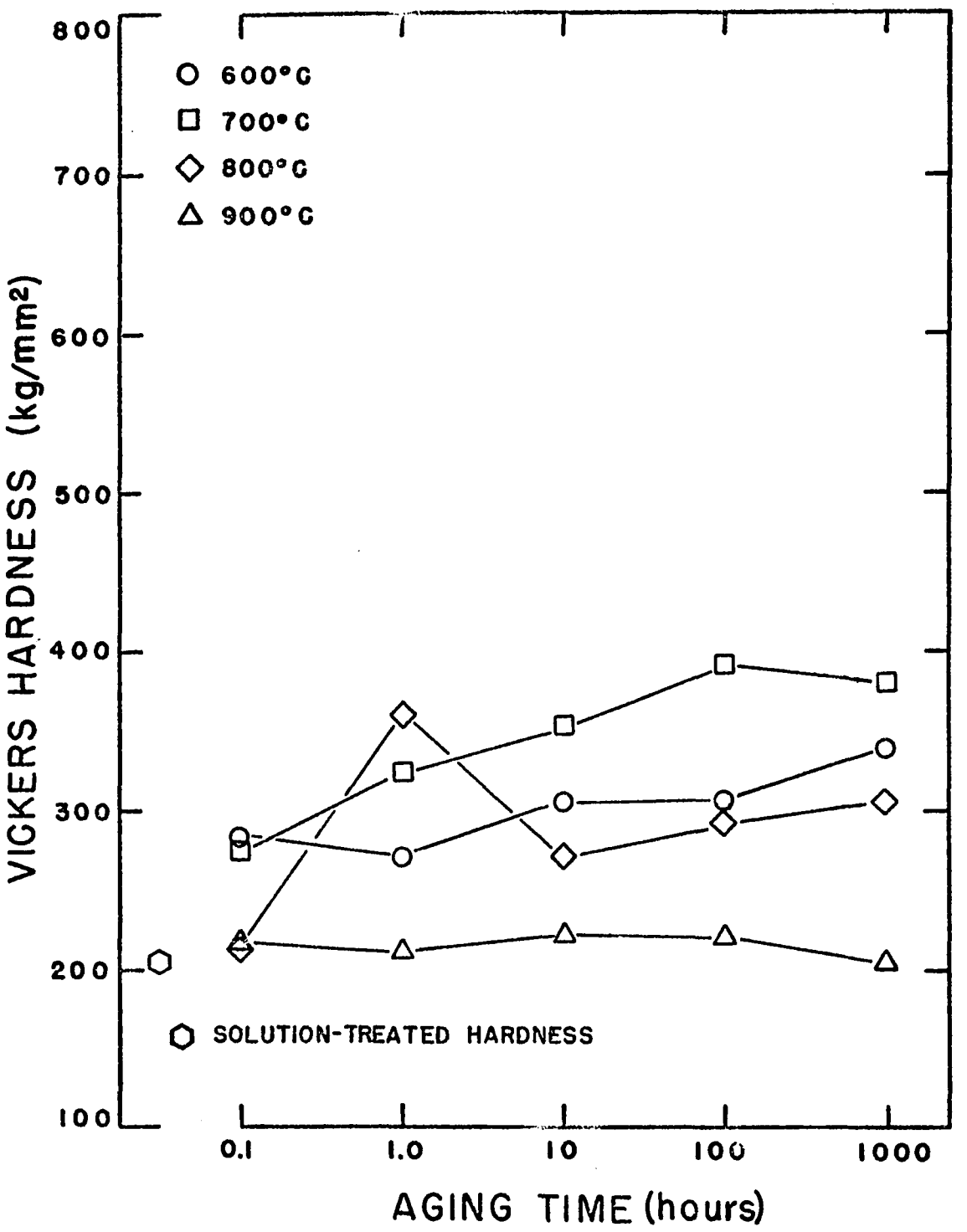

Fig. 15. Aging Curves for Co-4Al-5Ta

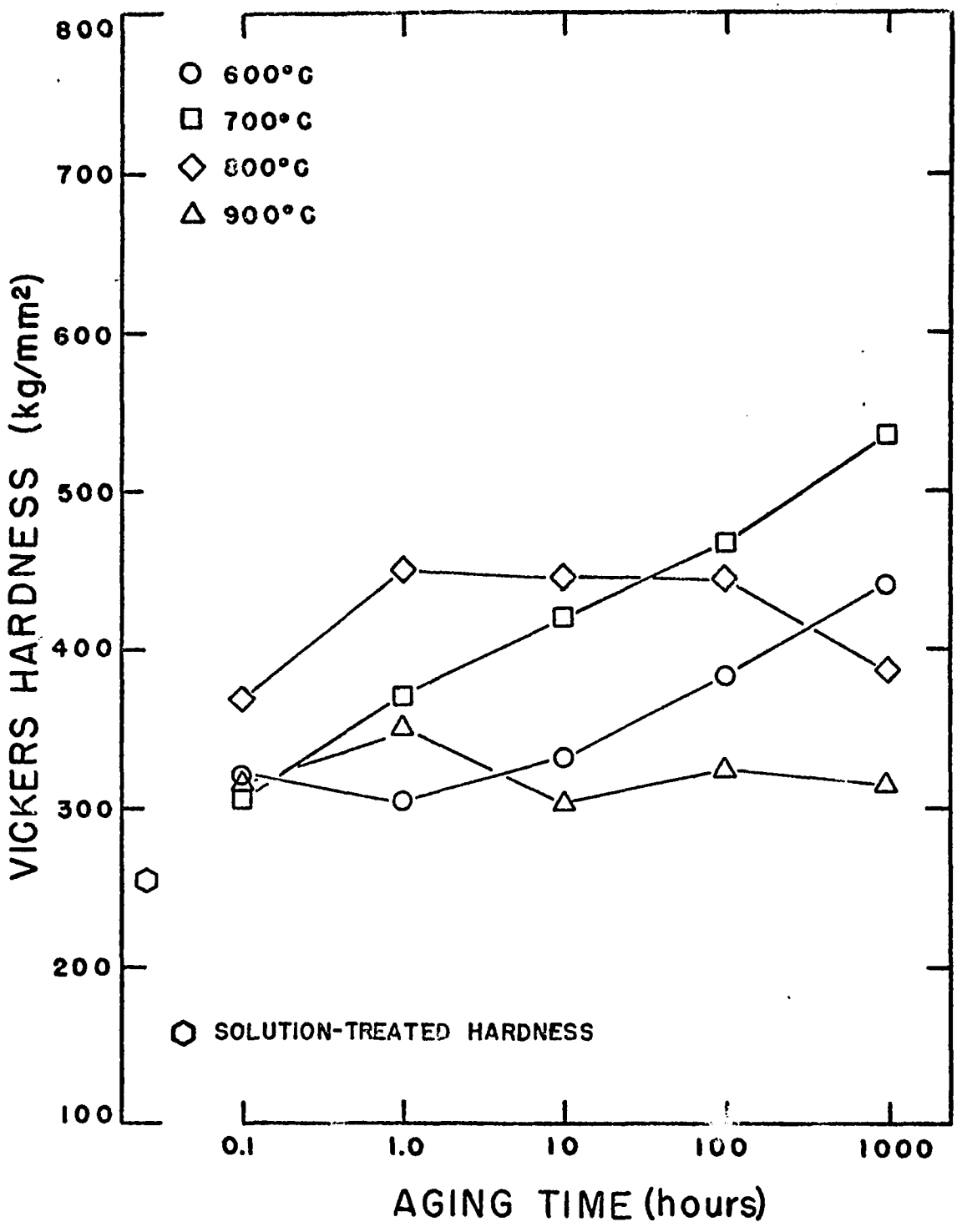

Fig. 16. Aging Curves for Co-4Al-10Ta

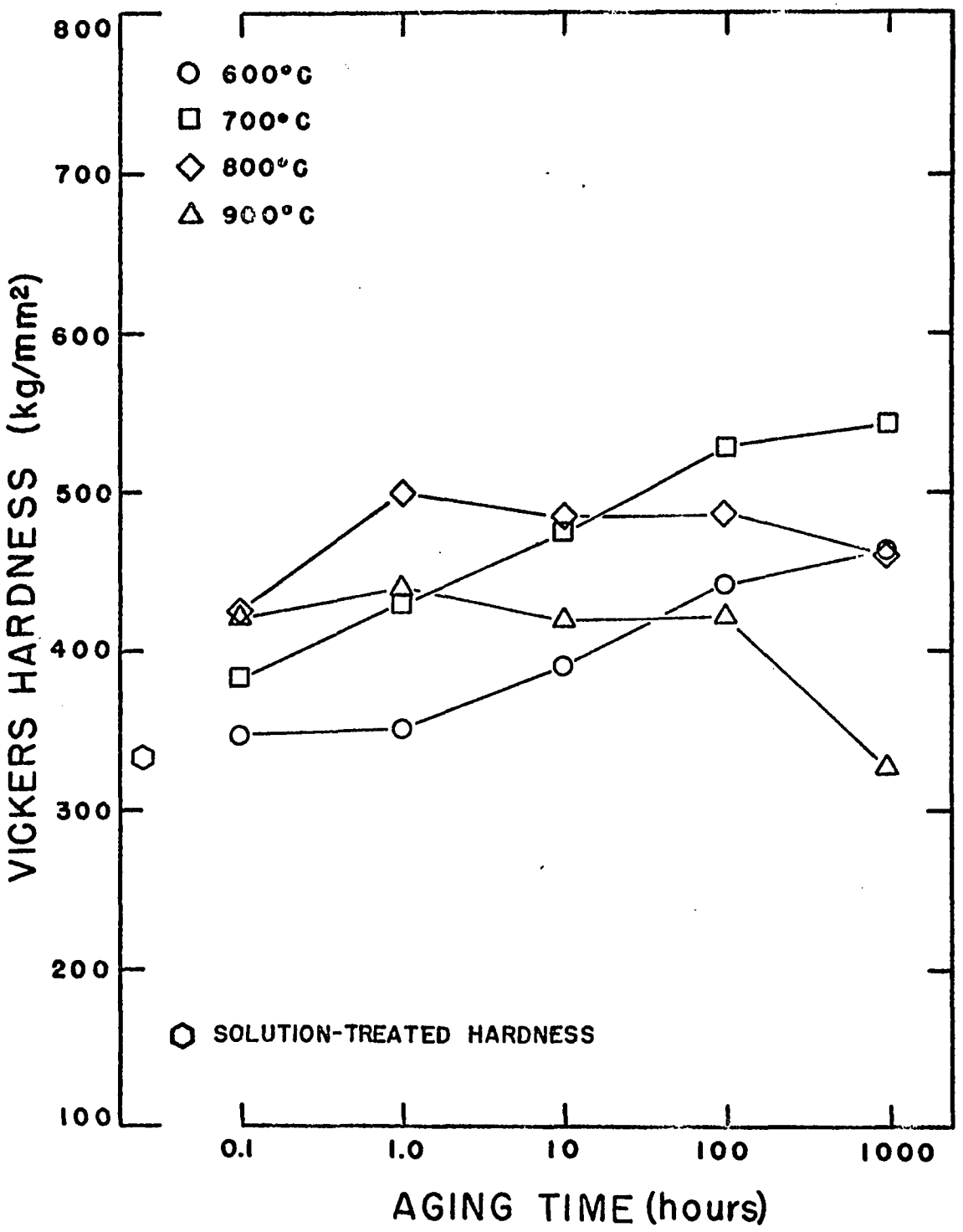

Fig. 17. Aging Curves for Co-4Al-15Ta

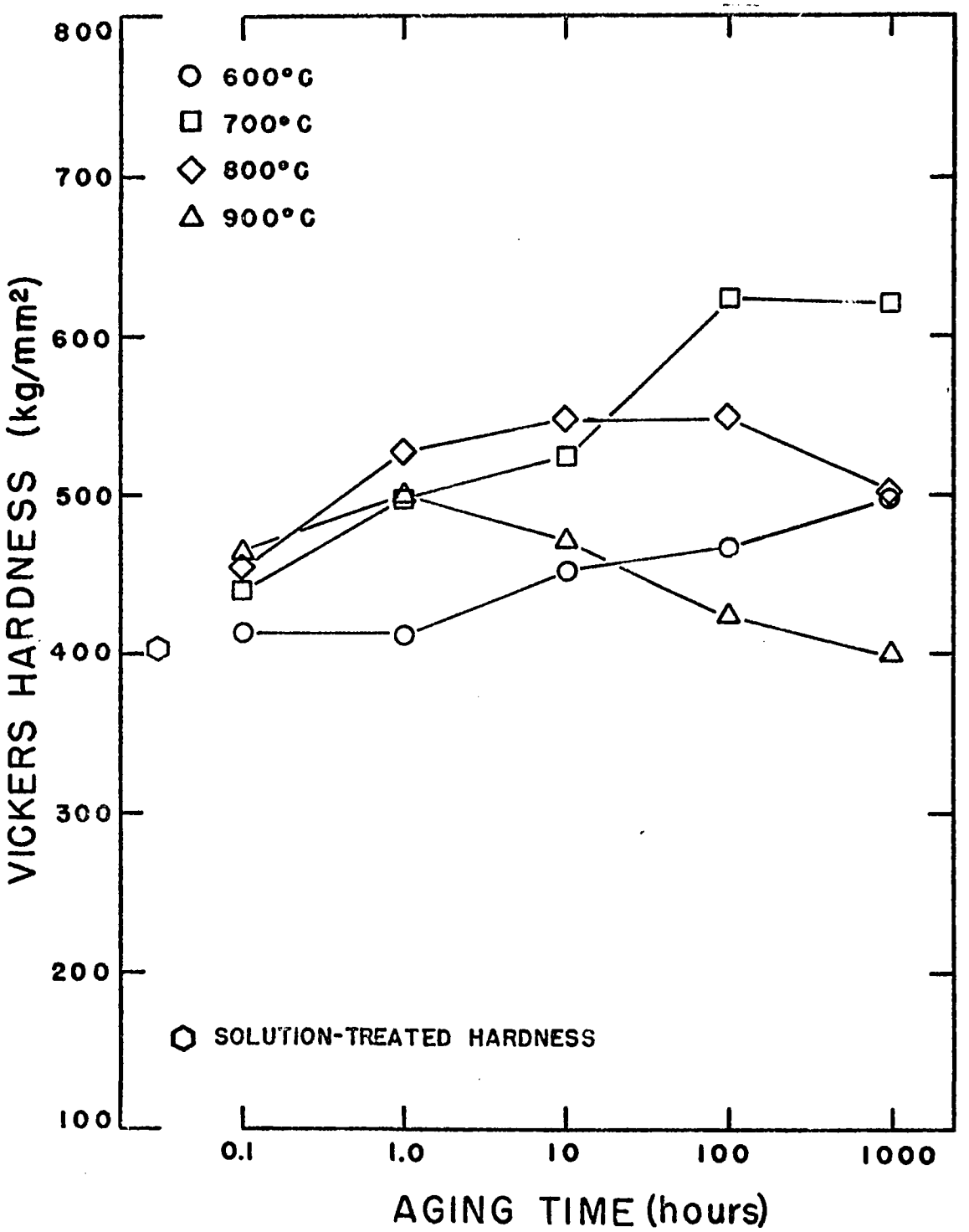

Fig. 18. Aging Curves for Co-4Al-20Ta

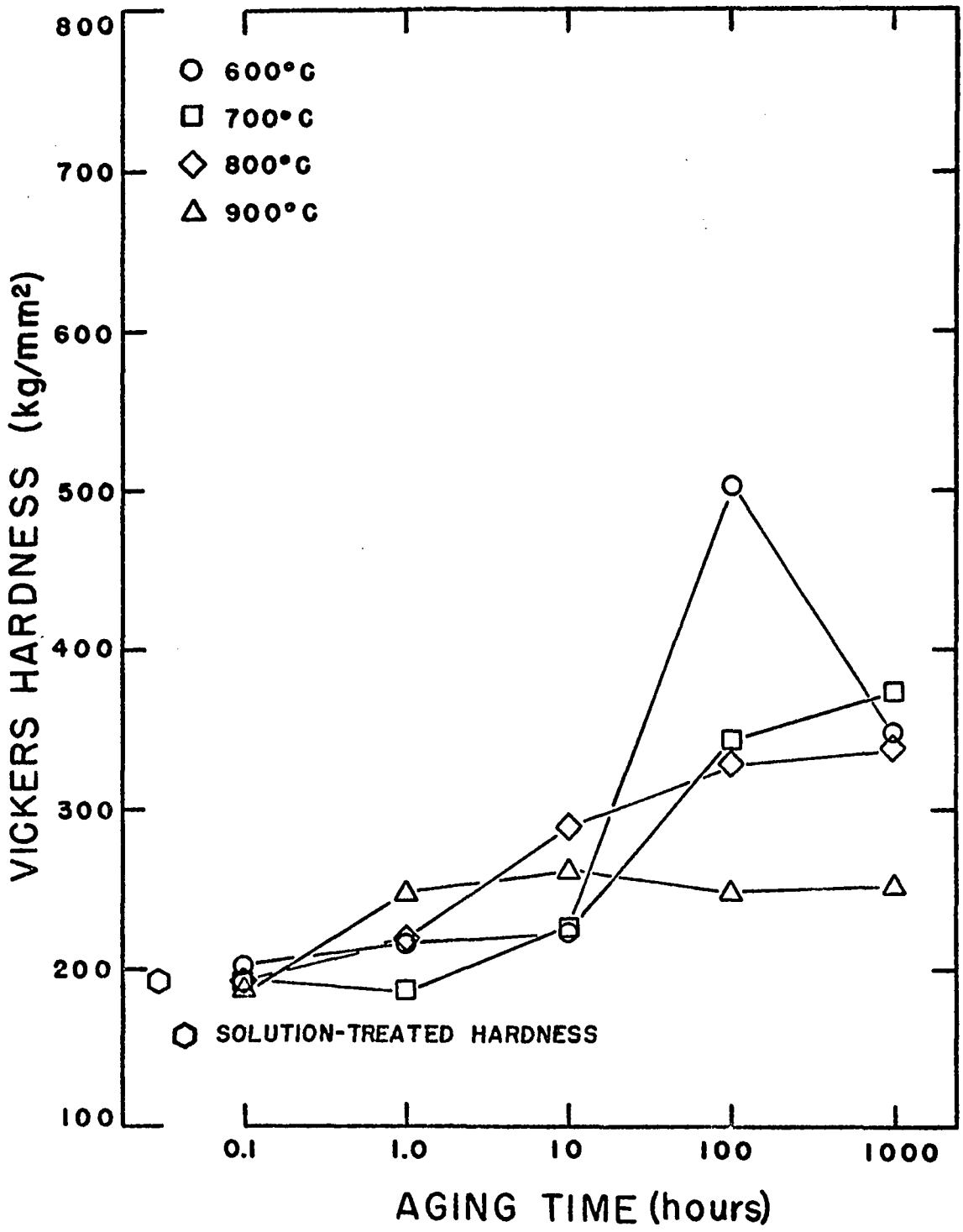

Fig. 19. Aging Curves for Co-4Al-3Ti

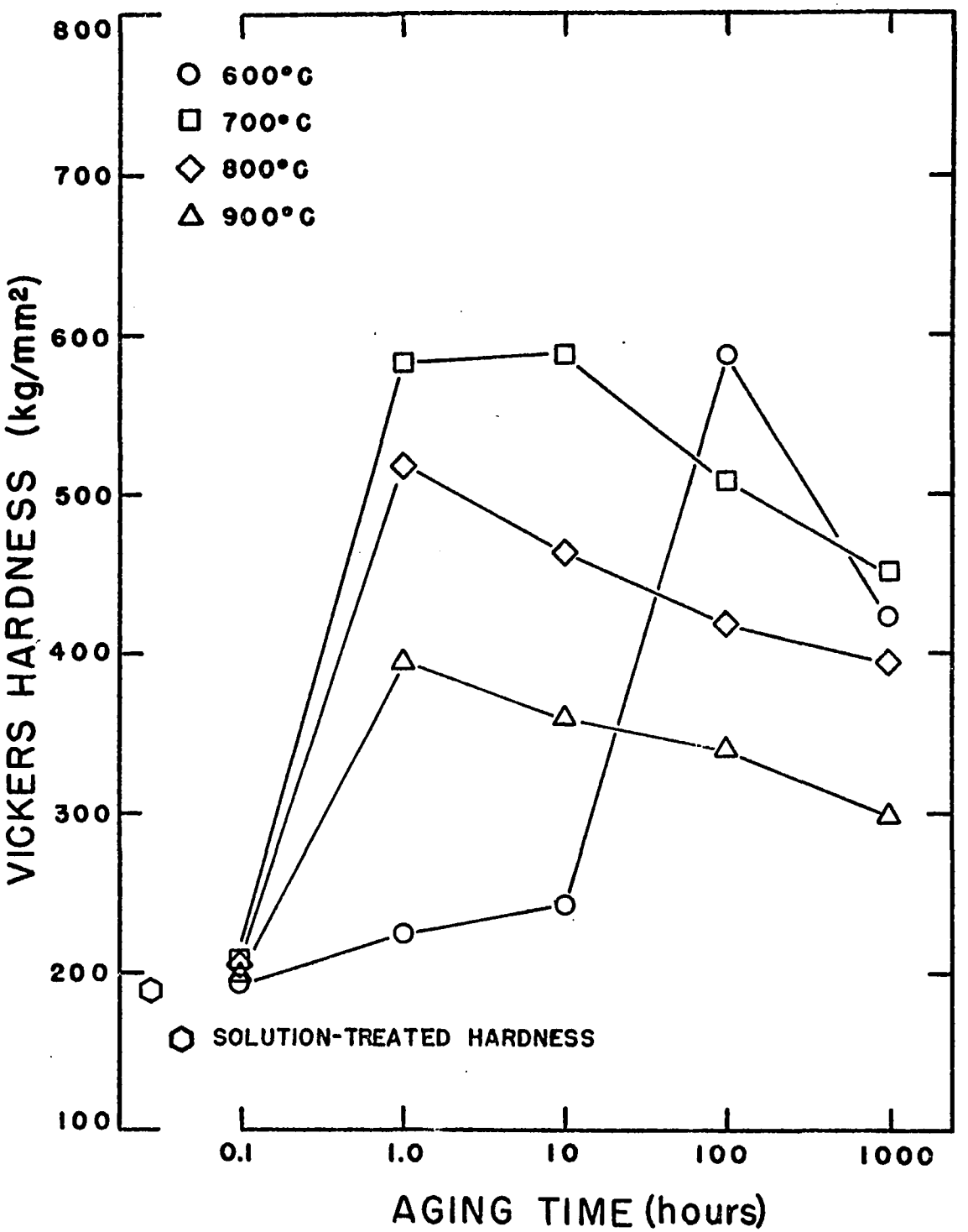

Fig. 20. Aging Curves for Co-4Al-6Ti

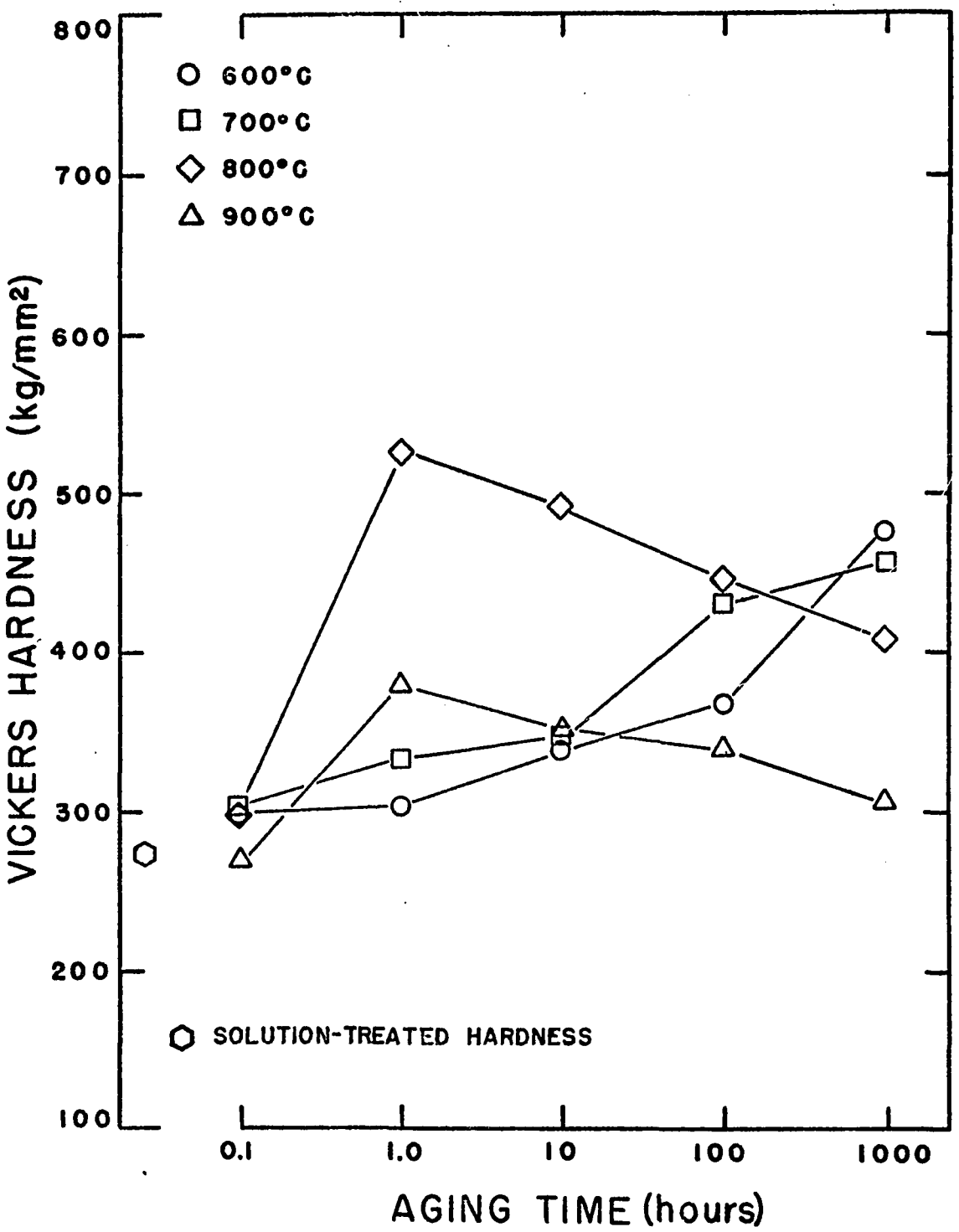

Fig. 21. Aging Curves for Co-4Al-9Ti

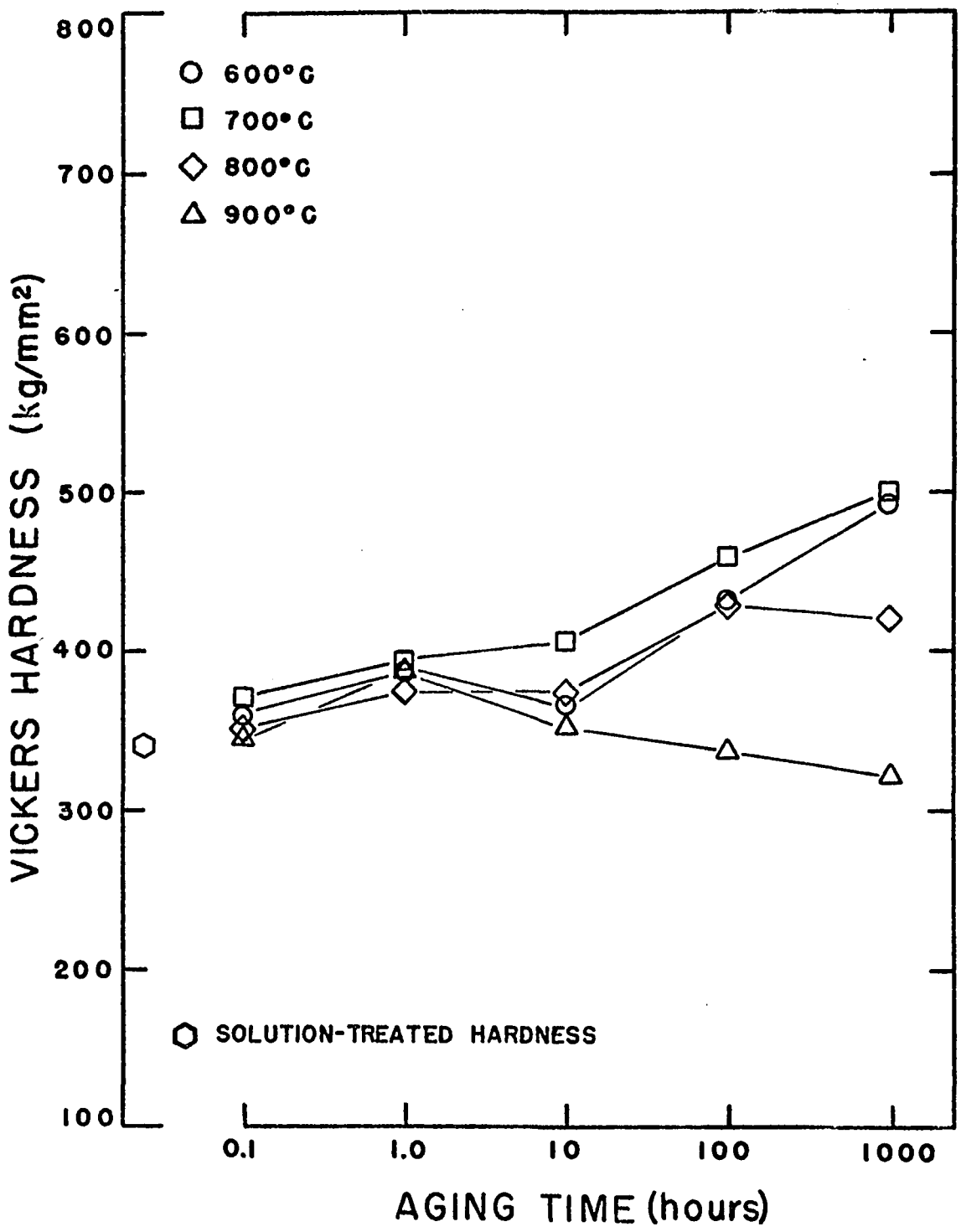

Fig. 22. Aging Curves for Co-4Al-12Ti

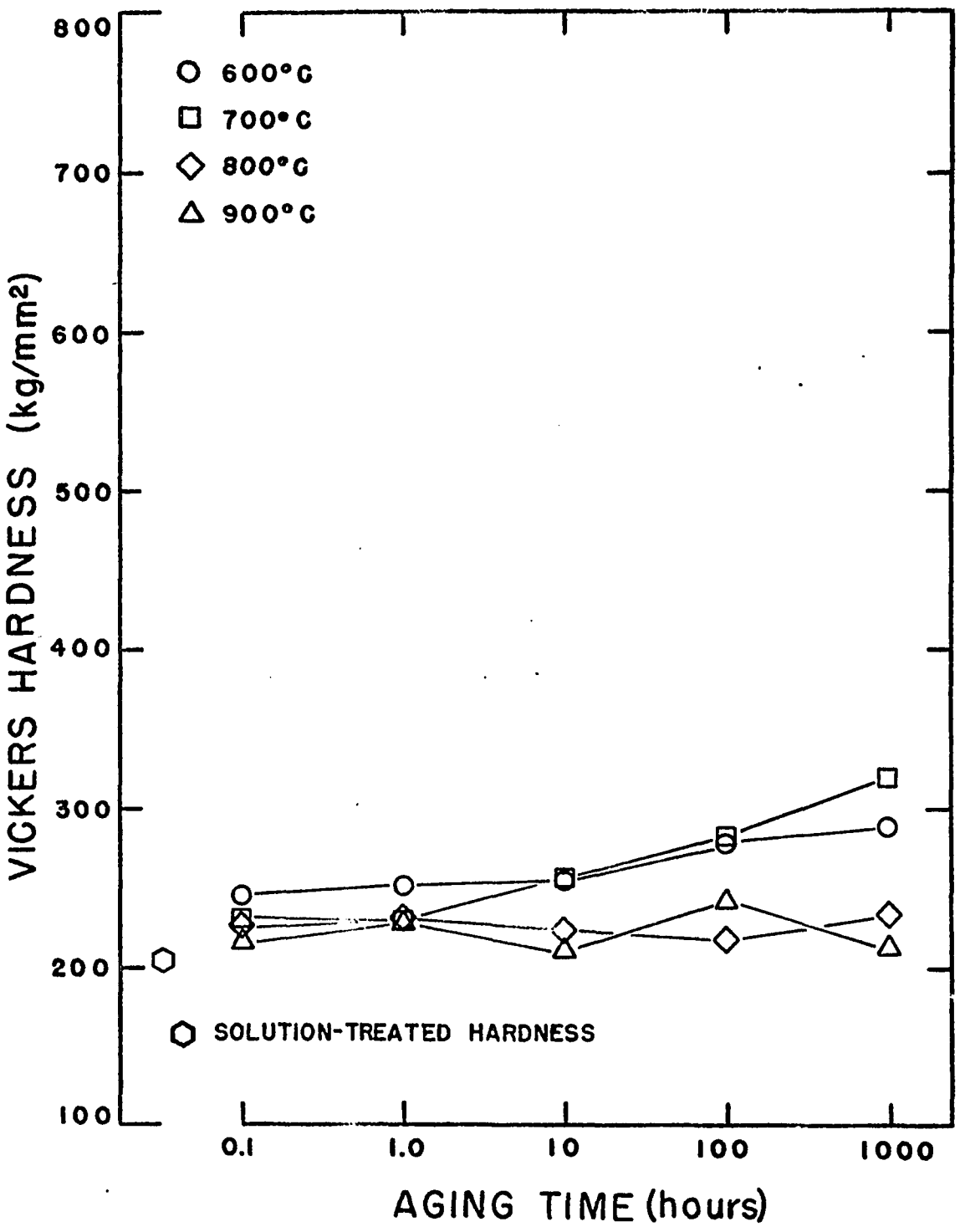

Fig. 23. Aging Curves for Co-4Al-5Mo

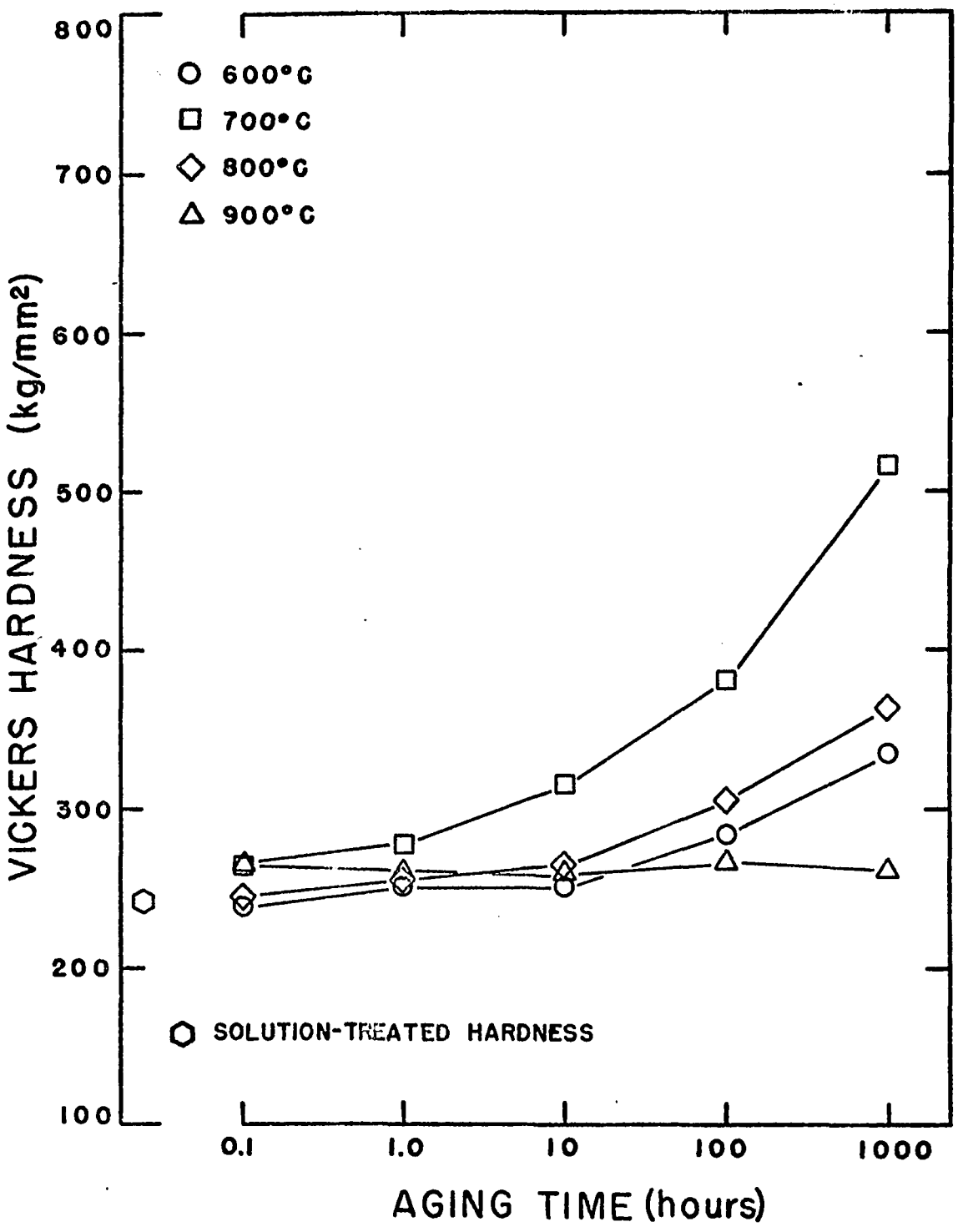

Fig. 24. Aging Curves for Co-4Al-12.5Mo

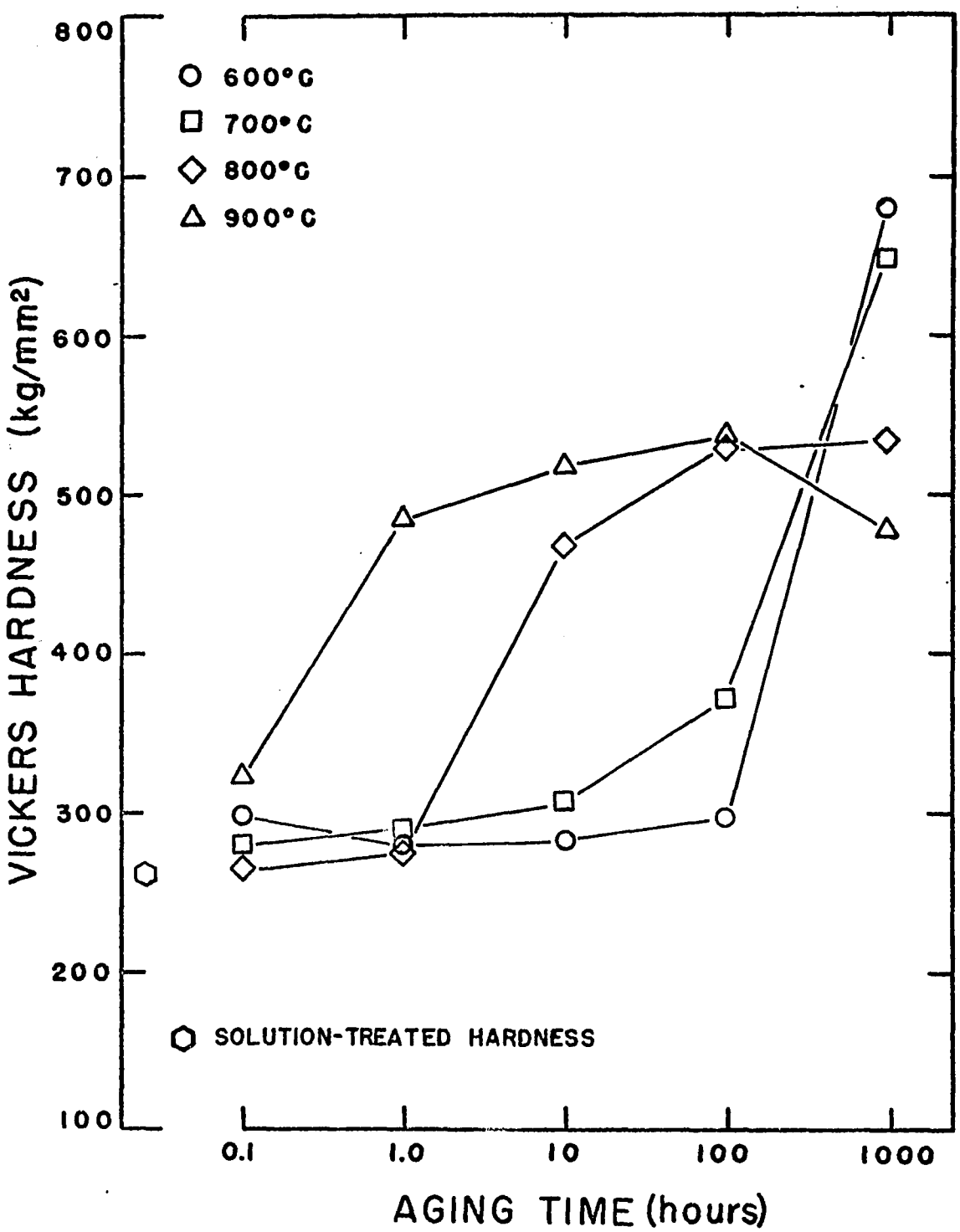

Fig. 25. Aging Curves for Co-4Al-20Mo

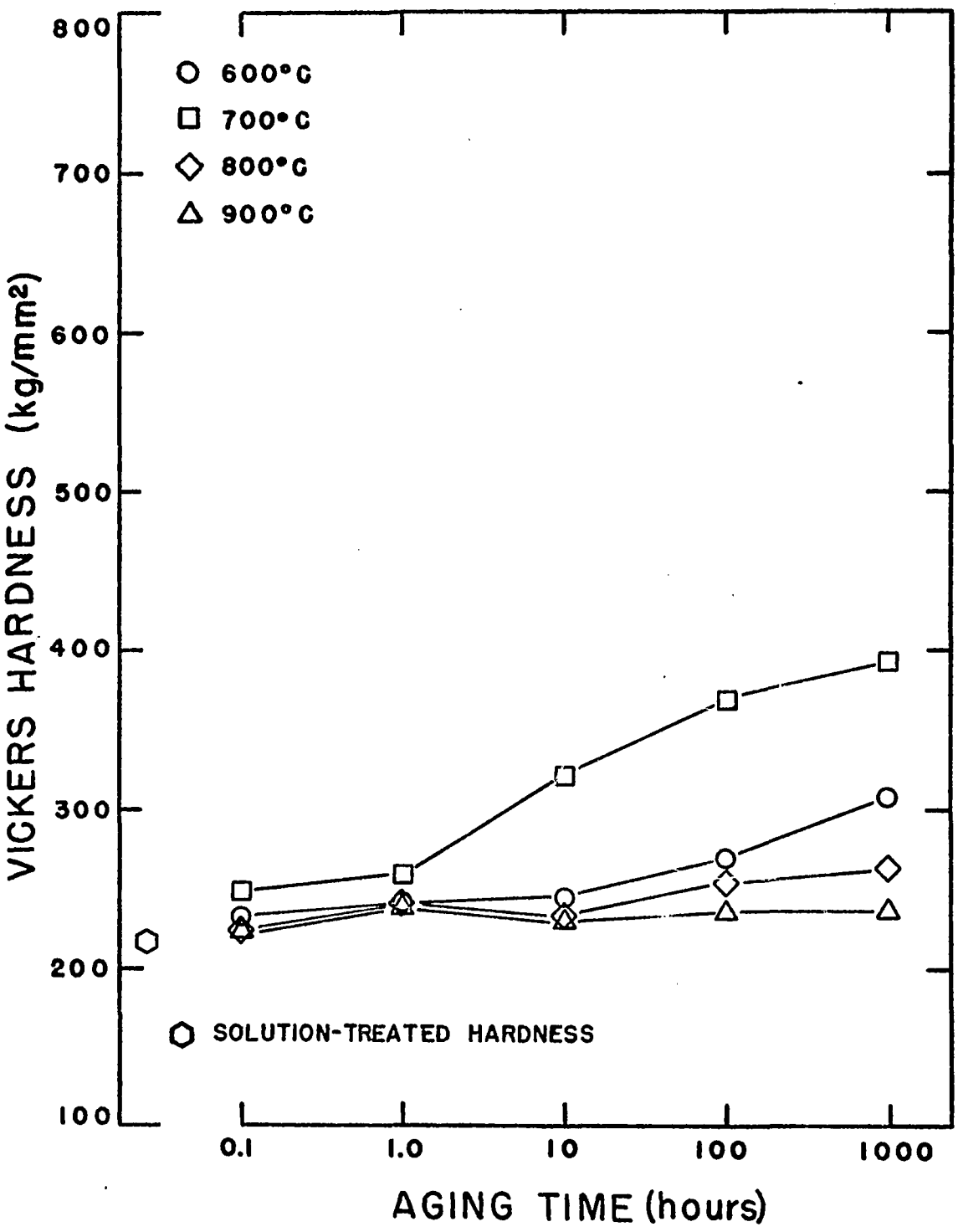

Fig. 26. Aging Curves for Co-4Al-10W

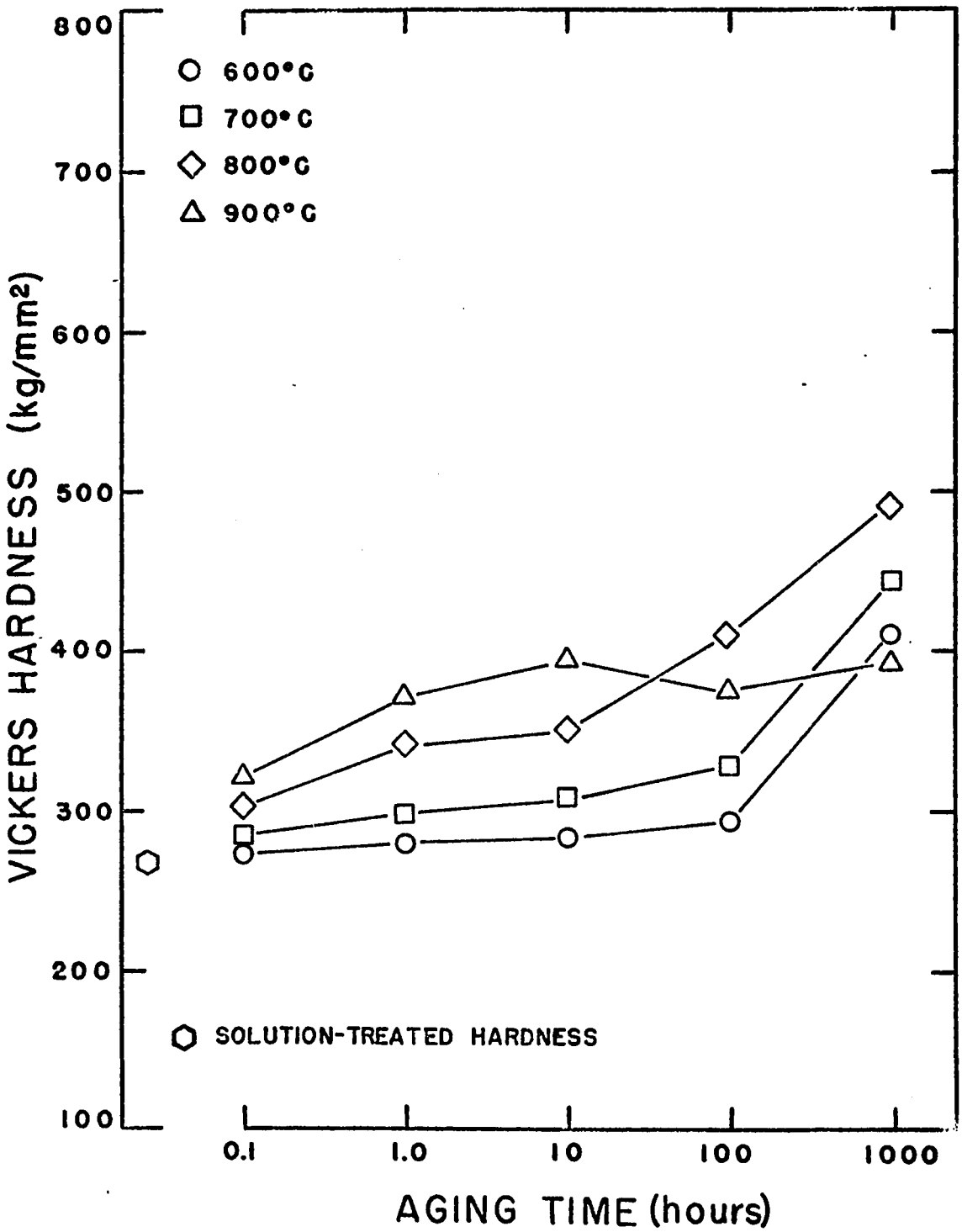

Fig. 27. Aging Curves for Co-4Al-25W

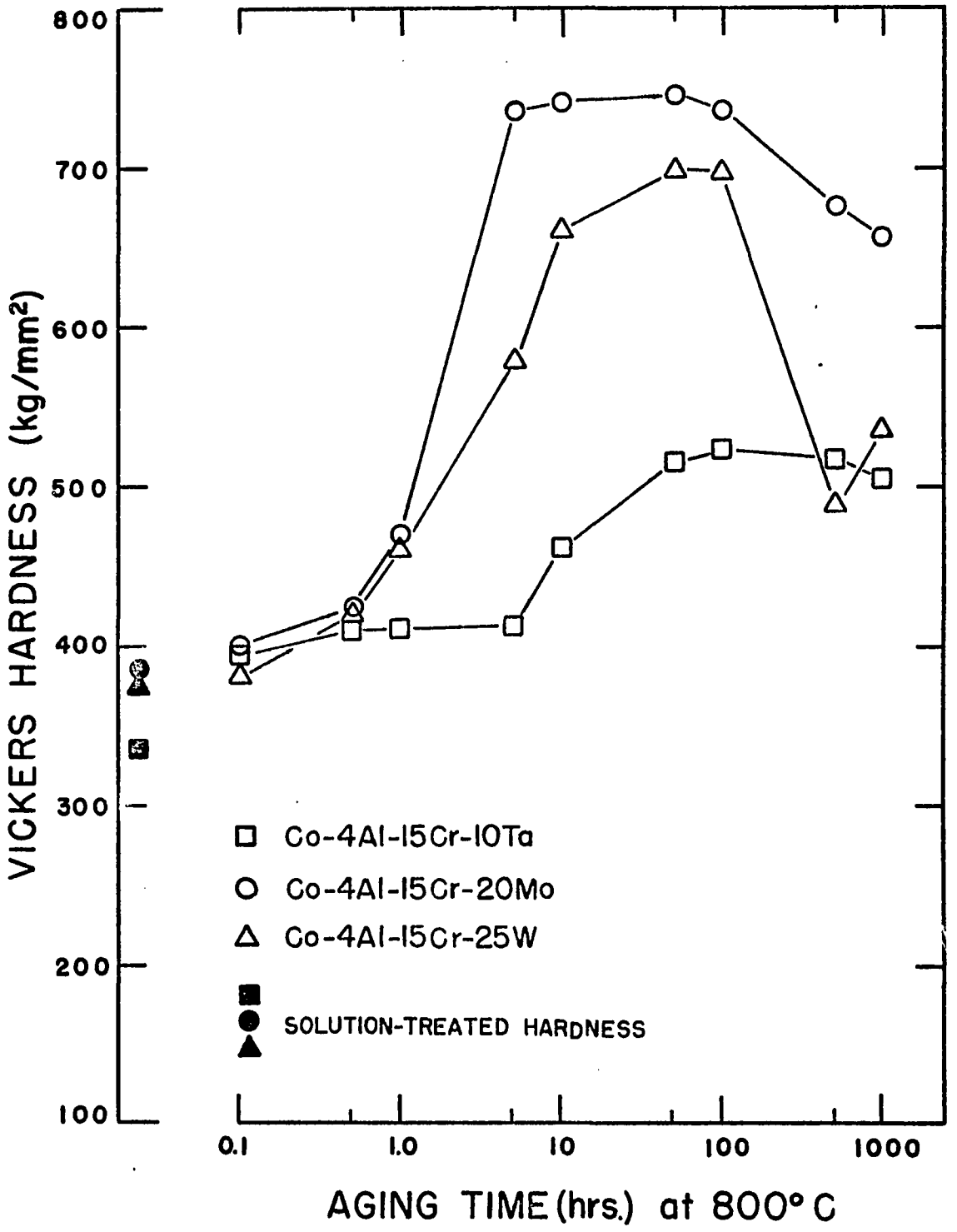

Fig. 28. Aging Curves for Co-4Al-15Cr-X Quartenaries

APPENDIX D

MICROGRAPHS OF SELECTED STRUCTURES

Fig. 29. Co-4Al-5Nb

A.	Solution treated at 1180°C-2 hrs.W.Q.	(PC)*	500X
B.	Aged 1 hour at 700°C		1000X
C.	Aged 1 hour at 800°C		1000X
D.	Aged 10 hours at 800°C		500X
E.	Aged 1000 hours at 800°C		500X
F.	Aged 10 hours at 900°C		1000X

The 5% Nb alloy was single phase as solution treated (A). Upon aging for one hour at 700° (B) or 800° (C), some localized precipitation of the Co_2Nb Laves phase ($MgNi_2$ type) was evident. Continued aging for longer times (D and E) resulted in a lower hardness as the precipitate agglomerated in the matrix and the grain boundaries. (D) corresponded to the maximum hardness at 800°C. After 100 hours, particle size grew throughout the matrix and a Widmanstätten pattern became visible. The needlelike nature of this phase was clearly shown in (F) where the Co_2Nb was well overaged after only 10 hours at 900°.

---

*Phase Contrast

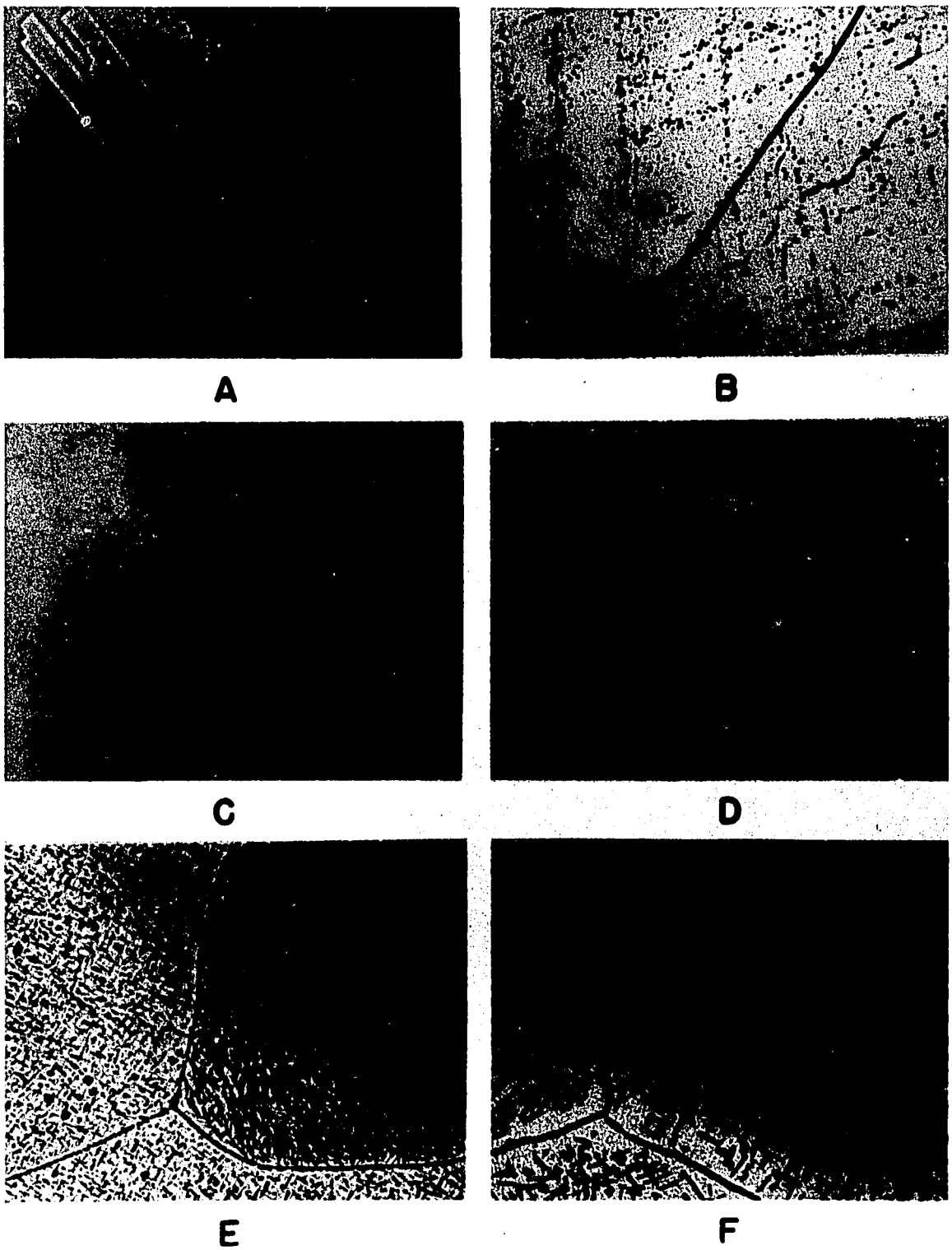

Figure 29. Co-4Al-5Nb

Fig. 30. Co-4Al-10Nb

A.	Solution treated at 1180°C-2 hrs./W.Q.	(PC)*	500X
B.	Aged 1 hour at 800°C		500X
C.	Aged 10 hours at 800°C		500X
D.	Aged 1 hour at 900°C		1000X
E.	Aged 10 hours at 900°C		1000X
F.	Aged 100 hours at 900°C		1000X

Primary Co_2Nb formed by a eutectic freezing reaction was still present after solution treatment (A). Although hardening was evident in (B), no sign of precipitation was seen until 10 hours had passed at 800°C (C). At 900°, the overaged needlelike phase was apparent after 1 hour (D). The primary Co_2Nb appeared little changed by the 900° heat treatment (E and F) although growth of the Co_2Nb needles was extensive.

---

*Phase Contrast

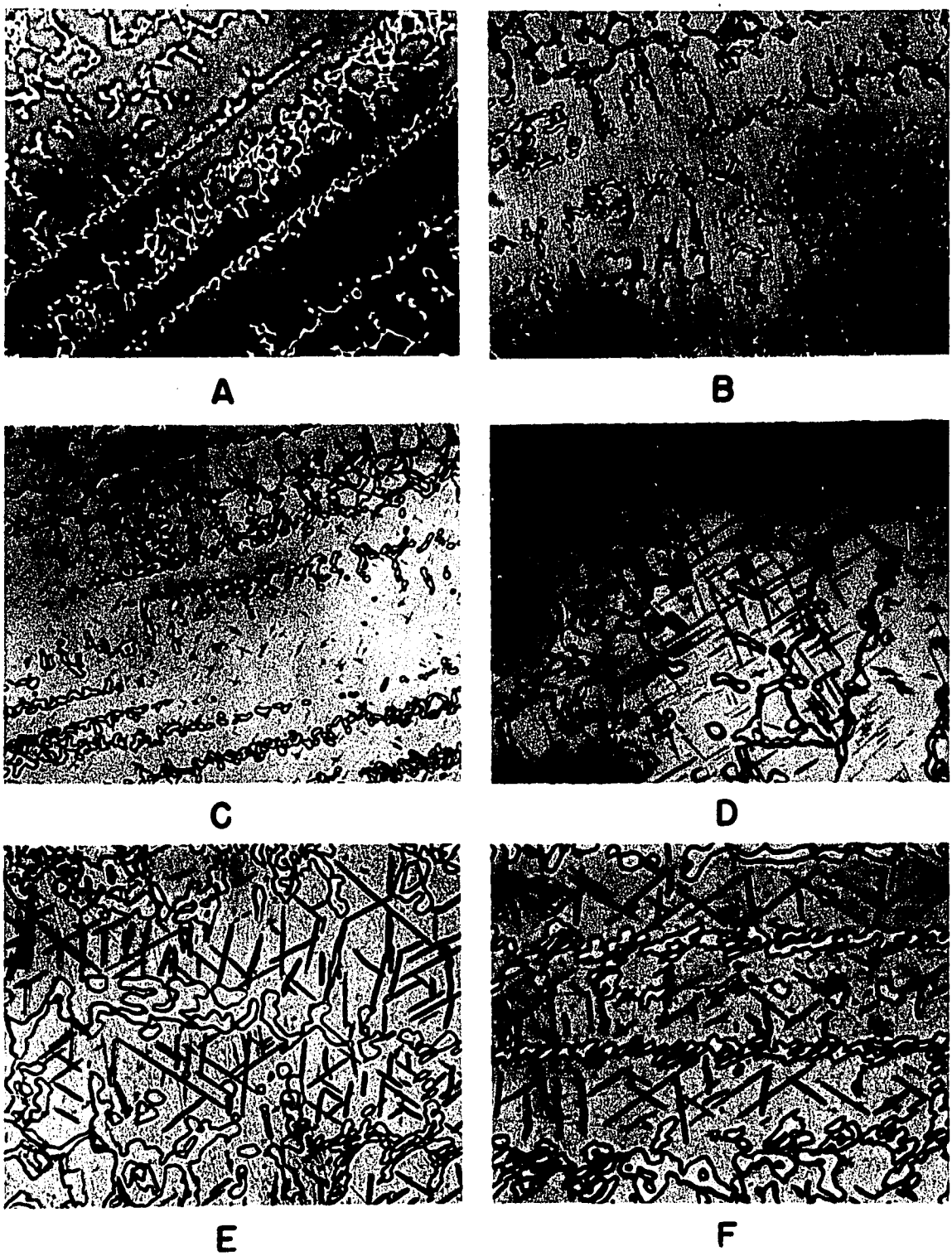

Figure 30. Co-4Al-10Nb

Fig. 31. Co-4Al-15Nb

A.	Solution treated at 1180°-2 hrs./W.Q.	(PC)*	500X
B.	Aged 1 hour at 700°C	(PC)	500X
C.	Aged 100 hours at 700°C		500X
D.	Aged 0.1 hour at 800°C	(PC)	500X
E.	Aged 1 hour at 900°C	(PC)	500X
F.	Aged 10 hours at 900°C		500X

Phase contrast photography clearly showed the hard, brittle Co_2Nb in the solution treated condition (A). Because of the large amount of primary Co_2Nb, the precipitation of this phase during aging was difficult to observe (B, D and E). After 100 hours at 700°, a general precipitate was present in the background (C). Aging at 900° resulted in a somewhat different appearing microstructure and in (F), agglomerated primary Co_2Nb can be seen in a matrix also containing precipitated needles of this intermetallic.

---

*Phase Contrast

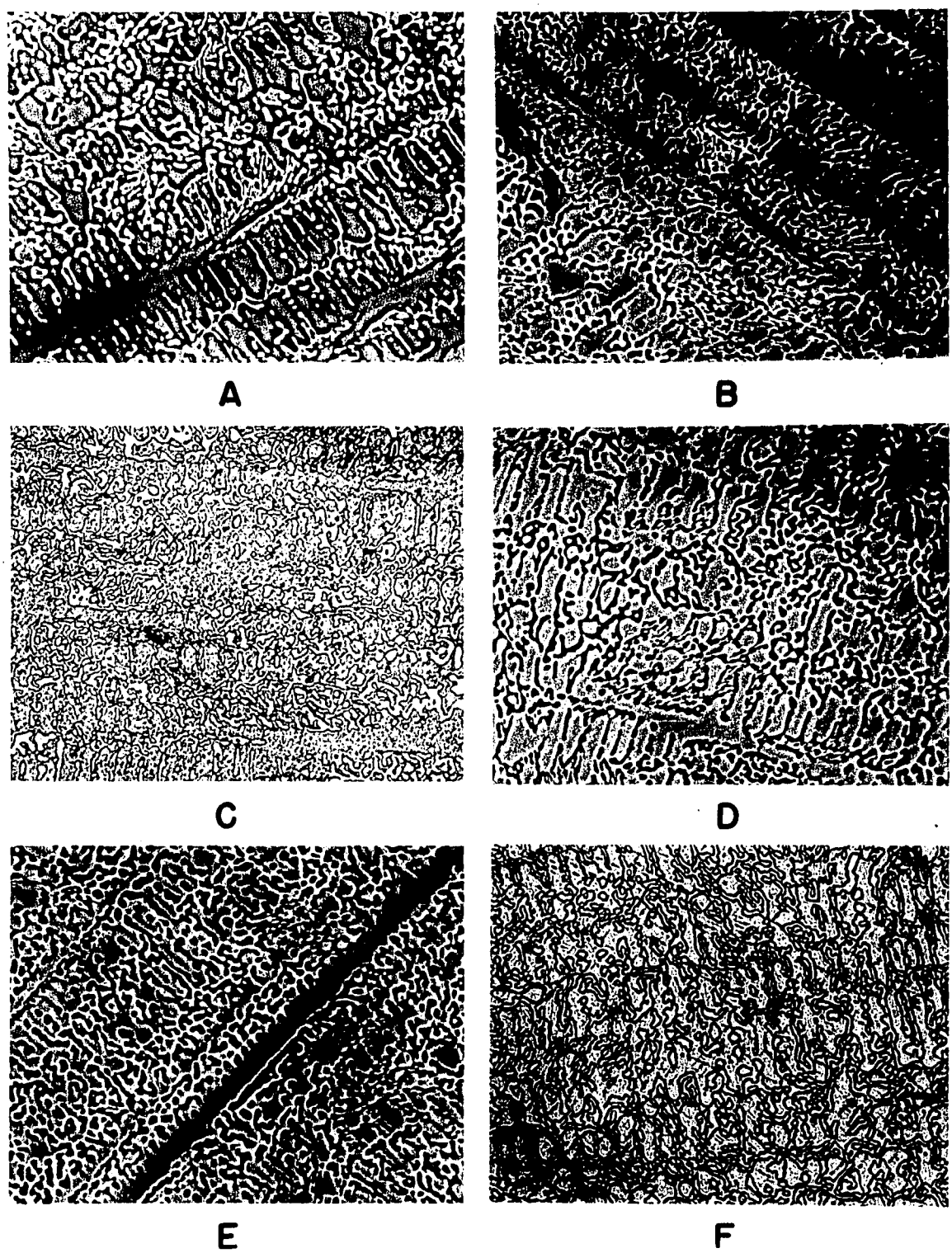

Figure 31. Co-4Al-15Nb

Fig. 32. Co-4Al-20Nb

A.	Solution treated at 1180°C-2 hrs./W.Q.	(PC)*	500X
B.	Aged 1 hour at 600°C	(PC)	1000X
C.	Aged 100 hours at 700°C		500X
D.	Aged 1 hour at 900°C	(PC)	500X
E.	Aged 10 hours at 900°C		500X
F.	Aged 100 hours at 900°C		1000X

This alloy (A) contained more primary Co_2Nb (white phase) than it did Co solid solution. It was so brittle it sustained cracks upon quenching. The morphology of this phase was evident in (B). The hardest value obtained by aging this alloy (773) resulted from a microstructure (C) containing both aged matrix and primary Co_2Nb. Aging at 900° produced an initial precipitation (D and E) which overaged and agglomerated at this temperature (F).

---

*Phase Contrast

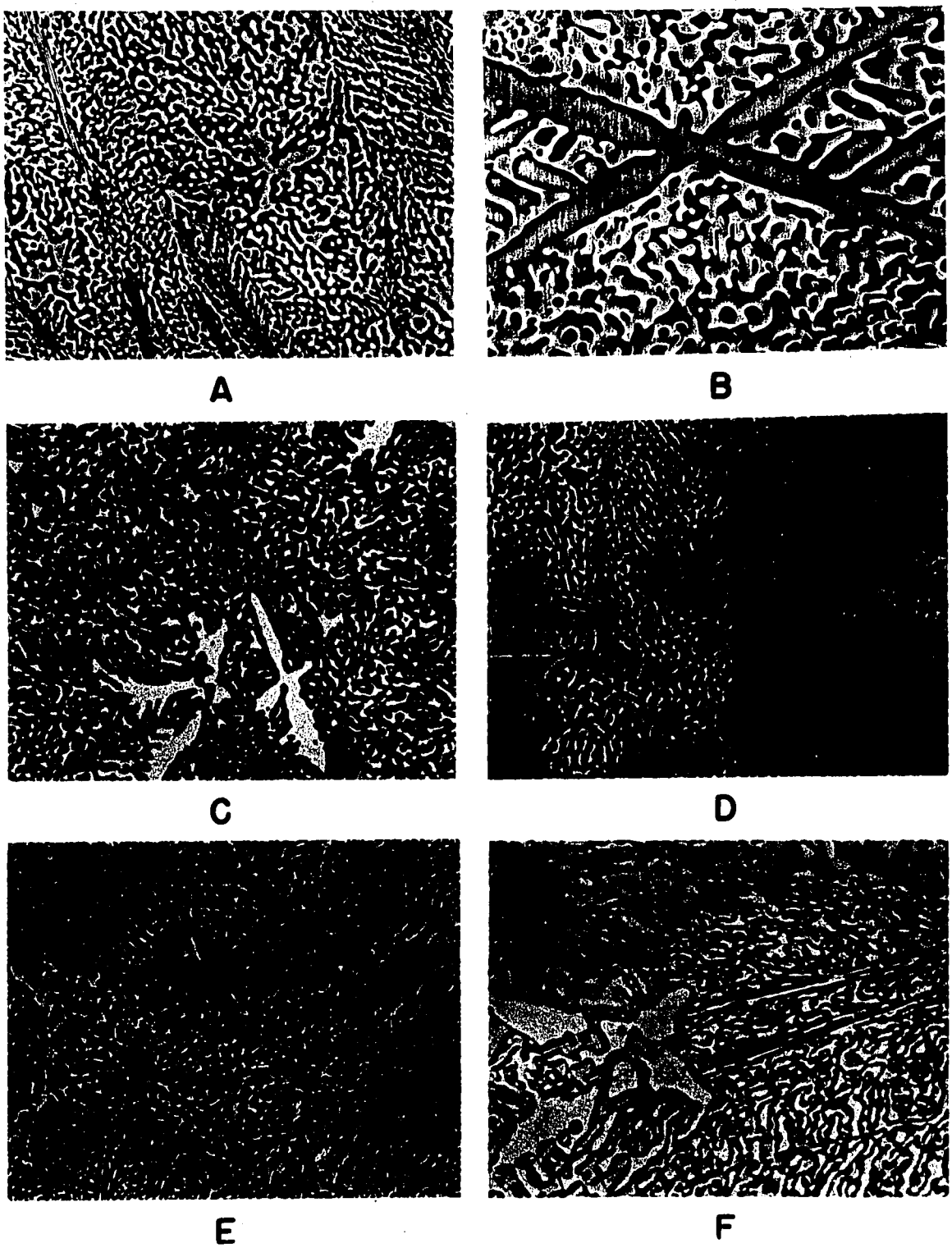

Figure 32. Co-4Al-20Nb

Fig. 33. Co-4Al-5Ta

A.	Solution treated at 1200°C-2 hrs./W.Q.	(PC)*	500X
B.	Aged 0.1 hour at 800°C	(PC)	500X
C.	Aged 1 hour at 800°C		500X
D.	Aged 10 hours at 800°C		500X
E.	Aged 1 hour at 900°C		1000X
F.	Aged 10 hours at 900°C		1000X

As solution treated (A), this alloy exhibited only the striations due to the fcc-to-hcp transformation. Aging at 800° (B, C and D) produced a visible precipitation along grain boundaries after 1 hour and a localized precipitation upon transformation markings after 10 hours. This initial precipitation was Co_2Ta ($MgNi_2$ type) which, at least partially, transformed to αCo_3Ta during aging at the higher temperatures. In E and F, the needlelike appearance of these phases was apparent. Precipitation in the grain boundaries led to denuded zones adjacent to the boundaries.

---

*Phase Contrast

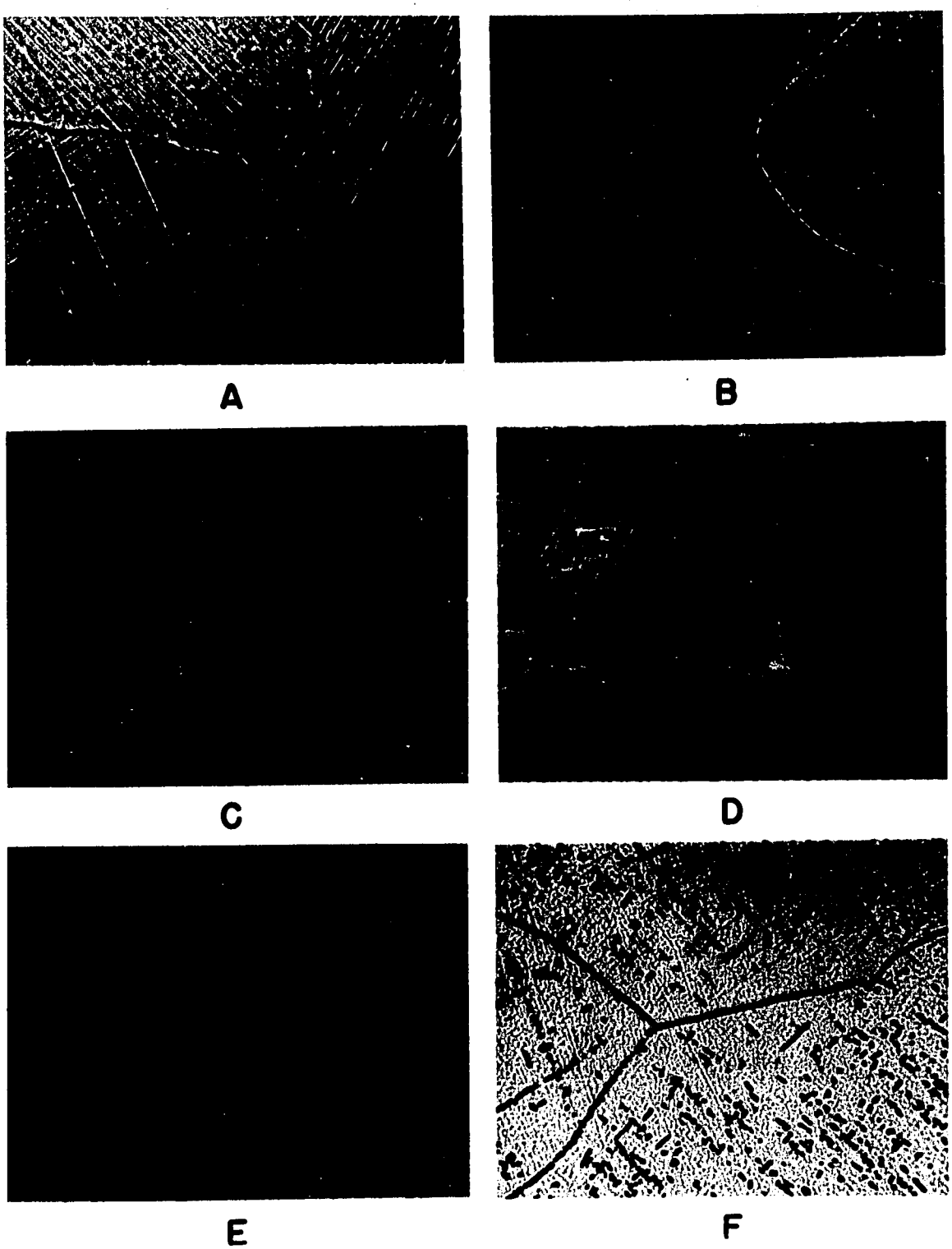

Figure 33. Co-4Al-5Ta

Fig. 34. Co-4Al-10Ta

A.	Solution treated at 1200°C-2 hrs./W.Q. (PC)*	500X
B.	Aged 1 hour at 700°C	1000X
C.	Aged 1000 hours at 700°C	500X
D.	Aged 1 hour at 800°C	1000X
E.	Aged 1000 hours at 800°C	500X
F.	Aged 10 hours at 900°C	1000X

At 10% Ta, the alloy was single phase after solution treatment (A). Precipitation of Co_2Ta was apparent after 1 hour at 700° (B) and the hardness was still increasing after 1000 hours at this temperature (C). At 800°, by comparison, more precipitation was evident at 1 hour (D) and overaging was evident after 1000 hours (E). At 900° (F), overaging was evident after 10 hours. Again, x-ray data showed that most of the precipitate after aging was cubic αCo_3Ta.

---

*Phase Contrast

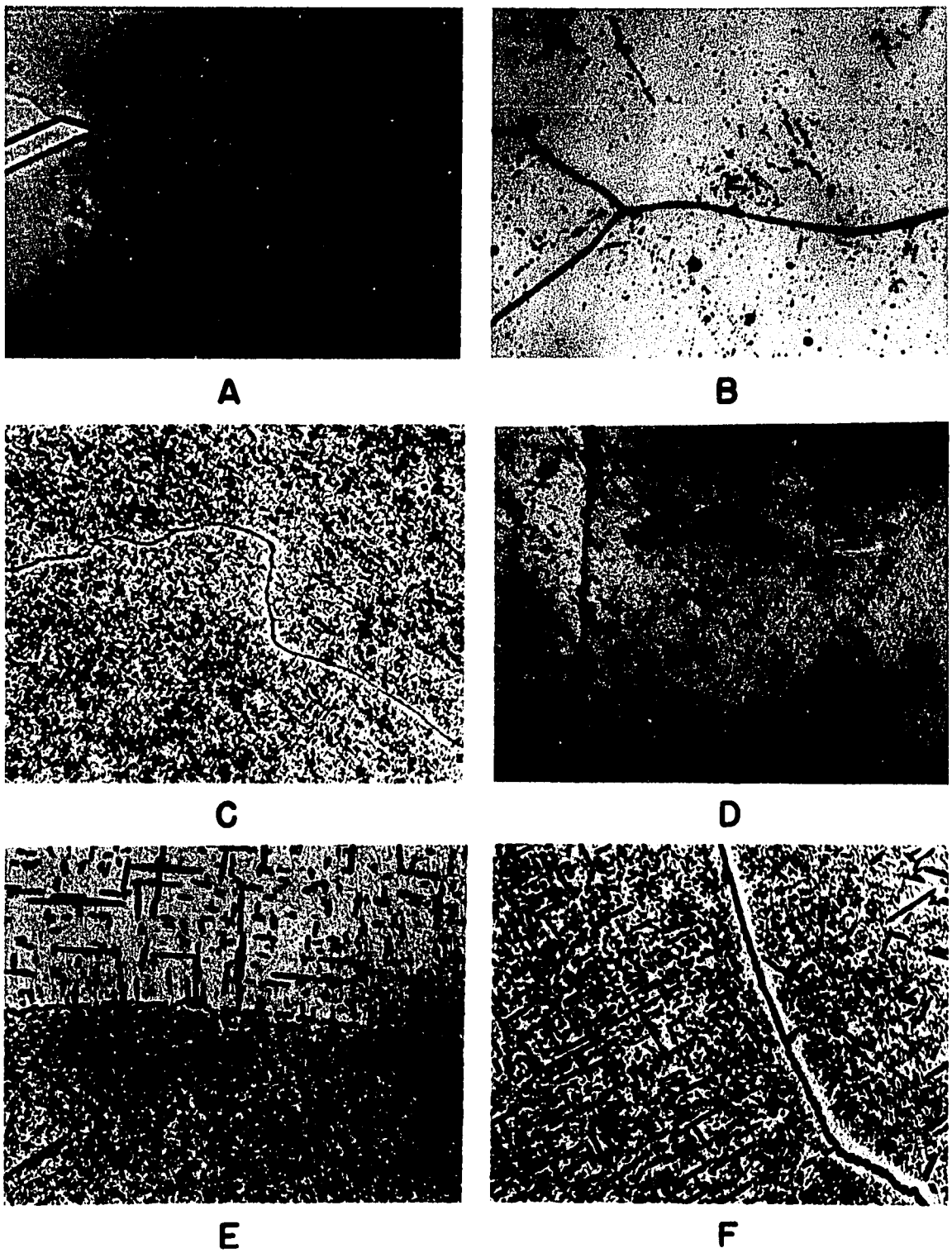

Figure 34. Co-4Al-10Ta

Fig. 35. Co-4Al-15Ta

A.	Solution treated at 1200°C-2 hrs./W.Q. (PC)*	500X
B.	Aged 100 hours at 700°C	500X
C.	Aged 100 hours at 800°C	500X
D.	Aged 1 hour at 900°C	500X
E.	Aged 10 hours at 900°C	1000X
F.	Aged 100 hours at 900°C	1000X

With 15% Ta, the solid solubility limit was exceeded and primary Co_2Ta was present after the solution treatment (A). At 700° (B), precipitation of Co_2Ta appeared as a general darkening in the matrix; whereas at 800° (C), the typical needles were present. In addition, the partial dissolution of the Co_2Ta in the matrix appears to be occurring in C. At 900°, the aging (D) and overaging (E and F) due to the formation of αCo_3Ta was apparent in the granular appearance of the matrix.

---

*Phase Contrast

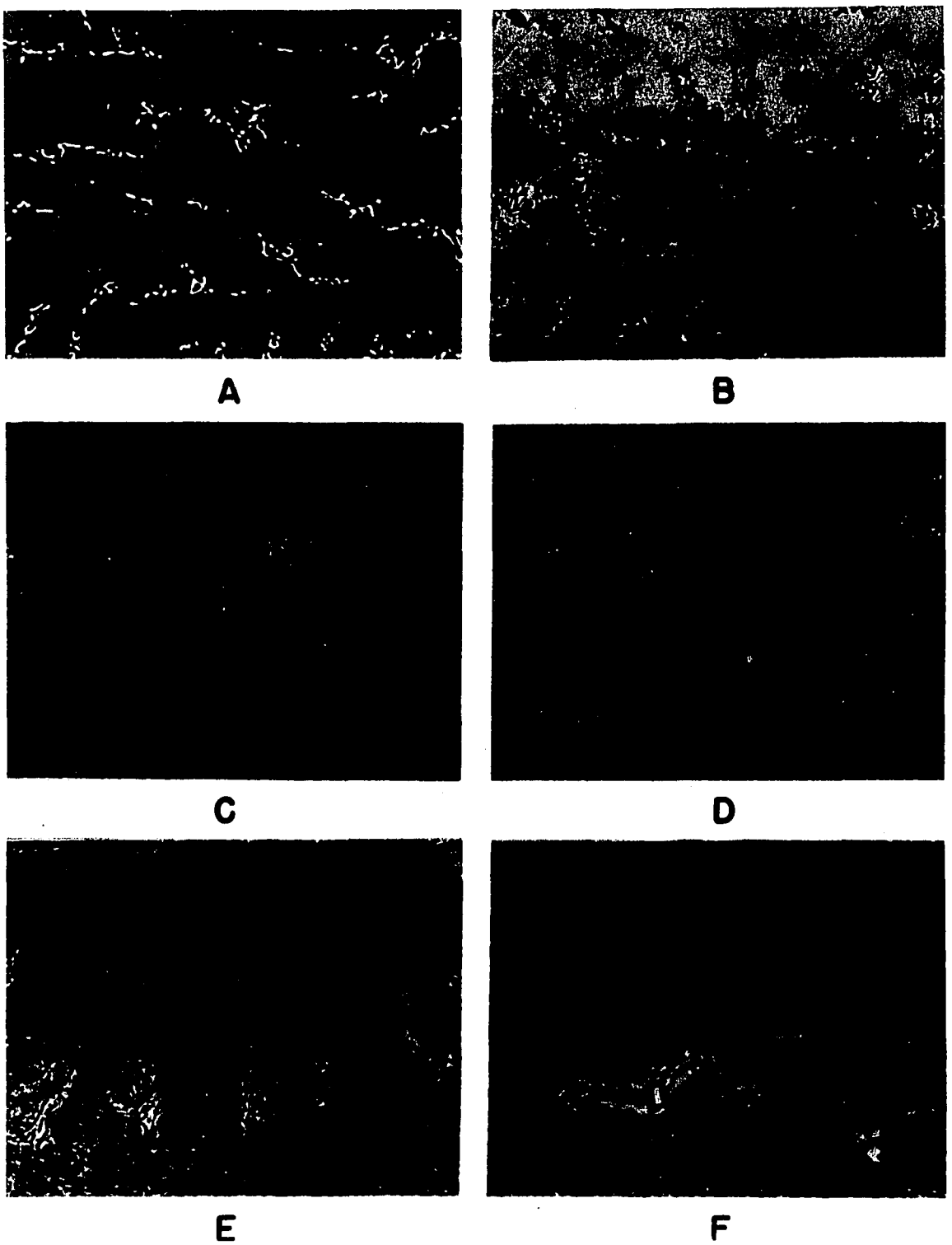

Figure 35. Co-4Al-15Ta

Fig. 36. Co-4Al-20Ta

A.	Solution treated at 1200°C-2 hrs./W.Q. (PC)*	500X
B.	Aged 1 hour at 700°C	500X
C.	Aged 1 hour at 800°C	500X
D.	Aged 100 hours at 800°C	500X
E.	Aged 10 hours at 900°C	1000X
F.	Aged 1000 hours at 900°C	1000X

Appreciable primary Co_2Ta was present in the alloy as solution treated (A). Aging 1 hour at 700° (B) increased the hardness without an appreciable change in appearance. Precipitation first appeared at 800° in 1 hour (C) and large quantities of Co_2Ta needles were present after 100 hours. At 900° the αCo_3Ta appeared in the matrix (E), and then formed the large needles seen after aging for 1000 hours (F).

---

*Phase Contrast

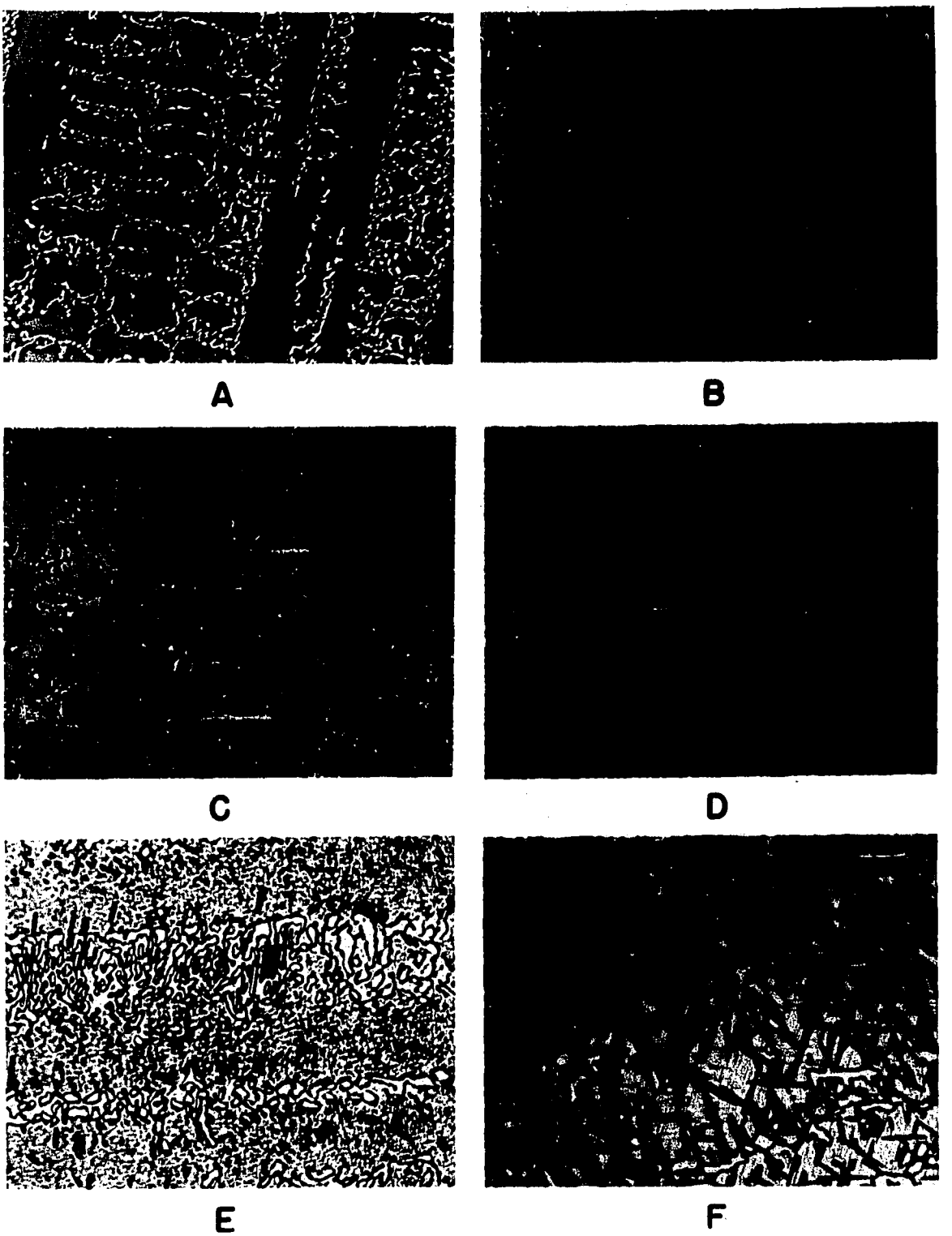

Figure 36. Co-4Al-20Ta

Fig. 37. Co-4Al-3Ti

A.	Solution treated at 1095°C-2 hrs./W.Q.	500X
B.	Aged 1 hour at 700°C	500X
C.	Aged 1 hour at 800°C	500X
D.	Aged 10 hours at 800°C	500X
E.	Aged 1 hour at 900°C	500X
F.	Aged 10 hours at 900°C	500X

The solution treated alloy (A) contained only trace amounts of $AlCo_2Ti$. After 1 hour at 700° (B) or 800° (C), a cellular precipitation occurred at grain boundaries along with what appeared to be a localized precipitate. No hardening was observed outside of the cellular precipitation area. After 10 hours at 800° (D), a definite Widmanstätten pattern was evident. Aging this alloy at 900° (E and F) produced only an overaged localized precipitation of the $AlCo_2Ti$ with some agglomeration in the grain boundaries.

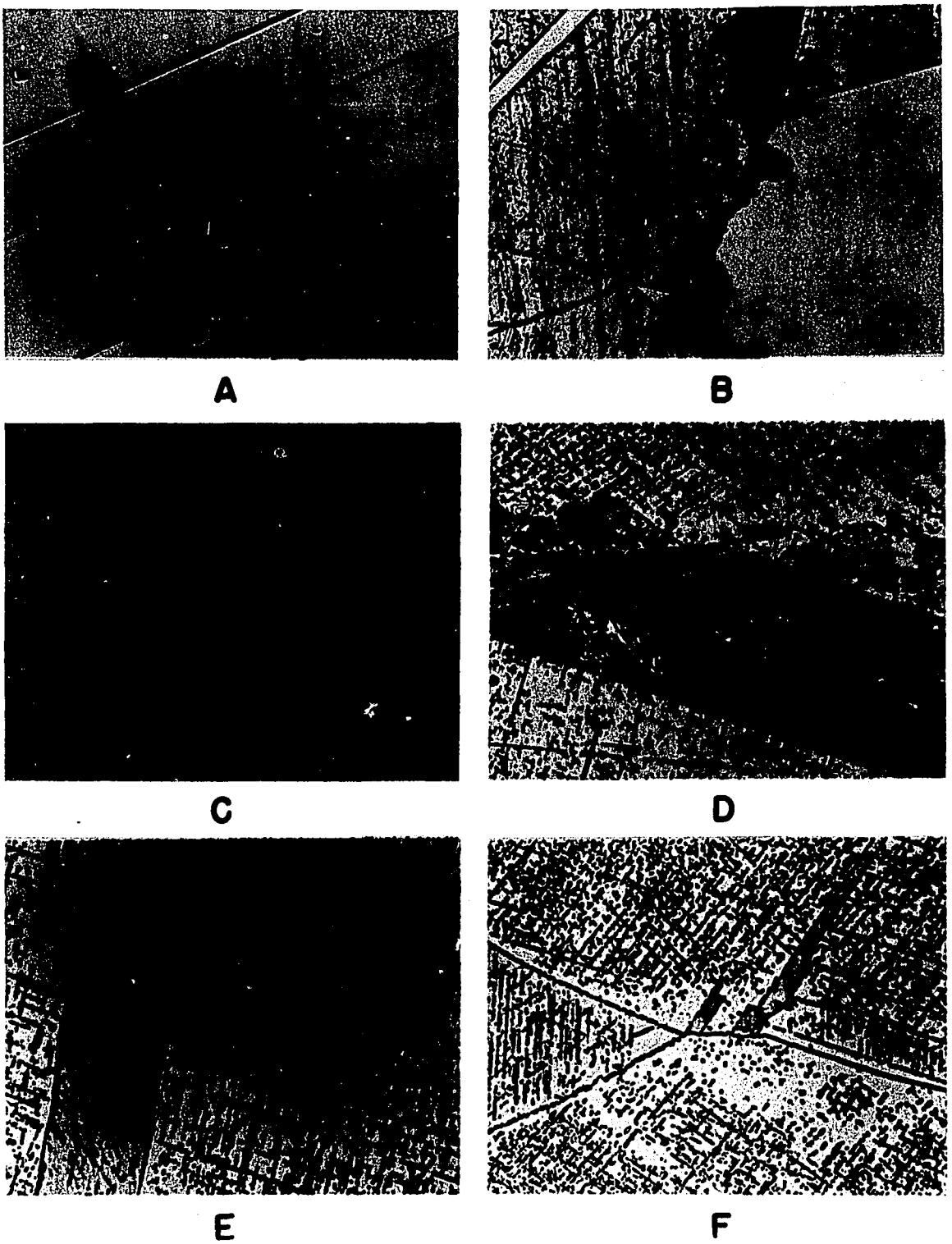

Figure 37. Co-4Al-3Ti

Fig. 38. Co-4Al-6Ti

A.	Solution treated at 1095°C-2 hrs./W.Q.	500X
B.	Aged 1 hour at 600°C	500X
C.	Aged 10 hours at 600°C	500X
D.	Aged 1 hour at 800°C	500X
E.	Aged 0.1 hour at 900°C	1000X
F.	Aged 1000 hours at 900°C	500X

Some primary $AlCo_2Ti$ was present in the solution treated condition (A). As with the 3% Ti alloy, cellular precipitation began at the grain boundaries (B and C) as the first sign of aging. With the increased amount of Ti, this cellular product completely engulfed the individual grains. The structure after aging for 1 hour at 800° (C) attained a hardness of 517 versus the solution treated hardness of 190. In (E) the lamellar structure of this precipitation can be seen. The light areas are Co solid solution while the dark lamellae are $AlCo_2Ti$. Prolonged heating at 900° caused a marked spheroidization of the lamellar phase (F).

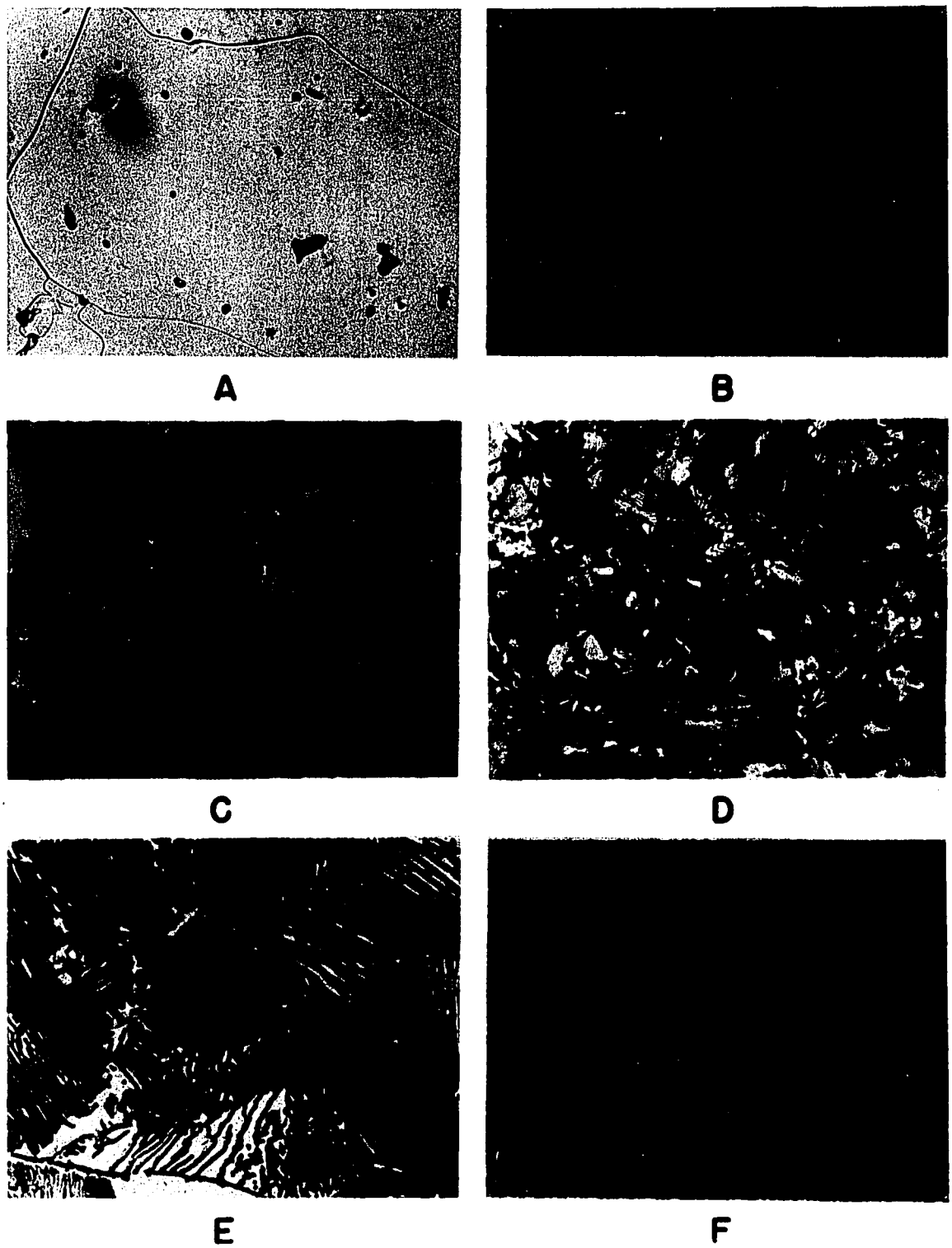

Figure 38. Co-4Al-6Ti

Fig. 39. Co-4Al-9Ti

A.	Solution treated at 1095°C-2 hrs./W.Q.	500X
B.	Aged 1000 hours at 600°C	500X
C.	Aged 100 hours at 700°C	500X
D.	Aged 1 hour at 800°C	500X
E.	Aged 10 hours at 900°C	500X
F.	Aged 1000 hours at 900°C	500X

Appreciable primary $AlCo_2Ti$ was present in this alloy (A). General precipitation in the matrix, after aging at 600° for 1000 hours, was quite heavy (B). At temperatures of 700° through 900°, the cellular precipitation was again evident, the only difference being that the lamellae were coarser at the higher temperatures (C, D and E). Spheroidization of the $AlCo_2Ti$ occurred after long time aging at 900° (F).

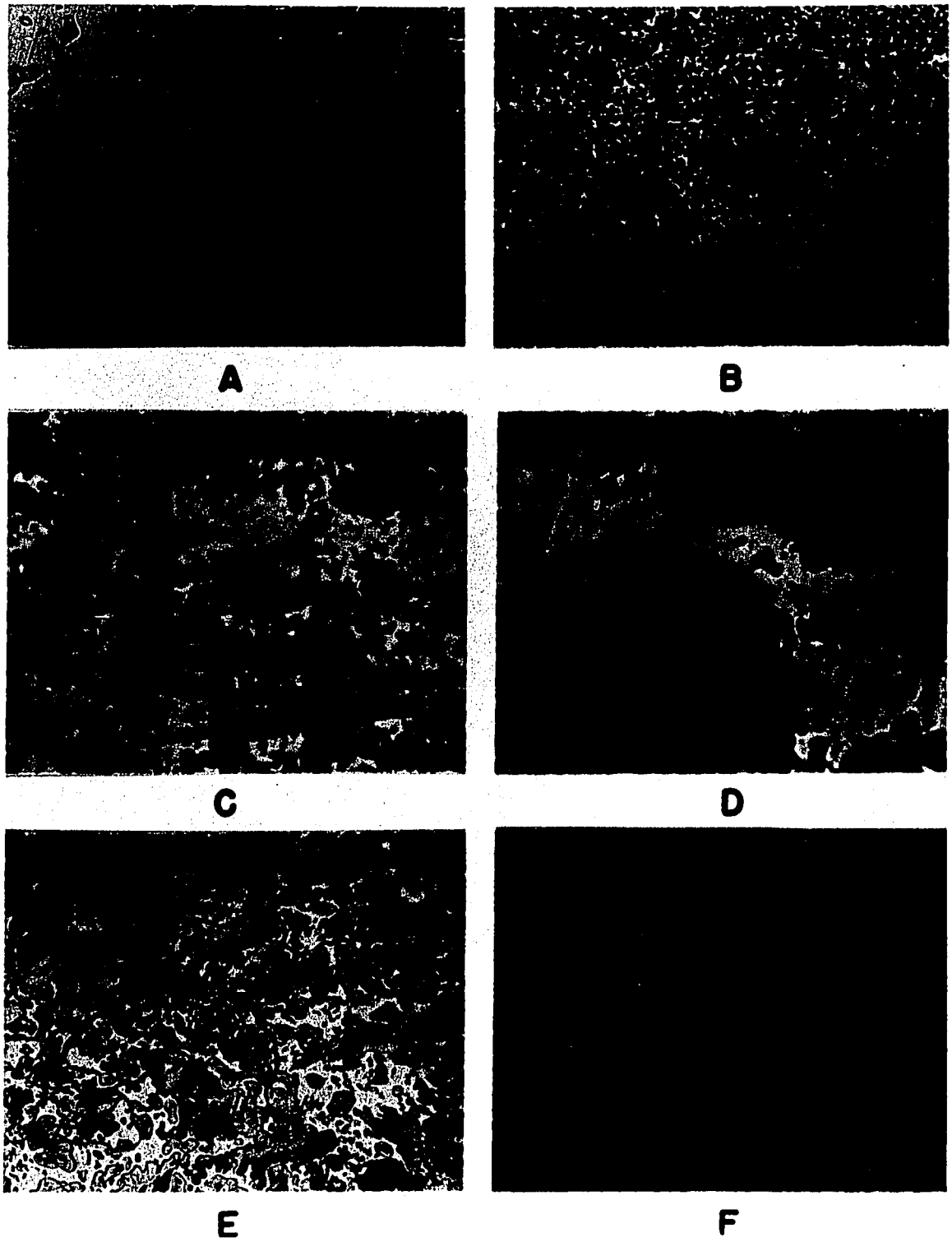

Figure 39. Co-4Al-9Ti

Fig. 40. Co-4Al-12Ti

A.	Solution treated at 1095°C-2 hrs./W.Q.	1000X
B.	Aged 100 hours at 600°C	500X
C.	Aged 1 hour at 800°C	500X
D.	Aged 100 hours at 800°C	500X
E.	Aged 1 hour at 900°C	500X
F.	Aged 1000 hours at 900°C	1000X

The solution treated structure of this alloy contained approximately 40% primary $AlCo_2Ti$ (A). Aging at 600° and 800° (B and C) showed what appeared to be a dissolving of some of this phase in the matrix followed by a reprecipitation later (D). At 900°, a general precipitation formed initially (E) but long time exposure for 1000 hours resulted in the previously seen agglomerated structure with a lower hardness than that of the solution treated condition.

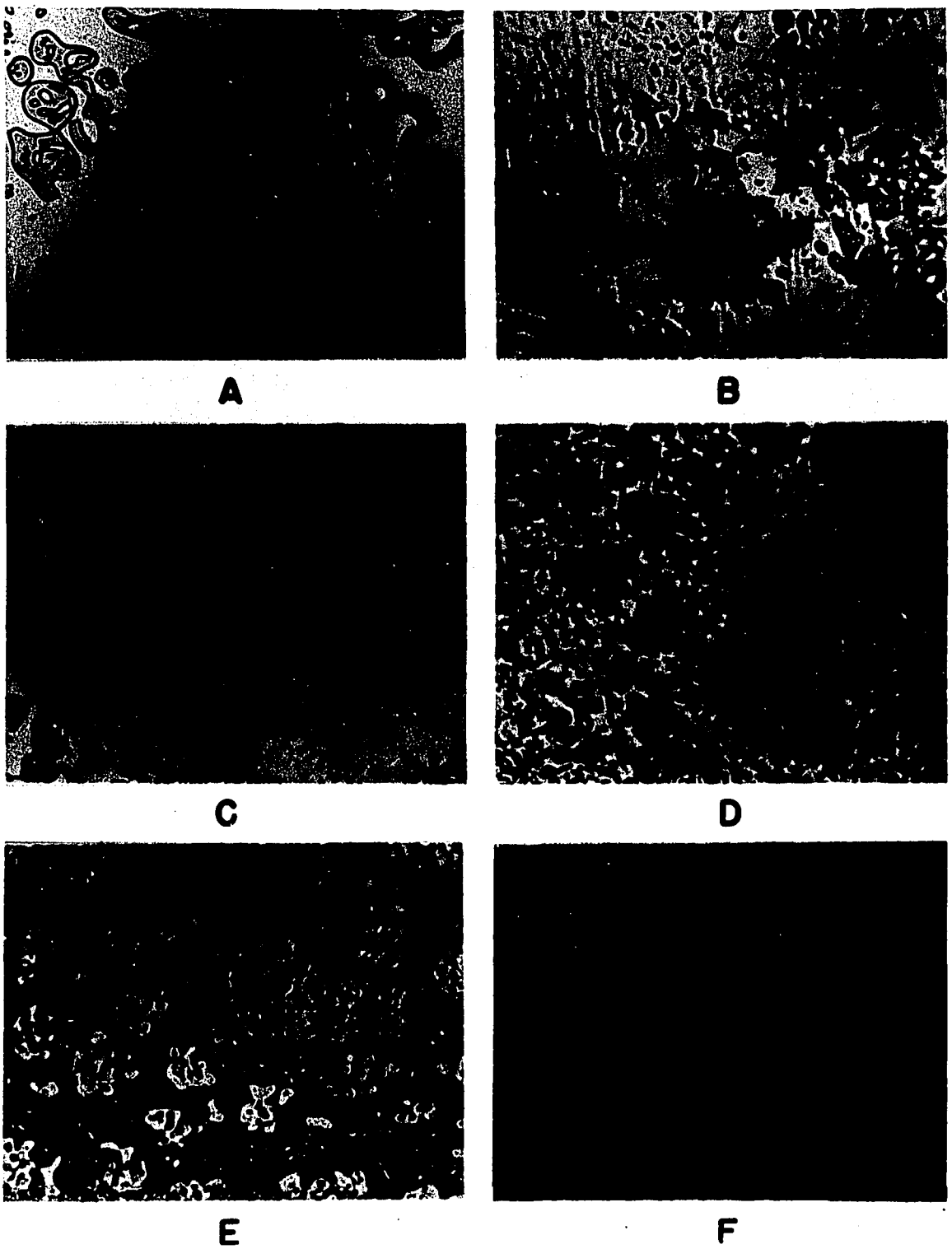

Figure 40. Co-4Al-12Ti

Fig. 41. Co-4Al-5Mo

A.	Solution treated at 1305°C-2 hrs./W.Q.	500X
B.	Aged 100 hours at 600°C	500X
C.	Aged 1000 hours at 700°C	500X
D.	Aged 0.1 hour at 800°C	500X
E.	Aged 1000 hours at 800°C	1000X
F.	Aged 0.1 hour at 900°C	500X

The clean matrix showed only some striations resulting from the fcc-to-hcp transformation (A). Aging this alloy at 600° resulted only in the cellular precipitation of Co_3Mo at the grain boundaries (B). No general precipitate was present. Aging at 700° for 1000 hours (C) produced a mixture of approximately 50% matrix, with some preferential localized precipitation, and 50% cellular structure. The hardness of these constituents was 265 and 369, respectively. Aging at 800° and 900° (D, E and F) showed no precipitation since at these temperatures the alloy was in the single phase cobalt solid-solution region. The transformation markings were quite evident, however.

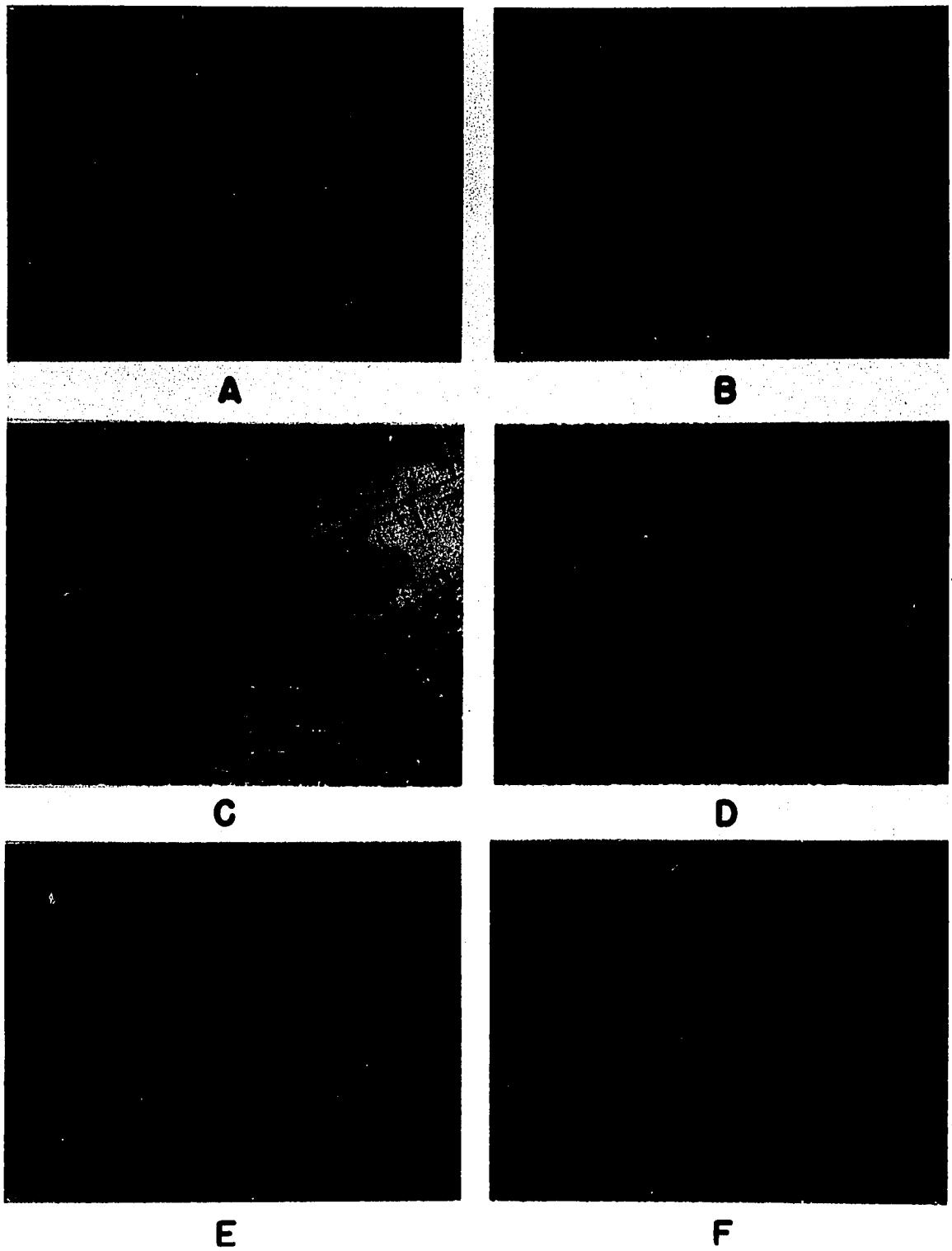

Figure 41. Co-4Al-5Mo

Fig. 42. Co-4Al-12.5Mo

A.	Solution treated at 1305°C-2 hrs./W.Q.	500X
B.	Aged 100 hours at 600°C	500X
C.	Aged 100 hours at 700°C	500X
D.	Aged 1000 hours at 700°C	500X
E.	Aged 100 hours at 800°C	500X
F.	Aged 1000 hours at 800°C	500X

Again, the solution treated structure was single phase (A). The first precipitate at 600° occurred after 100 hours (B). Aging at 700° for 100 hours produced the cellular precipitation of Co_3Mo at grain boundaries, plus what appeared to be a general matrix precipitate (C). After 1000 hours at this same temperature, the cellular precipitate had engulfed the entire specimen resulting in a large hardness increase (D). Aging at 800° resulted in much lesser amounts of precipitate, most of which appeared in grain boundaries (E) and agglomerated after long times at this temperature (F). At 900°, this alloy was entirely single phase.

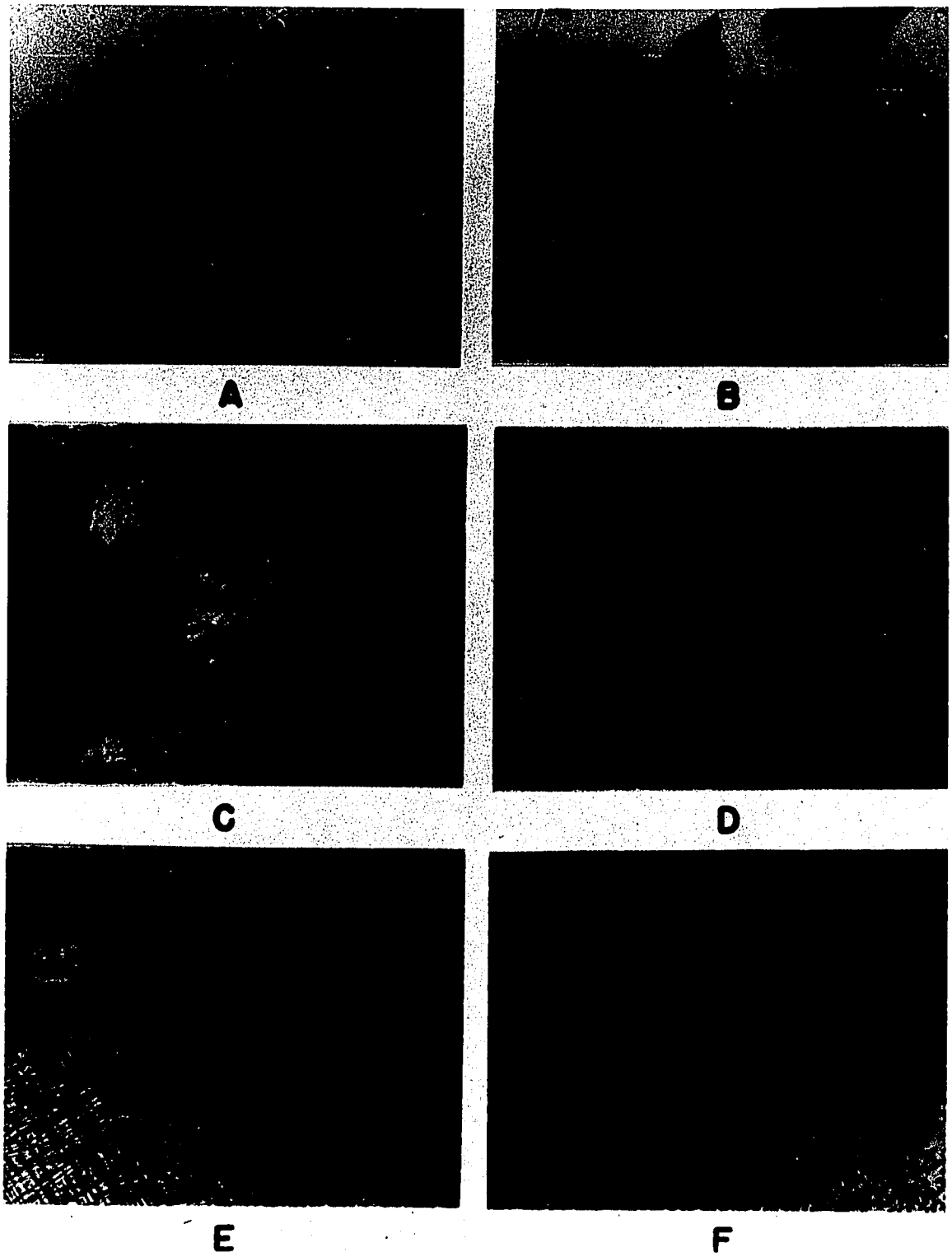

Figure 42. Co-4Al-12.5 Mo

Fig. 43. Co-4Al-20Mo

A.	Solution treated at 1305°C-2 hrs./W.Q.	500X
B.	Aged 10 hours at 800°C	500X
C.	Aged 1000 hours at 800°C	1000X
D.	Aged 0.1 hour at 900°C	500X
E.	Aged 1 hour at 900°C	500X
F.	Aged 10 hours at 900°C	500X

The solution treated alloy was again single phase (A). Cellular precipitation of Co_3Mo, beginning at grain boundaries, occurred in all alloys aged at 800° and below (B). Longer times at 800° resulted in a mixed structure of matrix and agglomerated Co_3Mo particles (C). Co_3Mo precipitation occurred in a localized and not a cellular fashion in specimens aged at 900° (D and E); however, for times above 100 hours, regions of agglomerated precipitate formed and grew in size (F). The hardness (510) of these two different appearing constituents was approximately the same.

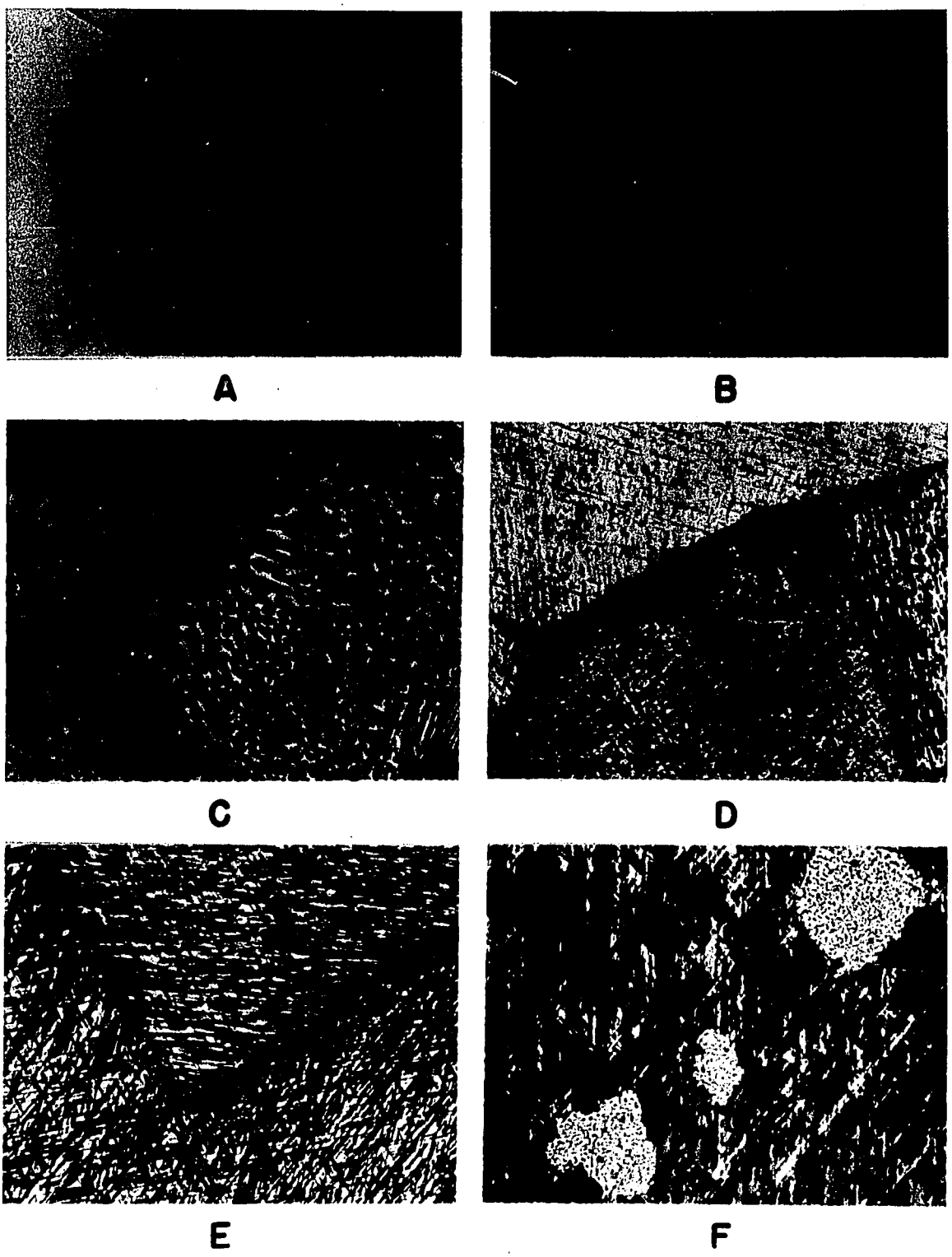

Figure 43. Co-4Al-20Mo

Fig. 44. Co-4Al-10W

A.	Solution treated at 1300°C-2 hrs./W.Q.	500X
B.	Aged 0.1 hour at 600°C	500X
C.	Aged 100 hours at 600°C	500X
D.	Aged 100 hours at 700°C	500X
E.	Aged 100 hours at 800°C	500X
F.	Aged 1000 hours at 800°C	1000X

This system was a single phase alloy in the solution treated condition (A). Aging even at 600° led to precipitation at the grain boundaries (B and C). The structure shown in (C) persisted even to 1000 hours. Since no x-ray pattern was obtained other than that of ordered fcc Co-solid solution, this precipitate may be simply hcp regions in the matrix. Aging at 700° and 800° caused a general darkening of the matrix (D and E) with a marked agglomeration in the grain boundaries which were denuded of solute atoms (F). The 900° structures, not shown, were aged in the single phase solid solution region and showed no precipitate on hardening.

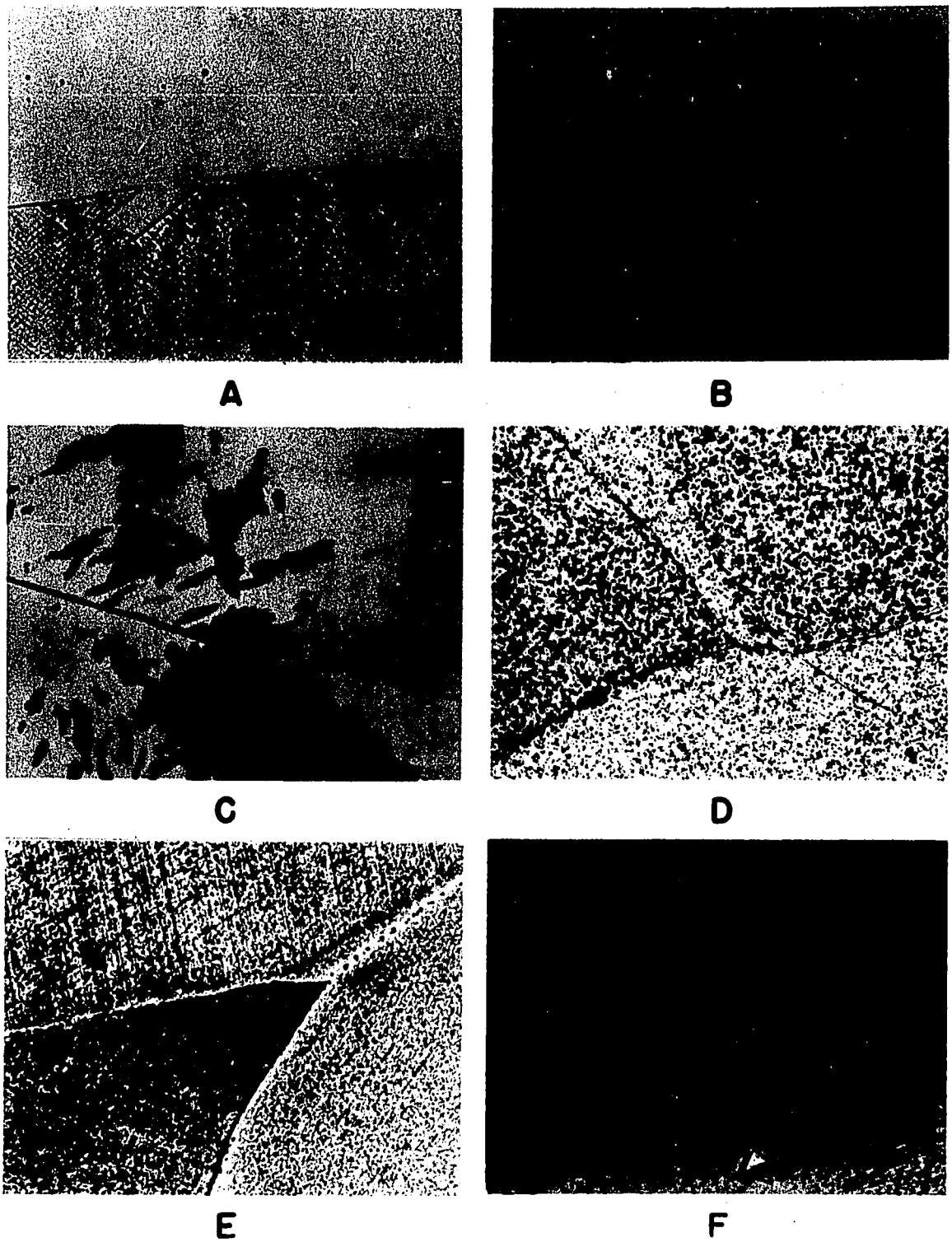

Figure 44. Co-4Al-10W

Fig. 45. Co-4Al-25W

A.	Solution treated at 1300°C-2 hrs./W.Q.	500X
B.	Aged 100 hours at 600°C	500X
C.	Aged 1000 hours at 600°C	500X
D.	Aged 1000 hours at 800°C	1000X
E.	Aged 1 hour at 900°C	500X
F.	Aged 1000 hours at 900°C	500X

This alloy also existed as a single phase following the solution treatment (A). As with the 10W alloy, a feathery precipitate appeared at the grain boundaries after aging at 600° (B and C). Aging at 800° (D) resulted in a general darkening of the matrix accompanied by a significant hardness increase which persisted through 1000 hours. At 900° (E and F), the matrix displayed a fine structure which x-ray analysis showed to be ordered Co solid solution.

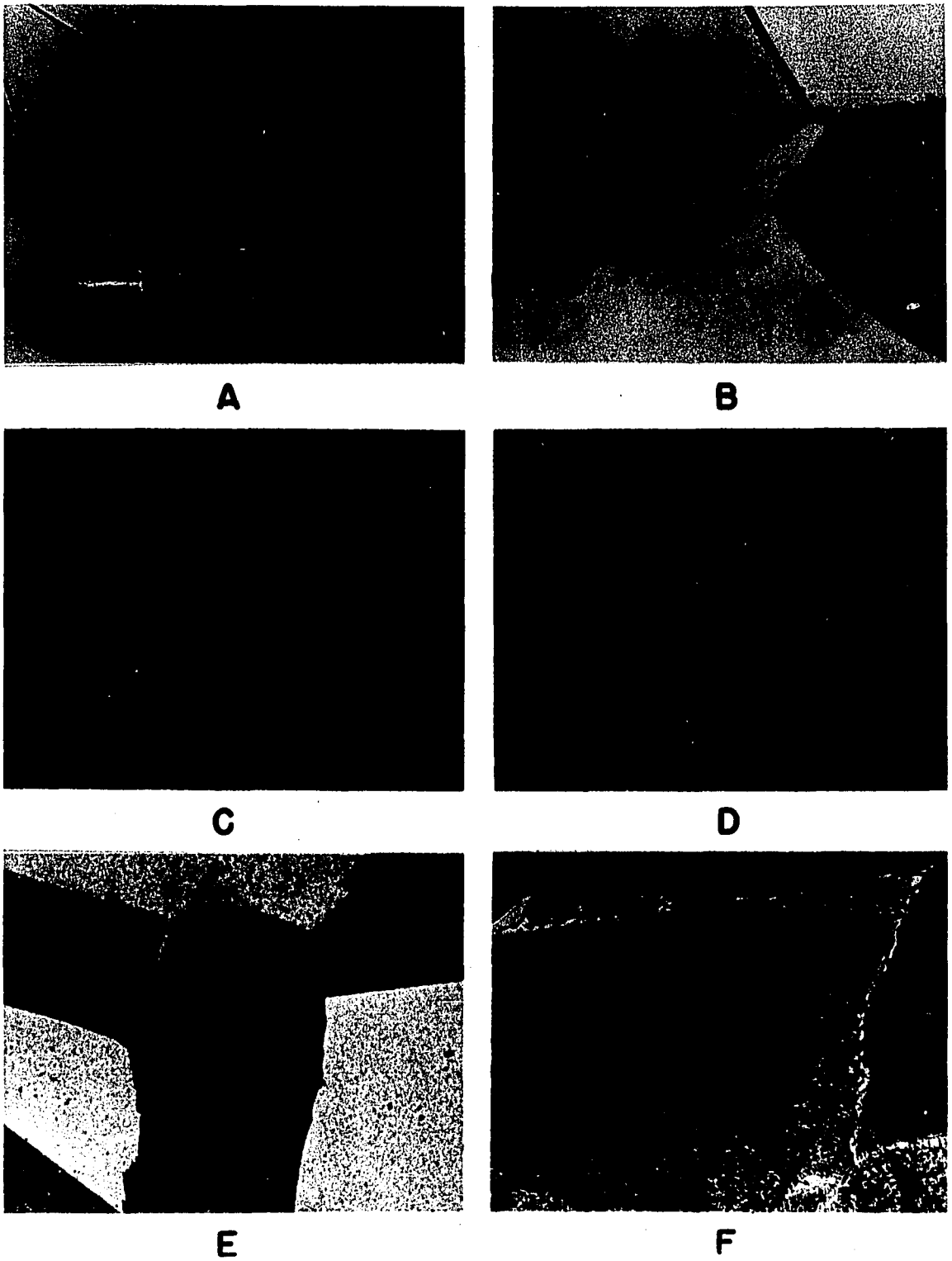

Figure 45. Co-4Al-25W

Fig. 46. Co-4Al-15Cr-10Ta

A.	As-cast	1000X
B.	Solution treated at 1200°C-8 hrs./W.Q.	500X
C.	Aged 10 hours at 800°C	1000X
D.	Aged 50 hours at 800°C	1000X
E.	Aged 100 hours at 800°C	1000X
F.	Aged 1000 hours at 800°C	1000X

The as-cast structure showed a solid-solution phase plus a eutectic structure with Co_2Ta ($MgNi_2$ form) (A). Solution treating agglomerated the Co_2Ta Laves phase (B). Subsequent aging at 800° produced a precipitate of Co_2Ta beginning at 10 hours (C) and continuing through to 1000 hours. The maximum hardness corresponded to the 100-hour treatment (E); however, there was essentially no significant hardness change for aging times of 50 hours (D) to 1000 hours (F) even though growth of the Co_2Ta platelets was appreciable.

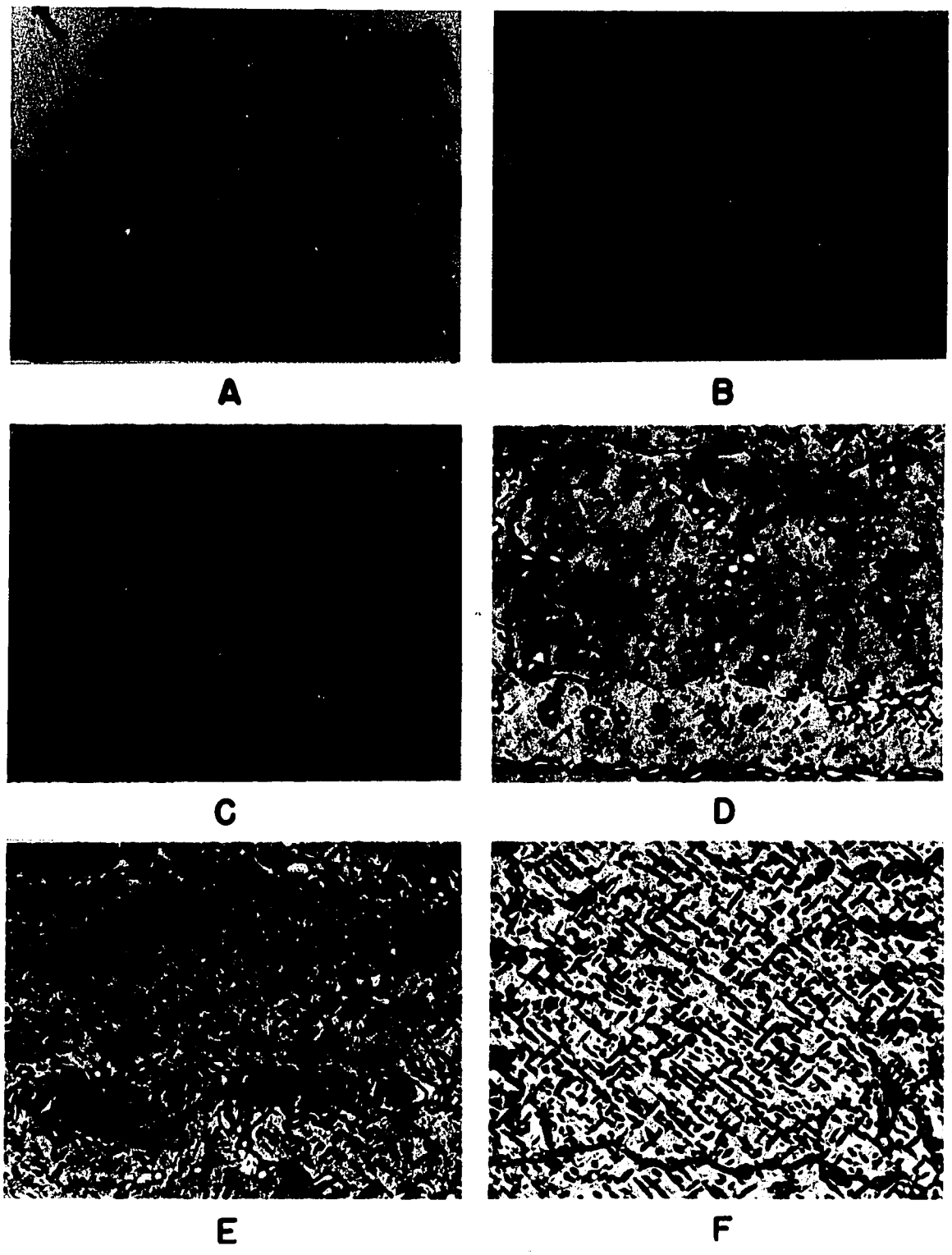

Figure 46. Co-4Al-15Cr-10Ta

Fig. 47. Co-4Al-15Cr-20Mo

A.	As-cast	1000X
B.	Solution treated at 1285°C-8 hrs./W.Q.	500X
C.	Aged 5 hours at 800°C	1000X
D.	Aged 50 hours at 800°C	1000X
E.	Aged 500 hours at 800°C	1000X
F.	Aged 1000 hours at 800°C	1000X

A eutectically formed R phase was present in the as-cast condition (A) which subsequently agglomerated during solution treatment (B). Aging at 800° resulted in the general precipitation of secondary R phase beginning at 5 hours (C). Maximum hardness was attained at 50 hours (D), followed by overaging after 500 and 1000 hours (E and F).

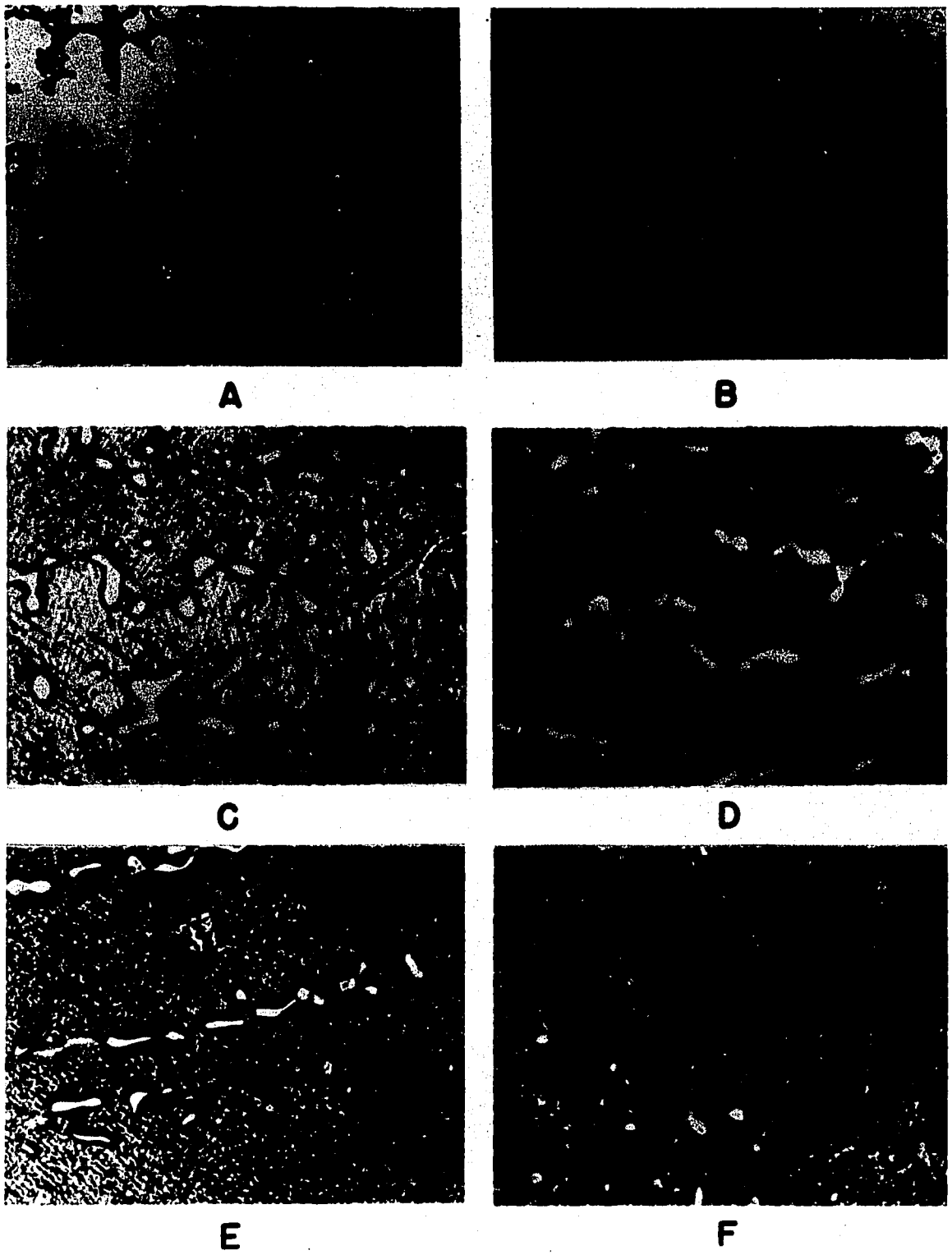

Figure 47. Co-4Al-15Cr-20Mo

Fig. 48. Co-4Al-15Cr-25W

A.	As-cast	1000X
B.	Solution treated at 1350°C-7 hrs./W.Q.	1000X
C.	Aged 1 hour at 800°C	1000X
D.	Aged 5 hours at 800°C	1000X
E.	Aged 50 hours at 800°C	1000X
F.	Aged 500 hours at 800°C	1000X

Eutectically formed Co_7W_6 (Mu-phase) was present in the as-cast (A) and solution treated condition (B). Aging at 800° initiated the precipitation of secondary Co_7W_6 after 1 hour (C). The amount of secondary Co_7W_6 increased as a general precipitate in the matrix (D). After the maximum hardness was attained at 50 hours (E), the Mu-phase overaged rapidly (F) by a coalescence into large globules.

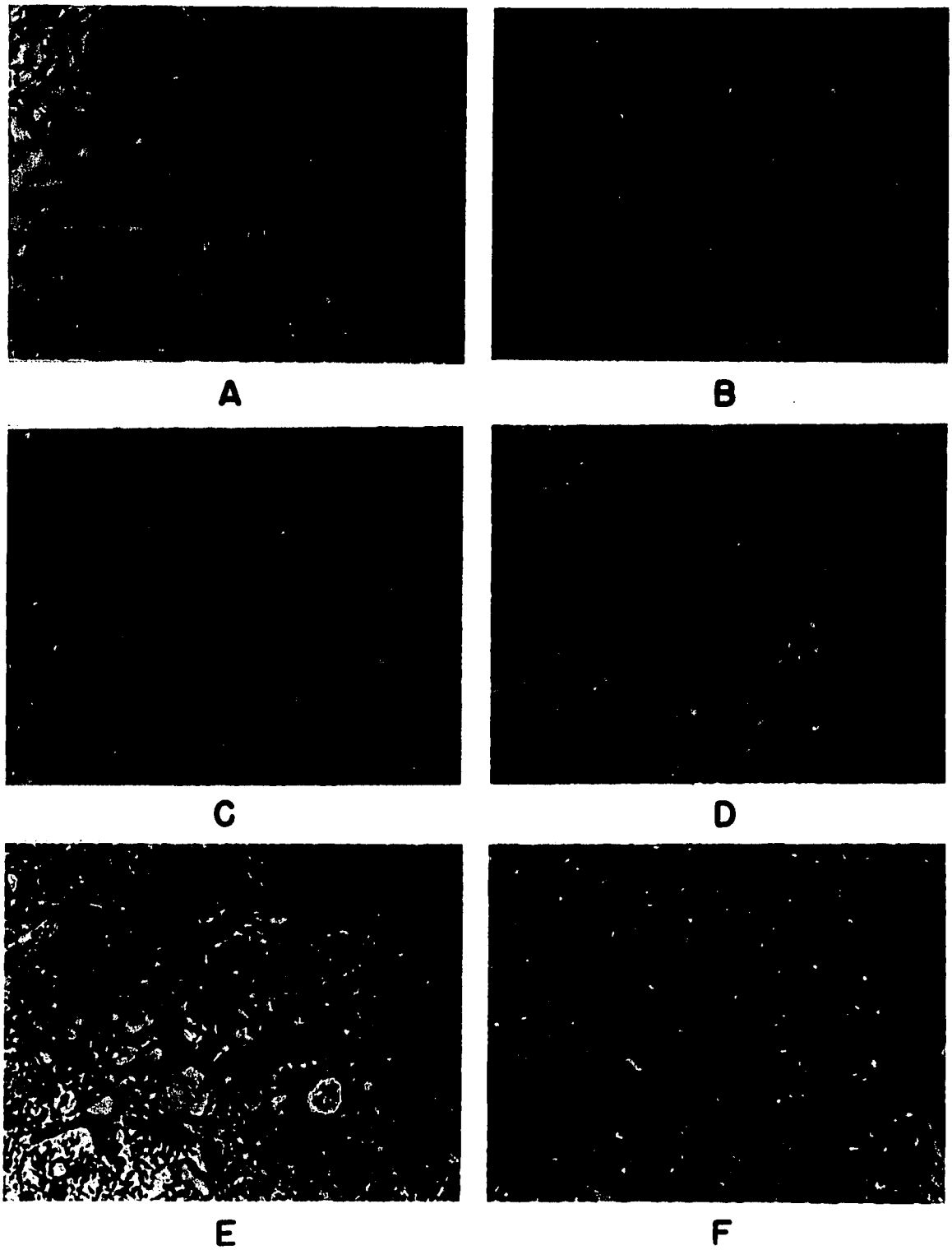

Figure 48. Co-4Al-15Cr-25W

Fig. 49. Co-4Al-10Ta

Aged 1000 hours at 800°C Magnification 1400X

This structure shows the Co_2Nb needles which appeared at the onset of aging plus a very fine textured precipitation of αCo_3Ta in the matrix.

Fig. 50. Co-4Al-15Cr-10Ta

Aged 50 hours at 800°C Magnification 13,000X

In the Ta alloy containing Cr, the blocky nature of the αCo_3Ta can be readily resolved at this magnification. Note the slight denuded regions adjacent to the grain boundary.

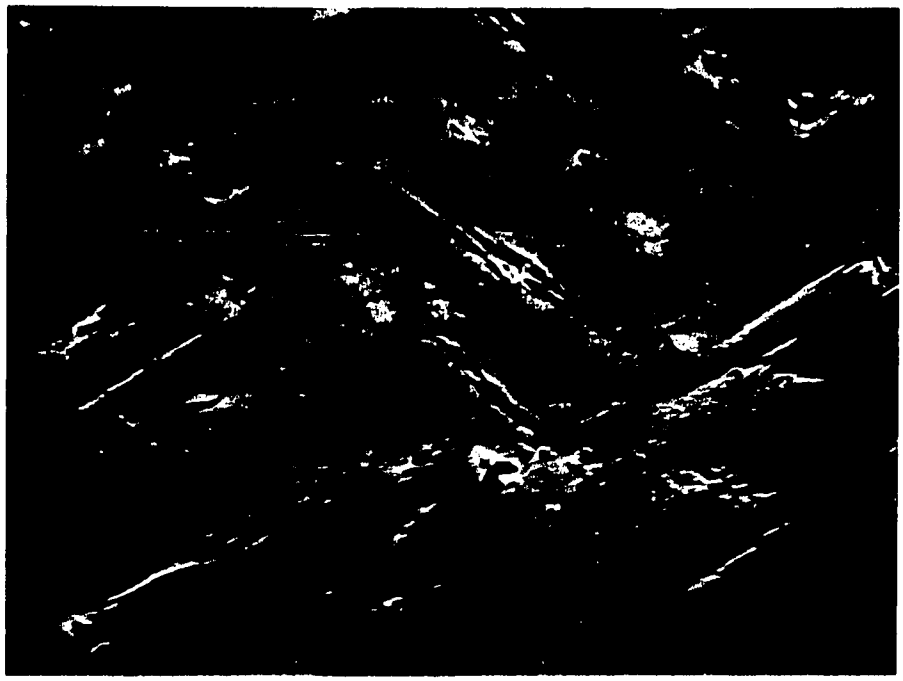

Figure 49. Co-4Al-10Ta

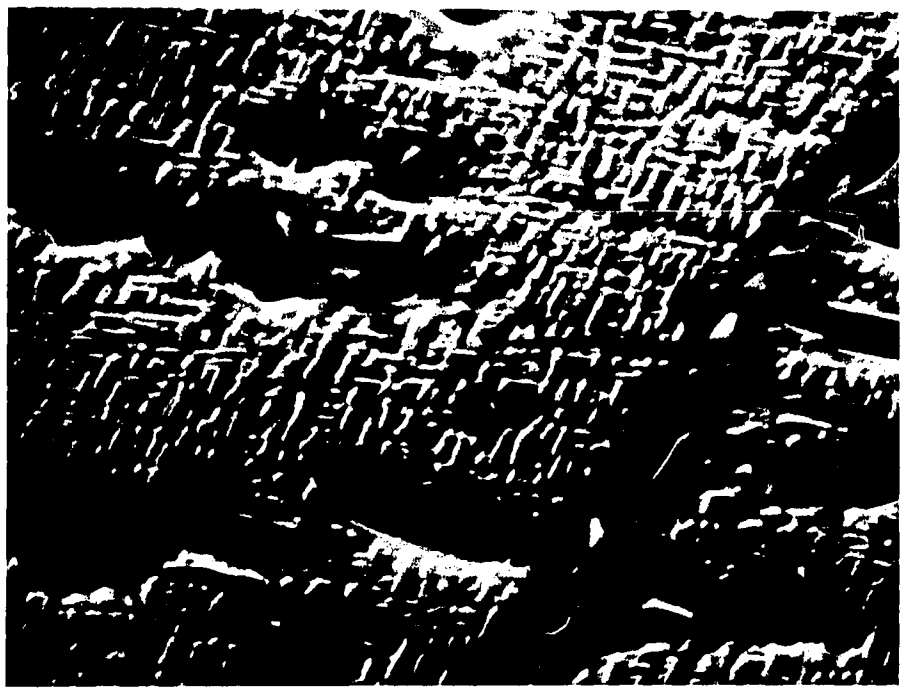

Figure 50. Co-4Al-15Cr-10Ta

Fig. 51. Co-4Al-20Mo

Aged 1000 hours at 700°C Magnification 7500X

This very hard structure was caused by the lamellar formation of Co_3Mo accompanying the decomposition of the alpha solid solution. The platelets of Co_3Mo seen here are approximately 2000 Å thick.

Fig. 52. Co-4Al-15Cr-20Mo

Aged 50 hours at 800°C Magnification 13,000X

When Cr is added to the basic 20Mo alloy, the precipitate is no longer Co_3Mo, but is instead the R-phase. Seen here is a large particle of the primary R-phase found during casting, plus a background of secondary R-phase in the molybdenum matrix. The hardness of this structure (Vickers hardness 750) was the maximum obtained by this alloy prior to overaging.

Figure 51. Co-4Al-20Mo

Figure 52. Co-4Al-15Cr-20Mo

Fig. 53. Co-4Al-25W

Aged 1000 hours at 800°C Magnification 10,500X

The structure adjacent to the grain boundary shows no distinct precipitation, but rather a modulated or textured structure suggesting the presence of a superlattice or transition phase in the matrix.

Fig. 54. Co-4Al-15Cr-25W

Aged 50 hours at 800°C Magnification 13,000X

The large light "blocks" are primary Co_7W_6 Mu-phase. The smaller light areas are precipitated Co_7W_6 which formed during aging.

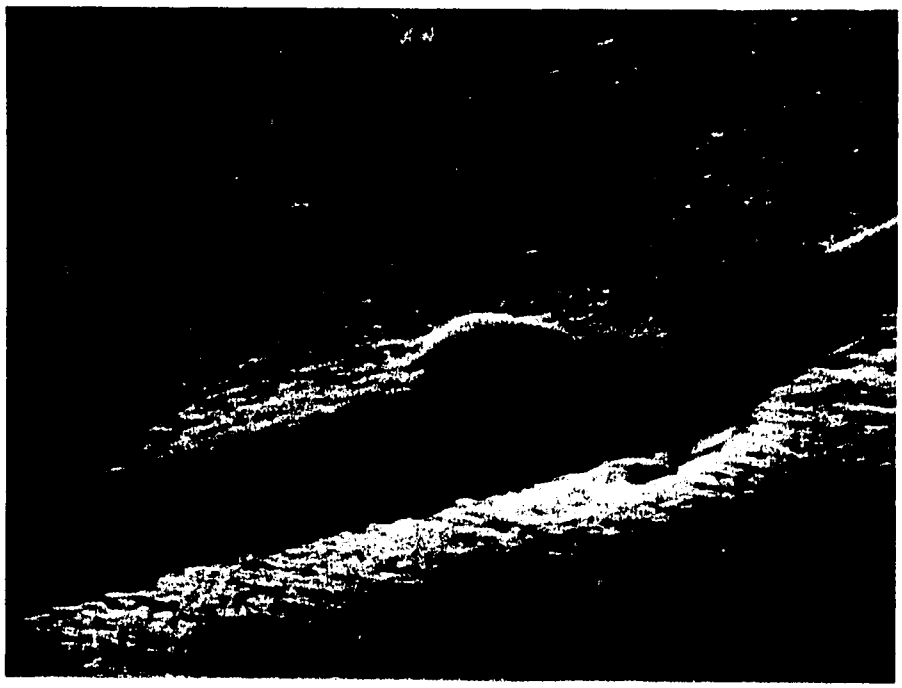

Figure 53. Co-4Al-25W

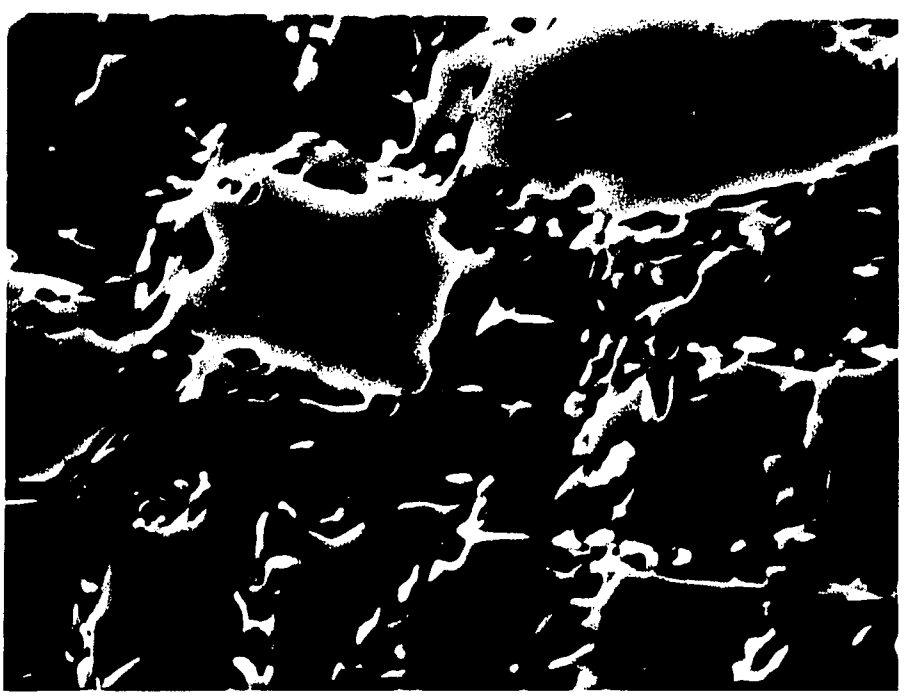

Figure 54. Co-4Al-15Cr-25W

REFERENCES

Adkins, E. F., Williams, D. N., and Jaffee, R. I. (1960), Cobalt, 8, 16.

AiResearch (1968), MP-5316-R, February 1, 1968, AiResearch Manufacturing Co. of Arizona, Phoenix, Arizona.

Beattie, H. J., Jr., (1967), "Close-Packed Structures," Intermetallic Compounds, John Wiley & Sons, New York, 144-165.

Bibring, H., and Graf, R. (1961), Comptes Rendus, Acad. Sci., 252, 4160.

Bibring, H., and Manenc, J. (1959), Comptes Rendus. Acad. Sci., 249, 16, 1508.

Bradley, A. J., and Seager, G. C. (1939), J. Inst. Metals, 64, 81.

Brown, J. F., Clark, W. D., and Parker, A. (1957), Metallurgia, 56, 215.

Coutsouradis, D. (1964), "Phenomenes de durcissement dans les alliages de Cobalt," Journees Internationales des Applications du Cobalt, Bruxelles.

Dragsdorf, R. D., and Forgeng, W. D. (1962), Acta Cryst, 15, 531.

Drapier, J. M., and Coutsouradis, D. (1968), Cobalt, 39, 63.

Drapier, J. M., deBrouwer, J. L., and Coutsouradis, D. (1965), Cobalt, 27, 59.

Dwight, A. E. (1961), Trans ASM. 53, 479.

Elliott, R. P. (1956), "A Study of a Family of Laves-Type Intermediate Phases," AFOSR-TR-56-22, ASTIA Document No. AD-88033.

Fink Inorganic Index to the Powder Diffraction File (1966), ASTM, Philadelphia, Pennsylvania.

Fountain, R. W., Faulring, G. M., and Forgeng, W. D. (1961), Trans AIME, 221, 747.

Fountain, R. W., and Forgeng, W. D. (1959), Trans AIME, 215, 998.

Fritzlen, G. A., Faulkner, W. H., Barnett, D. R., and Fountain, R. W. (1959), "Precipitation in Cobalt-Base Alloys," Precipitation from Solid Solution, ASM, Cleveland, Ohio, 449-494.

Hume-Rothery, W., and Raynor, G. V. (1962), The Structure of Metals and Alloys, Inst. of Metals, London.

Kokorin, V. V., and Chuistov, K. V. (1966), Fiz. Metal Metalloved, 21, 2, 311.

Kokorin, V. V., and Chuistov, K. V. (1968), Fiz. Metal Metalloved, 26, 2, 375.

Komura, Y., Sly, W. G., and Shoemaker, D. P. (1960), Acta Cryst, 13, 575.

Korchynsky, M., and Fountain, R. W. (1959), Trans. AIME, 215, 1033.

Lee, C. S. (1967), Cobalt, 37, 216.

Lux, B., and Bollman, W. (1961), Cobalt, 11, 4.

Markov, B. Ya. (1966), J. Acad Science USSR, 1, 156.

Neumeier, L. A., and Holman, J. L. (1967), "The Tungsten-Cobalt System for Compositions to 85 Atomic Percent Cobalt," Bureau of Mines Report 6956.

Piearcey, B. J., Jackson, R., and Argent, B. B. (1962-63), J. Inst. Metals, 91, 257.

Quinn, T. J., and Hume-Rothery, W. (1963), J. Less-Common Metals, 5, 314.

Rausch, J. J., and Simcoe, C. R. (1960), "Development of Cobalt-Base Alloys," Armour Research Foundation Proj. No. ARF 2131, ASTIA Document No. AD-234645.

Rideout, S. P., and Beck, P. A. (1953), "Survey of Portions of the Chromium-Cobalt-Nickel-Molybdenum Quartenary System at 1200°C," NACA-TR-1122.

Rizzo, F. J., and Lherbier, L. W. (1966), "Research Directed Toward the Development of a Wrought Superalloy," Air Force Materials Laboratory TR-66-364.

Saito, S., and Beck, P. A. (1960), Trans. AIME, 218, 670.

Sims, C. T. (1969), J. Metals, 21, Dec, 27.

Sykes, W. P. (1933), Trans ASM, 21, 385.

Sykes, W. P., and Graff, H. F. (1935), Trans ASM, 23, 249.

Wallbaum, H. J. (1941), Z. Krist, 103, 391.

Wheaton, H. L. (1965), Cobalt, 29, 163.

Vincent, F., and Figlarz, M. (1967), Comptes Rendus, Acad. Sci., 264, 1270.